Department of Physics and Astronomy

Heidelberg University

Master thesis

in Physics

submitted by

Aika Marie Tada

born in Göttingen

2022

Singlet-Assisted Electroweak Baryogenesis in Effective Field Theory and $SO(6)/SO(5)$ Composite Higgs Models

This Master thesis has been carried out by Aika Marie Tada

at the

Max-Planck-Institut für Kernphysik

under the supervision of

Dr. Florian Goertz

Elektroschwache Baryogenese mithilfe eines zusätzlichen Singlets in effektiver Feldtheorie und $SO(6)/SO(5)$ Composite Higgs Modellen

Die Baryonenasymmetrie des Universums (BAU) kann mit Elektroschwacher Baryogenese erklärt werden, allein indem das Standard Modell (SM) mit einem skalaren Singlet ergänzt wird. Besonders gut untersucht wurden Szenarien, die eine Z_2-Symmetrie des Singlets aufweisen, die auf elektroschwacher Skala spontan gebrochen wird, welches aber im Allgemeinen zu phänomenologisch problematischen Domänenwänden führt. Um dies zu umgehen, wird ein Modell eingeführt, in dem die Z_2-Symmetrie bei hohen Temperaturen nicht wiederhergestellt wird. Zu diesem Zweck wurde eine generelle, effektive Feldtheorie (EFT) mit $D \leq 6$ Operatoren analysiert. Nimmt man eine fundamentalere Theorie auf höheren Energieskalen an, würden solche nicht renormierbaren Operatoren dynamisch generiert werden. Dies ist z.B. in Modellen mit zusammengesetztem Higgs-Teilchen (CH) der Fall, welche gleichzeitig auch das Hierarchie-Problem und das Rätsel um die großen Unterschiede zwischen den Quarkmassen im SM lösen können. In dieser Arbeit wird eine komplette Übersicht der Yukawa-Lagrangedichte und des skalaren Potentials unter Annahme verschiedener $SO(6)/SO(5)$ CH Modelle präsentiert. Dazu wird eine Spurionen-Analyse mit SM Fermionen in den $(\mathbf{1}), \mathbf{6}, \mathbf{15}$ oder $\mathbf{20'}$ Repräsentationen von $SO(6)$ durchgeführt. Das erfolgsversprechenste Modell wird mit der EFT verglichen und gezeigt, dass damit die BAU erklärt werden kann.

Singlet-Assisted Electroweak Baryogenesis in Effective Field Theory and $SO(6)/SO(5)$ Composite Higgs Models

It is known that the Baryon-Asymmetry in the Universe (BAU) can be generated in Electroweak Baryogenesis when minimally extending the Standard Model (SM) with a scalar singlet. A particularly well-researched class of models features a Z_2 symmetry of the singlet that is spontaneously broken around the electroweak scale. However, such a scenario generically leads to phenomenologically problematic domain walls. Here, a thermal history in which the Z_2 symmetry is not restored at high temperatures is envisioned, as accomplished by introducing $D \leq 6$ operators in a general effective field theory (EFT). Introducing non-renormalizable operators is the logical consequence of understanding the theory as the low-energy tail of a more complete theory, such as in Composite Higgs (CH) scenarios, which can additionally address the hierarchy problem and the flavor hierarchy puzzle. Here I present a comprehensive analysis of the Yukawa terms and the scalar potential generated up to $D = 6$ terms in various $SO(6)/SO(5)$ CH models. To this end, a Spurion Analysis with SM fermions embedded in the $(\mathbf{1}), \mathbf{6}, \mathbf{15}$ or $\mathbf{20'}$ representations of $SO(6)$ is performed. The most promising model is successfully matched to the general EFT, showing that it can generate the correct BAU.

Contents

1 Introduction

To describe our world at the smallest scale, the Standard Model of particle physics (SM) is the most successful model up to date. Being completed with the discovery of the Higgs Boson in 2012 [1], so far, it withstood all further tests without breaking down. Nonetheless, our work is far from done – there are a number of reasons to search for so-called "new physics" (NP), particles or forces which we have not observed yet. One of the first and foremost issues is the *Baryon Asymmetry in the Universe (BAU)* which asks the most basic question of mankind: Why do we exist? The SM provides no answer to this, as we will see in the next chapter.

Now, if we assume new particles exist at a high energy scale, the SM can be seen as the renormalizable part of an effective field theory (EFT) which is valid only up to a scale Λ_{UV}. Having two or more scales - the Higgs mass m_h defining the SM scale and the scale of new physics Λ_{NP} - in the theory leads us into a *hierarchy problem*, with m_h being highly sensitive to quantum corrections of scale Λ_{NP}. Therefore, we wonder: why is the Higgs mass so small and should there not be a symmetry or other mechanism which protects it?

These two are the questions that mainly will be discussed in this thesis. Furthermore, one can ask for the nature of Dark Matter (DM), which makes up 84 % of the universe's matter density [2], the origin of dark energy, and the small value of neutrino masses. Unification of the electromagnetic and weak forces, as well as calculating the running couplings in the SM suggests the existence of a grand unified theory (GUT) of all forces at high energies. Another long-standing riddle is how to connect the quantum field theoretic (QFT) approach of the SM with the classical model of Einstein gravity. Last, but not least, when diving into the structure of the SM, there are more puzzles to be solved, e.g., why we do not observe CP-violation in strong interactions or why the top quark is much heavier than all other quarks (Flavor Hierarchy Puzzle).

Experiments obtain higher and higher precision, finding small – but promising – deviations from quantities predicted by the SM. Observed branching ratios in rare semileptonic B-meson decay, as well as hints of lepton flavor universality violation, e.g., are in tension with the SM. They point to a coherent pattern of "flavor anomalies", that may become proof of the existence of beyond the standard model physics [3]. Albeit experiments also continue to widen the energies accessible to us in direct search of new particles, none have been observed so far. Meanwhile, theorists try to address open issues by model building - not only out of curiosity, but also to point out where to search for the impacts of new physics. In such studies, effective field theories have proven to be very useful.

One particularly simple and well-researched model is given by adding one scalar

singlet, equipped with a $\mathbb{Z}_2$ symmetry to make it a DM candidate, to the SM. Thereby, one can e.g., explain the BAU in the context of *Electroweak Baryogenesis (EWBG)* by a two-step phase transition featuring spontaneous $\mathbb{Z}_2$ symmetry breaking at electroweak scale [4–13]. This, however, is known to be problematic due to the emergence of *domain walls* [14].

To avoid this problem and still allow for EWBG, in [15], we proposed a thermal history starting from a $\mathbb{Z}_2$-broken phase and undergoing a strong one-step phase transition. This thesis is based on this *symmetry non-restoration (SNR)* scenario, which we analyzed employing a general EFT. As a possible UV completion, a $SO(6)/SO(5)$ *Composite Higgs (CH)* model is introduced. In CH models, the Higgs is assumed to be a composite pseudo Nambu–Goldstone boson (pNGB) of a new, strongly coupled sector – similar to the pions in QCD – thus solving the hierarchy problem and paving the way to a calculable Higgs potential. The structure of the scalar potential is then determined by the interaction between the so-called composite and the standard model sector, where the SM fermions couple linearly to composite resonances in a framework called *Partial Compositeness (PC)*. The SM fermions are then lifted to full $SO(6)$ multiplets – so called spurions – and the potential can then be constructed in a *spurion analysis* by acknowledging that it needs to arise from the explicit $SO(6)$ symmetry breaking induced by the spurions taking their real values. It is therefore sensitive to what representation of $SO(6)$ the resonances transform in. A comprehensive overview of all Yukawa Lagrangians and potentials arising from combinations of the representations $\mathbf{1}, \mathbf{6}, \mathbf{15}$ and $\mathbf{20'}$ up to non-renormalizable order will be given and compared. The model most likely to fit the SNR scenario will be identified and matched to the parameters of the general EFT.

This thesis is structured as follows: first, the basic models, concepts and technicalities required to understand this work are summarized in Ch. 2. In Ch. 3, the thermal history of the $\mathbb{Z}_2$ symmetry non-restoration (SNR) scenario is considered and the parameter space in which it fulfills the conditions for EWBG is recapitulated. Ch. 4 considers concrete $SO(6)/SO(5)$ models, the different ways of how to embed SM fermions in $SO(6)$ multiplets and the calculation of the Yukawa Lagrangian and the potential, the implications of the resulting structures being analyzed in Sec. 4.5. In Sec. 4.6, the most promising model is matched to the SNR scenario. Finally, this work is summarized in Ch. 5 and a further lines of investigation are proposed.

2 Foundations

In this chapter, first, a short overview of the SM, Electroweak (EW) theory and the hierarchy problem is given in Sec. 2.1. It is followed by an explanation of the basic idea of electroweak baryogenesis in Sec. 2.2, and how additional scalar singlets can be employed to realize it in Sec. 2.3. The calculation of thermal corrections to the scalar potential needed in this context is the subject of Sec. 2.4. Sec. 2.5 then dives into the construction of composite Higgs models, explaining vacuum misalignment and giving a short overview of the *Callan-Coleman-Wess-Zumino (CCWZ)* framework, with which an EFT for any theory with a spontaneously broken symmetry can be obtained. It also includes how the new sector is coupled to the SM when assuming partial compositeness. Finally, the ingredients for the concrete $SO(6)/SO(5)$ model are introduced in Sec. 2.6, including how to calculate the resulting Higgs potential, using spurion analysis, the CCZW framework and dimensional analysis. Standard quantum field theory methods of textbook material as presented in [16] will be assumed in the following. Of particular importance for the present thesis are the language of effective field theory, especially the notion of dimensional analysis.

2.1 The Standard Model of Particle Physics

The SM is a description of our world at the smallest scale we can presently reach. It features three generations of fermions, consisting of each two quarks and two leptons as well as their antiparticles. The six quarks, u, d, s, c, t, b and the six leptons $e, \nu_e, \mu, \nu_\mu, \tau, \nu_\tau$ are also referred to as different "flavors". Additionally, the SM encompasses three fundamental forces, the strong, weak and electromagnetic force. These are described in terms of *gauge theories* and are mediated by their respective gauge bosons - eight gluons, $W^\pm$ and Z bosons, and the photon. Last but not least, the SM includes the Higgs boson, which generates particle masses via the *Higgs mechanism*. For an (experiment-centered) overview of Particles Physics, see e.g., Martin and Shaw [17], for a quantum field theoretic introduction, see Schwartz [18] or Peskin and Schroeder [16], where in the latter, especially chapters 11, 16, 20 and 21 are of interest for this thesis. The fermion content of the SM is summarized in Tab. 2.1.

The SM gauge group is given by $\mathcal{G}_{\text{SM}} = SU(3)_c \times SU(2)_L \times U(1)_Y$. The theory of the strong force, $SU(3)_c$, is called *Quantumchromodynamics (QCD)* and is responsible for forming quark bound-states like the proton or neutron. It will be mostly omitted, since it is not crucial to this thesis. The gauge groups $SU(2)_L \times U(1)_Y$ form the *Electroweak (EW) Theory*, a unification of the electromagnetic force $U(1)_{em}$ of *Quantum Electrodynamics (QED)* and the weak force (covered at small energies

Table 2.1: Fermion content of the standard model, adapted from [19].[1]The quarks are QCD color triplets, while the leptons are color singlets. The weak isospin I_3 and the hypercharge Y combine to the electric charge $Q = I_3 + Y$

	Generation						Notation
	I	II	III	I_3	Y	Q	$(SU(3), SU(2))_Y$
Leptons	$\begin{pmatrix} \nu_e \\ e \end{pmatrix}_L$	$\begin{pmatrix} \nu_\mu \\ \mu \end{pmatrix}_L$	$\begin{pmatrix} \nu_\tau \\ \tau \end{pmatrix}_L$	$+1/2$ $-1/2$	$-1/2$ $-1/2$	0 -1	$(\mathbf{1}, \mathbf{2})_{-1/2}$
	e_R	μ_R	τ_R	0	-1	-1	$(\mathbf{1}, \mathbf{1})_{-1}$
Quarks	$\begin{pmatrix} u \\ d \end{pmatrix}_L$	$\begin{pmatrix} c \\ s \end{pmatrix}_L$	$\begin{pmatrix} t \\ b \end{pmatrix}_L$	$+1/2$ $-1/2$	$+1/6$ $+1/6$	$+2/3$ $-1/3$	$(\mathbf{3}, \mathbf{2})_{1/6}$
	u_R	c_R	t_R	0	$+2/3$	$+2/3$	$(\mathbf{3}, \mathbf{1})_{2/3}$
	d_R	s_R	b_R	0	$-1/3$	$-1/3$	$(\mathbf{3}, \mathbf{1})_{-1/3}$

by *Fermi theory*). $U(1)_Y$ is the gauge group of the *weak hypercharge*, which in combination with the weak isospin I_3 of $SU(2)_L$ reproduces the correct electric charge $Q = I_3 + Y$. Elektroweak Symmetry Breaking (EWSB) $SU(2)_L \times U(1)_Y \to U(1)_{em}$ is described by the Higgs mechanism, where the Higgs boson acquires a non-zero vacuum expectation value v, spontaneously breaking EW symmetry and generating particle masses. When switching from interaction to mass eigenstates, one then recovers the low-energy massive W and Z bosons, as well as the massless photon.

In the history of particle physics, constructing a Lagrangian from symmetry principles has been proven very successful. In what representation of each symmetry group the ingredients transform is then of great importance to construct invariant terms. The quarks transform as fundamental triplets of $SU(3)_c$, while the leptons, which do not interact strongly, are singlets of it. As experimentally discovered [20], the weak force only couples to lefthanded (LH) particles and righthanded (RH) antiparticles, maximally violating parity (P) symmetry. Accordingly, the need to distinguish arises: RH quarks $q_R = u^i_R, d^i_R$ and LH antiquarks $\bar{q_R}^i$ are singlets, $i = 1, 2, 3$ denoting the three generations. LH quarks $q_L = (u^i_L, d^i_L)$ and RH antiquarks $\bar{q_L}^i$ form fundamental doublets of $SU(2)_L$. Similarly, the LH leptons form a doublet $l = (\nu^i_L, e^i_L)$ while the RH charged leptons e^i_R, ν^i_R are singlets. Although righthanded neutrinos could exist, they are not charged under $SU(2)_L$ and $SU(3)_c$ ("sterile") and therefore not considered part of the SM - a neutrino mass term then cannot arise.[2]

The gauge bosons are Lorentz vectors and transform in the adjoint representation of their respective group, meaning that they act like generators of the corresponding Lie group. Under all other forces they are singlets. The Higgs is a Lorentz scalar and a complex doublet of the EW gauge group.[3]

[1]Conventional notations for the hypercharge differ by a factor of 2.

[2]Neutrinos would need to be massive, however, to explain neutrino oscillation in a well-accepted extension of the SM [2].

[3]Actually, performing spontaneous symmetry breaking for a pure $SU(2)$ theory, one can not obtain three massive and one massless gauge boson (early versions of EW theory with only three gauge bosons were considered by Schwinger and Glashow [21, 22] before the Z boson was

The amount of symmetries one needs to take into account may seem overwhelming - obviously, Lorentz symmetry has to be considered in addition to any symmetry one imposes, be it the EW symmetry, the strong $SU(3)_c$, charge-parity (CP) symmetry or anything else. While it is crucial that any Lagrangian term is a singlet of all the assumed symmetries, they form direct tensor products with each other and thus one can check the invariance under each of them one by one.

By itself, the SM can be seen as a fundamental, self-consistent theory, meaning it does not exhibit any inherent problems. Even so, not including gravity and failing to explain many important experimental observations such as the BAU or DM, it needs to be thought of rather as a basis to expand on. That is where Beyond the Standard Model (BSM) physics comes in. Commonly, the Standard model is thought of as the renormalizable part of an effective field theory, SMEFT, located at scales much lower than the Planck scale $M_{\mathrm{Pl}} \sim G^{-1/2}$. The Planck scale is determined by the inverse gravitational constant G, where quantum gravity contributions are thought to become non-negligible. Assuming there is new physics (NP) in between the SM and the Planck scale, having more than one scale in a theory with a fundamental scalar, the hierarchy problem explained in the next section arises.

Even within the SM, there are some hitches: theorists wonder, for example, why CP-violation (CPV) in QCD is not observed, even though the corresponding Lagrangian term would not be forbidden and as a small amount of CPV is observed in EW interaction, CP cannot be an overall symmetry of nature. Also, quite many parameters have to be determined by experiment - e.g., there seems to be no theoretical motivation for the vastly different masses of different quark flavors. The discrepancy between the top mass at $m_t \approx 173\,\mathrm{GeV}$ and all other quark masses at $2\,\mathrm{MeV} \sim 4\,\mathrm{GeV}$ [2] is part of the *flavor hierarchy puzzle* and will be later addressed in the context of composite Higgs models. In the same context, the questions why there are three generations of quarks and leptons in particular and how to explain the amount of weak mixing between them (determined by the angles in the Cabibbo-Kobayashi-Maskawa (CKM) and Pontecorvo-Maki-Nakagawa-Sakata matrices) arise.

2.1.1 Electroweak Theory and the Higgs Mechanism

In the SM, due to the maximally P-violating nature of the weak interaction, no fermion masses of the type $\bar{q_R} m q_L$ can be written down, as q_R and q_L belong to different representations of $SU(2)$ and therefore cannot form invariants by themselves. In addition, in contrast to the massless photons and gluons, the gauge bosons of the weak interaction have non-zero masses - naively writing down mass terms would however destroy the gauge invariance. Both points can be solved by introducing the Higgs boson doublet H that spontaneously breaks $SU(2)_L \times U(1)_Y$ symmetry to the electromagnetic $U(1)_{\mathrm{em}}$ symmetry, generating three Goldstone bosons which are

discovered). To allow for both the photon and Z boson, an additional hypercharge $U(1)_Y$ needs to be introduced with the symmetry breaking Higgs charged under it, see e.g., [16, Ch. 20.2].

then "eaten" by the $W^{\pm}$ and Z bosons. This generation of gauge boson masses by spontaneous symmetry breaking is referred to as the *Higgs mechanism* and was first explored in non-abelian gauge theories in [23–25], extending the Goldstone theorem that predicts one massless boson for each generator of a broken global symmetry [26]. A small summary of the Higgs mechanism in EW theory, based on [16, Ch.20.2] follows. The same principles will be featured again in Subsec. 2.5.1, where *vacuum misalignment* in theories with spontaneously broken symmetries (SSB) and additional, explicit symmetry breaking is introduced. The complex Higgs doublet is written as

$$H(x) = \frac{1}{\sqrt{2}} \begin{pmatrix} \Pi_1(x) + \imath\Pi_2(x) \\ h(x) - \imath\Pi_3(x) \end{pmatrix} . \tag{2.1}$$

The part of the full Lagrangian $\mathcal{L}$ involving the Higgs field reads as follows:

$$\mathcal{L} \supset D_\mu H D^\mu H^\dagger - V(H) , \tag{2.2}$$

$$V(H) = \mu_h^2 H^\dagger H + \lambda_h \left(H^\dagger H\right)^2 , \tag{2.3}$$

given the electroweak covariant derivative

$$D_\mu = \partial_\mu - \imath g A_\mu^a T_L^a - \imath \frac{1}{2} g' B_\mu , \tag{2.4}$$

where T_L are the generators of $SU(2)_L$ with $a = 1, 2, 3$, and g, g' are the coupling constants of $SU(2)_L$ and $U(1)_Y$ gauge bosons. For $\mu_h^2 < 0$, the Higgs develops a vacuum expectation value (vev),

$$\frac{\partial V}{\partial H} = 0 \Leftrightarrow |H| = \sqrt{\frac{-\mu_h^2}{2\lambda_h}} =: \frac{1}{\sqrt{2}} v . \tag{2.5}$$

One can then choose one of the degenerate vacua and write the physical Higgs field $h(x)$ as fluctuations around it,

$$H = \frac{1}{\sqrt{2}} \begin{pmatrix} 0 \\ v + h(x) \end{pmatrix} . \tag{2.6}$$

The $\Pi_i(x)$ fields introduced above are then Goldstone bosons. They fluctuate in symmetry conserving directions and can therefore be gauged away by local $SU(2)$ transformations. Here, they are set to zero in what is called *unitary gauge*, where the Goldstone degrees of freedom are fully transferred to the gauge bosons, which thereby obtain mass:

$$|D_\mu H|^2 = \frac{v^2}{2} \left[g^2 \left(A_\mu^1 T_L^1\right)^2 + g^2 \left(A_\mu^2 T_L^2\right)^2 + \left(-g A_\mu^3 T_L^3 + g' B_\mu\right)^2 \right] . \tag{2.7}$$

Going to the mass eigenbasis of the EW gauge bosons, one recovers the three massive gauge bosons and the photon:

$$W_\mu^\pm = \frac{1}{\sqrt{2}}\left(A_\mu^1 \pm A_\mu^2\right) \qquad \text{with} \qquad m_W = g\frac{v}{2} \tag{2.8}$$

$$Z_\mu^0 = \frac{1}{\sqrt{g^2+g'^2}}\left(gA_\mu^3 - g'B_\mu\right) \qquad \text{with} \qquad m_Z = \sqrt{g^2+g'^2}\frac{v}{2} \tag{2.9}$$

$$A_\mu = \frac{1}{\sqrt{g^2+g'^2}}\left(g'A_\mu^3 + gB_\mu\right) \qquad \text{with} \qquad m_A = 0\,. \tag{2.10}$$

To realize fermion masses, for each flavor, one needs to introduce a Yukawa coupling y_q to the Higgs boson:

$$\mathcal{L}_{\text{Yuk}} \supset \sum_{q_R = u_R, d_R} (y_q)_{ij}\, \bar{q_L}^i H q_R^j + \text{h.c.}\ , \tag{2.11}$$

where $i,j = 1,2,3$ denote the quark generations and $H \to H^c = \imath\sigma_2 H^*$ for up-type u_R^i terms. Plugging the Higgs vev (2.6) in, in the basis of mass eigenstates one can write

$$m_q^i = \frac{1}{\sqrt{2}}\,(y_q)_{ii}\, v\,. \tag{2.12}$$

Note that while the generation of mass itself is explained, its size relies on the different coupling values which are theoretically not constrained.

The Higgs mass of $h(x)$ can easily be calculated, inserting (2.6) into (2.3) to be

$$m_h^2 = -2\mu^2 = 2\lambda_h v^2\,. \tag{2.13}$$

Experimentally, mass and electroweak vev have been determined to $m_h = 125\,\text{GeV}$ and $v = 246\,\text{GeV}$ [2].

2.1.2 The Hierarchy Problem

As quite clearly explained in [27], if there are two largely separated scales - for simplicity called $\Lambda_{\text{SM}} \approx m_h$ and Λ_{UV} here - in a theory with a light scalar, a fine tuning problem arises.[4] In particular, calculating the self energy of a scalar particle such as the Higgs, its squared bare mass m_0^2 obtains corrections quadratic in a large UV cutoff Λ_{UV}^2 for some regularization. Even when that is not the case, it will definitely be sensitive to M^2 when considering the influence of new particles with a high mass M, see e.g., the introduction of [30]. A heavy scalar S, interacting with the Higgs via $-\lambda_{hS}|H|^2|S|^2$, would e.g., give a one-loop correction of

$$\Delta m_h^2 = \frac{\lambda_{hS}}{16\pi^2}\left[\Lambda_{\text{UV}}^2 - 2M^2 \ln\left(\frac{\Lambda_{\text{UV}}}{M}\right) + \dots\right], \tag{2.14}$$

[4] Originally, this problem was pointed out in the context of GUTs, where in addition to EW symmetry breaking, another SSB scale was introduced to avoid proton decay [28, 29].

when regularizing the loop integral with an UV cutoff. The crux is that even though in the renormalization procedure, these corrections are absorbed into counterterms to fix the physical Higgs mass at low energies,

$$m_h^2 = m_0^2 - \Delta m_h^2 \,, \tag{2.15}$$

this relation is incredible finetuned. For one, Δm_h^2 is sensitive to the explicit mass of every single new particle there may be. Secondly, if one e.g., expects particles at Planck scale to play a role, this would imply a cancellation between two $M_{\mathrm{Pl}}^2 \sim 10^{38}\mathrm{GeV}^2$ scale values to yield a $\Lambda_{\mathrm{SM}}^2 \sim 10^4\mathrm{GeV}^2$ value, demanding a tuning of $\Lambda_{\mathrm{SM}}^2/M_{\mathrm{Pl}}^2 \approx 10^{-34}$.

Apart from the composite Higgs models introduced in this thesis, there are many other theories aiming to solve the hierarchy problem: supersymmetric models propose a symmetry between fermions and baryons, such that every known particle has a heavy "sparticle" partner of the respective other spin (for an introduction, see e.g. [30]). There are also technicolor models (see, e.g., [31]), which assume a new sector with a new strong force, and are in some ways the prequels of CH models. Another possibility is to propose one or more compact extra spatial dimensions, where the large Planck mass is only the 4D consequence of a smaller Planck scale in flat, higher dimensions. When instead assuming a warped extra dimension, the hierarchy problem can be solved instead by gravitational redshift – these warped extradimensional models can actually be identified with "holographic" 4D CH models [32].

2.2 Baryogenesis

All observations point to the fact that there is more matter than antimatter in the universe, see, for example, the constraints from gamma-ray astronomy in [33]. This asymmetry can be quantified by the ratio of baryon and photon number density $\eta_b = \frac{(n_b - n_{\bar{b}})}{n_\gamma} \approx 6 \cdot 10^{-10}$, the photons being from cosmic background radiation. The ratio can be extracted from measurements of element abundances at the time of big bang nucleosynthesis or from the cosmic microwave background (CMB) [34]. Oftentimes, it is measured and given in terms of $\Omega_b h^2 = 3.66 \cdot 10^7 \eta_b$, where Ω_b is the baryon fraction of the total energy density in the universe and h is the scaled Hubble parameter. The photon number may be calculated as a thermodynamic quantity from the temperature of the CMB, $T \approx 2.73\,\mathrm{K}$, to be $n_\gamma = \frac{2\zeta(3)}{\pi^2} T^3$ (in natural units), see e.g. [2]. Contributions from other photon sources are comparatively small.[5]

Any relic particle density in the very early universe, however, is exponentially diluted by inflation, a phase of accelerated expansion which is postulated to reconcile

[5] For a comprehensive overview of all sources of cosmic background radiation and their estimated energy densities, see [35]. If one then acknowledges that for smaller photon frequencies, one needs more photons to arrive at the same energy density than for higher frequencies, one can be qualitatively reassured that the CMB is dominating the number density and the above is a good estimate.

the large scale correlations in the CMB with the specific initial conditions of Big-Bang cosmology [2], and therefore cannot be used to explain the observed baryon asymmetry.[6] Therefore, it is assumed that the universe was initially matter-antimatter symmetric and an asymmetry needs to be created by *baryogenesis*.

While there is a whole range of different approaches to this (see, e.g., [37, 38]), assuming CPT is conserved, all must fulfill the three *Sakharov criteria*:

1. violation of baryon number conservation
2. C- and CP-violation
3. departure from thermal equilibrium

after [39], as explained, for example, in [34]. Most of the following overview is based on the latter reference. The SM actually features a significant amount of baryon number violation, fulfilling the first criterion. While baryon number B is a global symmetry of the SM Lagrangian, it is violated in the triangle anomaly for nonzero $SU(2)$ field strengths. Albeit this does not have any perturbative effects, tunneling between different topological vacua of $SU(2)$ - separated by potential barriers of height $E_{\text{sph}} \propto v$ - is possible, giving rise to varied field strengths. These intermediate field configurations are called instantons and thereby violate baryon number, as first discovered in [40]. Although the tunneling probability is very small, at higher temperatures T it becomes possible to hop over the barrier instead in what is referred to as a "sphaleron" process. The sphaleron transition rate can be semiclassically estimated to be

$$\Gamma_{\text{sph}} \propto e^{-E_{\text{sph}}/T} . \tag{2.16}$$

One may already notice that the barrier height and therefore the sphaleron rate is highly dependent on the Higgs vev, which changes in the course of the electroweak phase transition (EWPhT). The CP-violation (CPV) given by the CKM matrix of the SM, on the other hand, is thought to be insufficient for reproducing the observed BAU [41]. Lastly, the process at hand should be out of thermal equilibrium, meaning it should not be reversible - this proves difficult at low energies. Common ingredients are new, heavy particles decaying at temperatures $T < m$ or the universe going through a *strong first order phase transition (SFOPhT)* at some point. The obvious candidate for the latter would again be the EWPhT, but it is not strong enough to prevent a washout of generated baryon number. Interestingly, the SM therefore already hints at a solution to all three Sakharov criteria in form of the EWPhT – its CPV and phase transition are just not strong enough. This gives rise to a class of models called *electroweak baryogenesis*, which aims for a strong first order EWPhT (SFOEWPhT) and is explained in the next section. An additional singlet can, for example, be used to enhance the phase transition and introduce additional CPV – one such scenario being the basis of this thesis.

[6] In principle, as shown in [36], obtaining the BAU from a pre-inflationary initial condition is possible. However, the model in question requires severe fine-tuning and trans-Planckian field values.

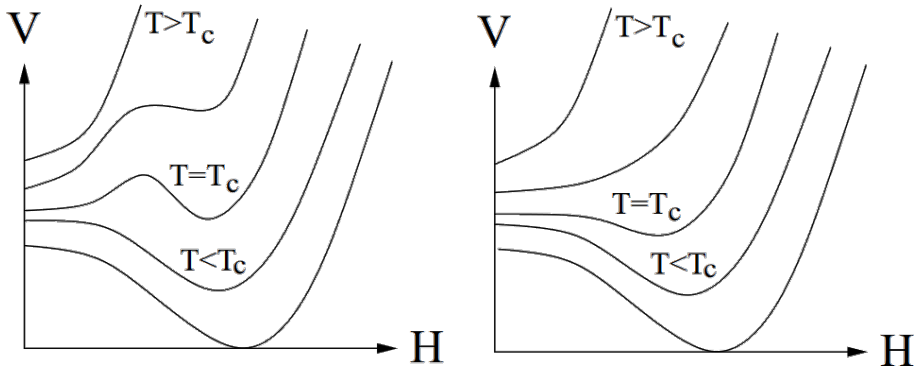

Figure 2.1: Schematic illustration of the Higgs potentials' thermal evolution for a (left) first and a (right) second order phase transition [34]

2.2.1 Electroweak Baryogenesis

Proposing to use the electroweak phase transition for baryogenesis has the main advantage that the scenario is testable at quite low energies – as is motivated below, to make the EWPhT strongly first order, one needs to introduce new physics at the weak scale, which could be discovered in future collider experiments. But how exactly is the BAU generated and what is a strong first order phase transition in this context?

A Phase Transition (PT) is of first order when at the *critical temperature* T_c, two degenerate vacua, in this case the symmetric one at $\langle h \rangle = 0$ and the symmetry breaking $v(T_c) = v_c$, separated by a potential barrier, are present. In contrast, in a second order phase transition, the system smoothly transitions into a new global minimum. The critical temperature is then determined by the point at which the origin becomes unstable, here $\frac{\partial^2 V}{\partial h^2} = 0$. Both scenarios are depicted in Fig. 2.1 for the evolution of the Higgs potential, which features the EW vacuum v at zero temperatures and goes through a first (left) or second order phase transition (right) at T_c, above which the electroweak symmetry becomes fully restored at high temperature. Obviously, to analyze the thermal history, the finite temperature scalar potential has to be calculated, which is briefly summarized in Sec. 2.4.

A first order phase transition proceeds by *bubble nucleation*: the system hops into the new vacuum v_c. Inside these bubbles, the sphalerons are out of equilibrium and their rate $\propto e^{-\#v/T}$ is dampened, while outside, they are still unsuppressed and in equilibrium. Eventually, the bubbles expand to fill the whole space. The idea is to have CP-violating interactions inside the bubble wall, such that a lefthanded vs righthanded quark overhang is created in the symmetric phase in front of the wall. Sphalerons try to relax this CP asymmetry, thereby creating a baryon surplus, which transmits into the bubbles as they expand. To ensure this surplus is not washed out by inverse sphaleron processes in the inside, the sphaleron rate there must be heavily suppressed. A sufficient suppression of $\xi = v_c/T_c \gtrsim 1$ – or, more conservatively, $\xi \gtrsim 1.3$, as in [42] – therefore defines a *strong* PT. Second order phase transitions on

the other hand always allow a washout by the inverse sphaleron processes.

Calculating the finite temperature Higgs potential, it can be shown that a SFOEWPhT in the SM would require a Higgs mass of $m_h < 32\,\text{GeV}$, which is refuted by experiment. Results from lattice calculations show that the SM EWPhT is not even of first or second order, but rather a crossover [43]. Hence, the SM needs to be extended to account for not only additional CP-violation but also make the phase transition strongly first order, e.g., by introducing an additional scalar singlet as explained in the next section. For more details on EWBG, see e.g., the lectures by Cline [34].

Note that in addition to the critical temperature and vev, there is another important parameter in cosmological phase transitions: the *nucleation temperature* T_n is given by the temperature at which the probability of finding one bubble per Hubble volume becomes order one and signifies the actual starting point of the phase transition. While the critical temperature is easy to calculate by finding the degenerate vacua, for the lower nucleation temperature one would need to solve a so-called bounce equation which describes the bubble dynamics, see, e.g. [42, 44]. The bounce solutions can be only obtained for thin bubble walls analytically, which is why one often needs to rely on numerical simulations, as, e.g., in [45, 46].

2.3 Singlet Assisted Electroweak Baryogenesis

Singlet-extensions of the SM, allowing additional sources of CP-violation and providing a strong first order phase transition, are promising candidates for realizing EWSB. One particularly well researched class of models features a real scalar singlet S with a $\mathbb{Z}_2 : S \leftrightarrow -S$ symmetry, allowing it to act as a dark matter candidate without being ruled out by current collider limits and accounting for the correct BAU [4–13].[7] EWBG is then usually realized using a two-step phase transition $(\langle h\rangle, \langle S\rangle) = (0,0) \to (0,w) \to (v,0)$, where in the first step, the $\mathbb{Z}_2$ symmetry is spontaneously broken to $\langle S\rangle = w$, before the electroweak vacuum with $\langle h\rangle = v$ becomes the global minimum. While the singlet vev needs to change over the course of the phase transition in these scenarios (otherwise, the singlet basically stays a spectator and cannot enhance the phase transition), $\mathbb{Z}_2$ symmetry breaking at low energies is known to be problematic. In particular, if one does not introduce at least a small explicitly $\mathbb{Z}_2$ breaking term, bubbles with $+w$ and $-w$ populate equally. When they expand, domain walls form between the different patches, which have been shown to have a high energy density [14]. It should therefore be possible to either observe such domain walls today or observe the radiation from their decay, both of which are not the case. Espinosa et al. note in [7], however, that the temperature at which a decay of domain walls would start to dominate observations is at $\sim 10^{-7}$GeV, long after the EWPhT at $T_{\text{EW}} \sim 100\,\text{GeV}$, making a SSB scenario safe as long as the symmetry is restored after EWSB. On the other hand, they also note

[7] Such a scenario can be readily obtained in a non-minimal composite Higgs model [7, 47], which is the subject of Sec. 2.6.

that an equal population of the vacua and subsequent decay of the domain walls would lead to a cancellation of a net baryon asymmetry from w patches with an antibaryon asymmetry from $-w$ patches.[8] In [7] and [46], this is circumvented by introducing explicit symmetry breaking. This thesis instead relies on the possibility that the universe starts from a $\mathbb{Z}_2$ broken phase at high temperatures ("symmetry non-restoration") and undergoes only a one-step phase transition $(0, w) \to (0, v)$, as proposed in [15]. Such a thermal history is made possible if one allows for $D = 6$ operators in the potential. Higher dimensional operators are sometimes used to introduce additional CPV as in [7, 10, 48], which will also be the subject of the next subsection. As the Lagrangian is then already an EFT, there is no reason to omit similar terms in the potential. If one introduces new physics at a higher scale to solve other problems of the SM, the low energy description is indeed expected to feature higher dimensional terms.

In singlet extended models, the potential barrier needed for a first order phase transition can either be obtained by singlet loop corrections to the tree level scalar potential $V_0(h, S)$ or by introducing such a barrier at tree level in the first place, i.e., by choosing the coupling of the "portal" term h^2S^2 accordingly. The latter is generally more successful in making the phase transition strongly first order [7] and will be employed in the scenario of Ch. 3.

2.3.1 CP-violation in singlet extended model

There are two common ways of introducing additional CP-violation in the singlet extended model: if one wants to conserve $\mathbb{Z}_2$ symmetry not only in the scalar potential, but also in the Yukawa Lagrangian, the $D = 6$ modification of the top mass

$$\bar{t}_L m_t t_R = \bar{q}_L H^c \left(y_t + (a + \imath b) \frac{S^2}{\Lambda_{\mathrm{NP}}^2} \right) u_R + \mathrm{h.c.} \tag{2.17}$$

may be introduced, where a, b are real parameters and Λ_{NP} is some new physics scale [10, 48]. (For the singlet arising as a Goldstone boson in a composite Higgs model, Λ_{NP} will be identified with the Goldstone decay constant f.) In this way, decay of a single S into SM particles can be prevented. If we do not strive to conserve this symmetry, a $D = 5$ modification

$$\bar{t}_L m_t t_R = \bar{q}_L H^c \left(y_t + (a + \imath b) \frac{S}{\Lambda_{\mathrm{NP}}} \right) u_R + \mathrm{h.c.}\,, \tag{2.18}$$

as in [7] suffices and – being less suppressed – may be preferred. In both cases, the top mass obtains a complex phase $m_t = |m_t| e^{\imath \Theta_t}$ for $b \neq 0$. At zero temperature, where the scalar vevs are constant, this phase can be absorbed into the top quark

[8] Note that $\mathbb{Z}_2$ symmetry and CP-invariance are sometimes used synonymously when considering the potential of a pseudoscalar singlet. This may be a source of confusion when comparing different papers.

field and is thus unphysical. For finite temperatures on the other hand, the singlet vev w is subject to change (in particular to enhance the EWPhT), such that an absorption of the phase $\Theta_t(t)$ into the top quark would appear in the quark's kinetic term. In this way, intermediate complex masses and thereby CP-violation can be introduced. Espinosa et al. [7] then proceed to analyze the change in phase needed to reproduce the correct BAU with the $D = 5$ term and find numerically that

$$\Delta\Theta_t \approx \frac{b}{y_t}\frac{\Delta w_c}{f} \gtrsim 0.1\,, \tag{2.19}$$

where Δw_c is the total change in the singlet vev w at the critical temperature.

The five dimensional term in (2.18) can be made explicitly CP-conserving, if either $a \neq 0$, $b = 0$ for a CP-even scalar or $a = 0$, $b \neq 0$ for a CP-odd pseudoscalar S. To make use of *spontaneous* CP-violation, a pseudoscalar singlet is then needed.[9] In contrast, the six dimensional term in (2.17) can only *explicitly* violate CP. When introducing such a term, one usually wants it to be the only extra source of CP-violation, meaning that S would be assumed to be fully CP even or odd regardless.

2.4 Finite Temperature Corrections to a Scalar Potential

In [49], it was shown that quantum fluctuations can tip a system into a symmetry broken state even if the naive vev is symmetry conserving, motivating the need for and introducing the effective action. Indeed, the true vacuum expectation value ϕ_c of a quantum theory then extremizes the effective action $\Gamma[\phi_c] = -\int dx V_{\text{eff}}(\phi_c)$ (also see, e.g., [16, Ch. 11] and other QFT textbooks).[10] A potential appearing in the Lagrangian, such as (2.3) is also called the classical or tree level potential V_0, as loop corrections have not been taken into account yet. The effective action formalism can be extended to include finite temperature corrections, making use of the fact that an imaginary time path τ in the path integral corresponds to taking a thermodynamic average at $\beta = \imath\tau = 1/T$. One can then formulate finite temperature Feynman rules. An overview of how to use both conventional and finite temperature field theory for calculating loop corrections to the scalar Higgs potential in the SM and in particular also for analyzing cosmological phase transitions is, for example, given in [42]. Following this reference, one can make a loop expansion

$$V_{\text{eff}}^T(\phi_c) = V_0(\phi_c) + V_{\text{1-loop}}(\phi_c) + \dots\,. \tag{2.20}$$

[9] Imposing explicit CP-conservation on singlet terms then automatically forbids uneven powers of S in the potential, thereby enforcing $\mathbb{Z}_2$ symmetry in it – this will be convenient when considering the UV completion later on.

[10] As we assume the theory to be translation invariant, the effective potential differs from the action only by a volume factor.

The 1-loop approximation reads

$$V_{\text{1-loop}}\left(\phi_c\right) = \sum_{i=bosons,fermions} \frac{n_i T}{2} \sum_{n=-\infty}^{+\infty} \int \frac{d^3\vec{k}}{\left(2\pi\right)^3} \ln\left[\vec{k}^2 + \omega_n^2 + m_i^2\left(\phi_c\right)\right] \tag{2.21}$$

where ω_n are the Matsubara frequencies in the imaginary time formalism, with $\omega_n = 2n\pi T$ for bosons and $\omega_n = 2\left(n+1\right)\pi T$ for fermions. The n_i denote the number of degrees of freedom for each virtual particle φ_i and the shifted masses $m_i^2\left(\phi_c\right)$ are calculated by taking two field derivatives of the tree-level Lagrangian and setting all fields to their background values at zero temperature – in case mixed field terms appear, the mass matrix should be diagonalized.

$$m_{ij}^2\left(\phi_c\right) = -\frac{\partial}{\partial\varphi_i}\frac{\partial}{\partial\varphi_j}\mathcal{L}_0\left(\phi_c\right) . \tag{2.22}$$

The 1-loop correction can be split into

$$V_{\text{1-loop}}\left(\phi_c\right) = V_{\text{1-loop}}^0\left(\phi_c\right) + V_{\text{1-loop}}^T\left(\phi_c\right) , \tag{2.23}$$

$$V_{\text{1-loop}}^0\left(\phi_c\right) = \sum_{i=h,S,\Pi,W,Z,\gamma,q} \frac{n_i}{2} \int \frac{d^4k}{\left(2\pi\right)^4} \ln\left(k^2 + m_i^2\left(\phi_c\right)\right) , \tag{2.24}$$

$$V_{\text{1-loop}}^T\left(\phi_c\right) = \sum_{i=h,S,\Pi,W,Z,\gamma,q} n_i T \int \frac{d^3\vec{k}}{\left(2\pi\right)^3} \ln\left(1 \mp e^{-\sqrt{\vec{k}^2+m_i^2(\phi_c)}/T}\right) \tag{2.25}$$

$$= \sum_{i=h,S,\Pi,W,Z,\gamma} \frac{n_i T^4}{2\pi^2} J_B\left[\frac{m_i^2\left(\phi_c\right)}{T^2}\right] + \sum_{i=q} \frac{n_i T^4}{2\pi^2} J_F\left[\frac{m_i^2\left(\phi_c\right)}{T^2}\right] , \tag{2.26}$$

with Euclidean loop 4-momentum k, recovering the zero temperature one-loop result and introducing the thermal bosonic (fermionic) function

$$J_{B/F}\left[m_i^2/T^2\right] = \int_0^\infty dx\, x^2 \ln\left[1 \mp e^{-\sqrt{x^2+m_i^2/T^2}}\right] , \tag{2.27}$$

see, e.g., [42, 50]. Given that for the cosmological evolution only large temperature corrections, where $T^2 \gg m_i^2$, are of interest, $V_{\text{1-loop}}^0$ may be omitted and the thermal functions can be extended to

$$J_B\left[m_i^2/T^2\right] = -\frac{\pi^4}{45} + \frac{\pi^2}{12}\frac{m_i^2}{T^2} + \mathcal{O}\left(\frac{1}{T^3}\right) \tag{2.28}$$

$$J_F\left[m_i^2/T^2\right] = \frac{7\pi^4}{360} - \frac{\pi^2}{24}\frac{m_i^2}{T^2} + \mathcal{O}\left(\frac{1}{T^4}\right) . \tag{2.29}$$

Perturbation theory in terms of a small coupling constant actually breaks down when going to finite temperatures. For $T > m_{boson}$, IR-divergences in the boson propagators arise and some multiloop corrections become of the same order as the one-loop result. The leading part of those corrections is contained in daisy diagrams,

where any number of loops $N-1$ is direcly attached to one central loop - they need to be resummed in the IR limit [50], see also, e.g., [42, 51]. Usually, this has to be taken into account when analyzing the electroweak phase transition. As they only contribute with terms $\propto T$ and the SNR scenario in this thesis is more of a proof of concept than a detailed analysis, they are omitted, together with the other terms of the same order, such that in the high temperature approximation,

$$V^{T}_{\text{1-loop}}(h,S) = \frac{1}{24}\sum_{i=bosons} n_i m_i^2(h,S)\,T^2 + \frac{1}{48}\sum_{i=fermions} n_i m_i^2(h,S)\,T^2\,. \quad (2.30)$$

2.5 Composite Higgs Models

As explained in Subsec. 2.1.2, when assuming the SM to be only the low energy part of a greater theory, the Higgs as a supposedly elementary scalar particle would be very sensitive to higher energy scale quantum corrections on its mass. The physical Higgs mass of $m_h = 125\,\text{GeV}$ would thus be heavily fine-tuned.

Assuming the Higgs to be a composite particle of a new strong force (e.g., $SU(N)$) can eliminate the sensitivity to effects from virtual particles above a compositeness scale $\Lambda_c \sim 1/l_h$, where l_h is the assumed finite size of the Higgs. Essentially, the Higgs is thought to only appear elementary at energies below Λ_c, whereas above, the inner structure is resolved, as is the case for e.g., the proton or pions at high energies. Mass corrections are then at most proportional to this scale – often assumed to be $\Lambda_c = 4\pi f \approx 10\,\text{TeV}$, given the current bounds on the Goldstone decay constant $f \gtrsim 800\,\text{GeV}$ [52] – instead of M_{Pl}. The strongly coupled theory, from which CH models emerge at Λ_c is, however, not thought to be the final theory of nature. In general, one would expect other new physics – in form of a GUT at $\Lambda_{\text{UV}} \gg \text{TeV}$, for example, and definitely at the Planck scale M_{Pl} –, posing the question if this does not generate another hierarchy problem. It can however be shown that the compositeness scale can be generated naturally by "dimensional transmutation", in analogy to QCD (see, e.g, [53]). The Higgs mass would, at this point, still be expected at TeV scale, emerging together with a heap of other massive resonances Ψ.

Georgi, Kaplan and others already pointed out in the eighties [54–59] that realizing the Higgs as a pNGB of an enlarged global symmetry $\mathcal{G}$ of such a *composite sector* can make it naturally light as compared to the compositeness scale and the other, massive resonances. This idea will be explained in more detail in the following sections. To give a short overview: By condensation of the strongly coupled particles of the composite sector, $\langle\bar{\Psi}\Psi\rangle \neq 0$, $\mathcal{G}$ is spontaneously broken to a subgroup $\mathcal{H}_1$, thus generating $\dim(\mathcal{G}) - \dim(\mathcal{H}_1)$ Goldstone bosons and a number of massive composite fermionic and bosonic resonances ψ, ρ, as in low energy QCD. The complex Higgs doublet can then be identified with four of the Goldstone degrees of freedom.

A true Goldstone boson is protected by the non-linearly realized ("broken") symmetry and as such cannot obtain a potential or mass. Therefore, *explicit* symmetry breaking is needed, which is obtained by interactions with the SM sector: While on one hand, only a subgroup $\mathcal{H}_0 \subset \mathcal{G}$, which contains the SM gauge group

$\mathcal{G}_{\text{SM}} = SU(2)_L \times U(1)_Y$, is gauged, on the other hand, the SM fermions also do not transform in full representations of $\mathcal{G}$.

The interaction between composite and SM fermions is assumed to be linear to suppress flavor-changing neutral currents (FCNCs) and address the flavor hierarchy puzzle [60], see also [53]. The physical quarks are then mixtures of both sectors and the amount of compositeness determines their mass. This *partial fermion compositeness* is briefly explained in Subsec. 2.5.3. Only the top quark contribution to the explicit breaking will be considered in this thesis, as due to its mass of 173 GeV, it is much heavier than the EW gauge bosons (80, 90 GeV) or other fermions (few GeV), meaning it also contributes most to the Higgs potential. The theory can be readily extended to include the other particles as well, c.f. [53].

Given the mixing between SM and composite sector, the Lagrangian can now be obtained by a spurion analysis. For this, one initially assumes that the SM particles are part of full multiplets of the global symmetry group $\mathcal{G}$. Using the *Callan-Coleman-Wess-Zumino* construction [61, 62] described in Subsec. 2.5.2, one can construct the $\mathcal{G}$-invariant Lagrangian in the spontaneously symmetry broken phase. Then, the truly incomplete multiplets ("spurions"), are set to the actual SM fermion embeddings, thereby breaking the symmetry explicitly. Through this trick, one is able to deduce the structure of the Higgs potential, relying on the fact that it has to include explicitly symmetry breaking interactions and that it needs to be invariant under the SM gauge group $\mathcal{G}_{\text{SM}} = SU(2)_L \times SU(2)_R$. The scaling can be obtained by dimensional analysis, assuming a one-scale-one-coupling scenario.

The following discussion of the main ingredients of CH models described above heavily relies on an extensive review by Panico and Wulzer [53]. The examples in the review focus on an $SO(5)/SO(4)$ model, the minimal incarnation of CH models that contains the electroweak (EW) gauge group and which delivers the Higgs as a pNGB and includes an unbroken custodial symmetry [63]. This will be adapted to the next-to minimal $SO(6)/SO(5)$ in Sec. 2.6, which yields an additional degree of freedom to encode a scalar singlet for baryogenesis.

2.5.1 The Goldstone-Boson Higgs: Vacuum Misalignment

The underlying mechanism of all CH models is vacuum misalignment. Let us assume a global symmetry $\mathcal{G}$, which is spontaneously broken to $\mathcal{H}_1$. The set of generators is chosen to be

$$T^A = \left\{ T^a, \hat{T}^r \right\} \tag{2.31}$$

with $A = 1, \dots \dim[\mathcal{G}]$, including the generators $\hat{T}^r, r = 1, \dots, \dim[\mathcal{G}/\mathcal{H}_1]$ of the non-linearly realized (for simplicity "broken") group and the generators $T^a, a = 1, \dots \dim[\mathcal{H}_1]$ of the linearly realized ("unbroken") group. Linearly realized means that the Lagrangian, after expanding around the ground state, is invariant under $\exp\{\imath\alpha_a T^a\}$ transformations of the fields. The $\mathcal{G}/\mathcal{H}_1$ symmetry is instead hidden – it is manifested in the invariance of the Lagrangian under a shift in the Goldstone

bosons (see, e.g., [53] for further details). It is therefore also called the *shift symmetry* and has to be broken if a Goldstone boson should acquire a potential.

Let Σ_0 now be a vacuum expectation value that induces the spontaneous symmetry breaking, i.e., is not invariant under linear transformations generated by $\hat{T}^r$:

$$T^a\Sigma_0 = 0, \qquad \hat{T}^r\Sigma_0 \neq 0. \tag{2.32}$$

Although the splitting between broken and unbroken generators is arbitrary, it is convenient to include the SM gauge group generators in the unbroken subgroup [53].

The Goldstone bosons $\Pi^r(x)$ are local transformations in the symmetry-broken directions. Using them, the general symmetry breaking vacuum can be obtained:

$$\begin{aligned}\Sigma(x) &= e^{i\frac{\sqrt{2}}{f}\Pi_r(x)\hat{T}^r}\Sigma_0 \\ &=: U\left[\Pi_r(x)\right]\Sigma_0,\end{aligned} \tag{2.33}$$

where $|\Sigma_0| = f$ is the Goldstone decay constant and U is called the *Goldstone matrix*.[11] If the global symmetry is exact, $\langle\Pi\rangle$ is arbitrary and can be set to zero. If the symmetry is explicitly broken, however, Π obtains a potential, from which its vev can be calculated by minimization. For $\langle\Pi\rangle \neq 0$, the vacuum is displaced from the original $\mathcal{H}_1$ conserving vacuum Σ_0, with $\langle\Pi\rangle/f$ being the displacement angle, c.f. Fig. 2.2 (left). One then needs to distinguish between the new $\langle\Sigma\rangle$, conserving $\mathcal{H}_1$ and the gauged symmetry group $\mathcal{H}_0 \supset \mathcal{G}_{\text{SM}}$, which before overlapped with $\mathcal{H}_1$, c.f. Fig. 2.2 (right). Thereby, the projection of the displaced SSB vacuum $\langle\Sigma\rangle$ onto $\mathcal{H}_0$ triggers electroweak symmetry breaking (EWSB) at a scale $v = f\sin\frac{\langle\Pi\rangle}{f}$. The electromagnetic $U(1)_{\text{em}}$ is then included in the unbroken group $\mathcal{H} = \mathcal{H}_0 \cap \mathcal{H}_1$. To suppress large corrections to SM predictions and as no massive composite resonances have been observed, a sizable gap between the two scales, generally expressed as $\xi_{\text{CH}} = \frac{v^2}{f^2} \ll 1$ is necessary. Although having no tuning at all ($\xi_{\text{CH}} \to 1$) would be preferred, the fine-tuning of $\xi_{\text{CH}} \approx 0.1$ necessary to fulfill current bounds is acceptable as opposed to the huge amount of tuning necessary in the SM, c.f. Subsec. 2.1.2.

Note that not all Goldstone bosons necessarily obtain a vev by explicit breaking. The remaining degrees of freedom can be rotated away by $\mathcal{H}_0$ gauge transformations, making the respective gauge bosons heavy.

In light of the discussion above, the conditions for a working CH model are the following [32]:

1. the SM gauge group has to be embeddable in the unbroken subgroup, $\mathcal{G}_{\text{SM}} \subset \mathcal{H}_1$

2. to realize the Higgs, at least one $SU(2)_L$ doublet needs to be included in $\mathcal{G}/\mathcal{H}_1$

Now that the general mechanism is clear, the Lagrangian may be constructed.

[11] Note that the factors in the exponential are due to normalization and not strictly necessary for the general discussion.

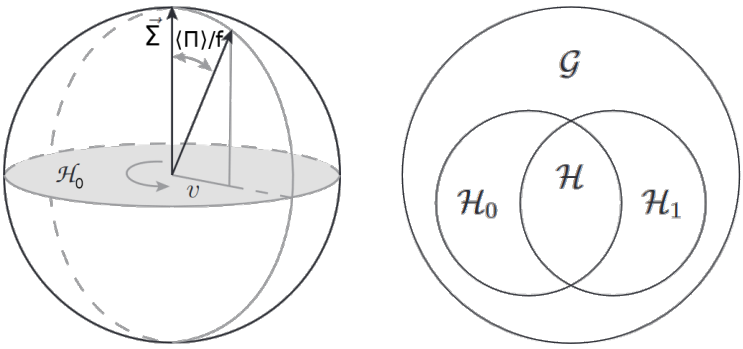

Figure 2.2: Left: Vacuum misalignment in an $SO(3)/SO(2)$ example, adapted from [53]. Right: The pattern of symmetry breaking in CH models [32]

2.5.2 CCWZ construction in general

Using the Callan-Coleman-Wess-Zumino framework [61, 62] one can write down the Lagrangian for any theory with a spontaneous symmetry breaking $\mathcal{G} \to \mathcal{H}$. Explicit symmetry breaking can then easily be incorporated using spurions. While the theory is quite extensive and can be looked up e.g., in [53], for this thesis only a small part is needed. The construction relies on the Goldstone matrix U transforming under $g \in \mathcal{G}$ as

$$U\left[\Pi\right] \to U\left[\Pi^{(g)}\right] = g \cdot U\left[\Pi\right] \cdot h^{-1}\left[\Pi; g\right] \tag{2.34}$$

where $h \in \mathcal{H}$.[12] Given that h leaves Σ_0 invariant, this is equivalent to a transformation $\Sigma \to g\Sigma$ under which the original Lagrangian is invariant. The original symmetry is not really broken, but rather encoded in the way the Π's transform, which is essentially described by (2.34). To obtain the $\mathcal{H}$-invariant Lagrangian with a $\mathcal{G}/\mathcal{H}$ shift symmetry in the Goldstone fields, one "dresses" $\mathcal{G}$-transforming objects with U to split them into $\mathcal{H}$-transforming parts and then use the latter to construct the Lagrangian. All terms in the SSB theory are thereby invariant under linear $\mathcal{H}$-transformations and invariant under the above transformation of the U matrix.

For the kinetic terms, e.g., one can use the decomposition of the Maurer-Cartan-form into

$$iU\left[\Pi\right]^{-1} \cdot \partial_\mu U\left[\Pi\right] = d_{\mu,r}\hat{T}^r + e_{\mu,a}T^a = d_\mu + e_\mu\,, \tag{2.35}$$

where d_μ transforms linearly under $\mathcal{H}$ and e_μ transforms like a gauge field. The first order Goldstone derivative term is then given by

$$\frac{f^2}{4}\mathrm{Tr}\left(d_\mu d^\mu\right)\,. \tag{2.36}$$

Especially interesting for this thesis is the generation of the potential by interactions with fermions. One can make use of this formalism by assuming the fermions to be full

[12] The explicit form depends on the commutation relation between generators, see e.g., [53].

multiplets of $\mathcal{G}$, the aforementioned spurions, and only in the end setting them to their original values. This will become clearer in Sec. 2.6, where the $SO(6)/SO(5)$ picture will be employed.

2.5.3 Partial Compositeness

In order to realize explicit breaking and realize fermion masses, the PC framework is employed, which features a linear mixing between SM and vector-like composite fermions $\Psi^{Q,T}$ below the compositeness scale Λ_c,

$$\mathcal{L}_{\text{PC}} = -m_Q \bar{\Psi}^Q \Psi^Q - m_T \bar{\Psi}^T \Psi^T - \frac{m_*}{g_*} a^Q y_L^Q \bar{Q}_L \Psi^Q - \frac{m_*}{g_*} a^t y_R^t \bar{t}_R \Psi^T + \text{h.c.}\,, \tag{2.37}$$

where Q_L, t_R are a stand-in for all quark flavors, g_* is the strong coupling constant of the composite sector and $y_{L,R}$ are the couplings at the cutoff scale Λ_{UV}. Arising from the composite sector confinement and not being protected by the Goldstone symmetry, the "partner" resonances have Dirac masses of scale $m_{Q,T} \approx m_* = g_* f < \Lambda_c$. The low energy Yukawa couplings in (2.37) are obtained by running the UV-coupling down to the mass resonance scale,

$$a^{Q,T}(m_*)\, y_{L,R} \approx y_{L,R} \left(\frac{m_*}{\Lambda_{\text{UV}}} \right)^{d_{L,R}-5/2}\,, \tag{2.38}$$

where $d_{L,R}$ stands for the mass dimension of fermionic operators above the compositeness scale which generate the resonances Ψ. In particular, these operators (and thereby resonances) can be different for different flavors, such that the same $\mathcal{O}(1)$ coupling $y_{L,R}$ at Λ_{UV} can evolve to different $a^{Q,t} y_{L,R}$ in the IR. More precisely, the $\mathcal{O}(1)$ coupling for the top quark can be obtained with a $d \approx 5/2$ operator and the other quarks smaller couplings with $d > 5/2$, thereby generating IR flavor hierarchies from the same initial coupling at high scales.

As the partner resonances fill complete multiplets of the global symmetry $\mathcal{G}$, to couple them formally $\mathcal{G}$-invariantly to the SM fermions, one needs to embed the latter into such multiplets, as will become clear in the next section. More importantly, the Lagrangian must be invariant under the SM gauge group, so the part of the resonances multiplets actually mixing with the SM fermions when they are set to their real values must feature the same quantum numbers as the latter (displayed in Tab. 2.1). When decomposing the resonance multiplet under the SM group, there will therefore be other particles of different quantum numbers present, too. The PC Lagrangian is then diagonalized and the physical fermions correspond to the massless eigenstates (before EWSB), which are mixtures of SM elementary and composite particles.

In this thesis, the resonances are only shown to motivate the PC scenario - as they are heavy in comparison to the Goldstone boson scale f at which the potential is calculated, they can be integrated out and a pure non-linear sigma model will be employed. How low-energy form factors are calculated from a PC setting is, e.g., shown in [64, 65].

2.6 The $SO(6)/SO(5)$ model

In this section, the ingredients for a next to minimal composite Higgs model $SO(6)/SO(5)$, which accounts for the additional singlet used to make electroweak baryogenesis possible are gathered. After specifying the framework of the theory, namely the generators and the Goldstone matrix, the various embeddings available to realize partial compositeness are introduced in Subsec. 2.6.1. This is followed by an example calculation of the scalar potential to leading order in spurions, reproducing the results of [66]. The whole section has been written as part of [15] and therefore sticks closely to it.

The composite Higgs Lagrangian below the compositeness structure Λ_c and after integrating out heavy resonances Ψ, ρ reads

$$\mathcal{L}_{\text{CH}} \supset \mathcal{L}_{\text{kin}}^{H,S} + \mathcal{L}_{\text{Yuk}} + \mathcal{L}_{\text{WZW}} - V(H,S), \tag{2.39}$$

where $\mathcal{L}_{\text{kin}}^{H,S}$ denotes the kinetic term for the scalars, $\mathcal{L}_{\text{Yuk}}$ contains the interaction between SM fermions and the light scalars arising from partial compositeness and $\mathcal{L}_{\text{WZW}}$ stands for Wess-Zumino-Witten (WZW) couplings of the singlet to gauge bosons, which will play no role in the following, where we only look at the top quark sector.[13]

In line with the previous section, a global symmetry $\mathcal{G} = SO(6)$ is introduced, which is spontaneously broken to $\mathcal{H}_1 = SO(5)$. As any Lie group $SO(N)$ has $N(N-1)/2$ generators, there will be $15 - 10 = 5$ generators of the "broken" symmetry group. The 15 generators of $SO(6)$ are denoted as $T^A = \{T^{\bar{A}}, \hat{T}_6^r\}$, with $T^{\bar{A}} = \{T_L^a, T_R^a, T_5^i\}$ being the 10 generators of $SO(5)$, where T_L^a, T_R^a correspond to the $SU(2)_L, SU(2)_R$ subgroups, respectively. On the other hand, $\hat{T}_6^r$ are the 5 broken generators of $SO(6)/SO(5)$, containing a $SU(2)_L \times SU(2)_R$ bi-doublet ($r = 1, \dots, 4$) and a singlet ($r = 5$). They can be written as [64, 67]

$$\begin{aligned}
\left[T_L^a\right]_{IJ} &= -\frac{\imath}{2}\left[\frac{1}{2}\epsilon^{abc}\left(\delta_{bI}\delta_{cJ} - \delta_{bJ}\delta_{cI}\right) + \left(\delta_{aI}\delta_{4J} - \delta_{aJ}\delta_{4I}\right)\right] \\
\left[T_R^a\right]_{IJ} &= -\frac{\imath}{2}\left[\frac{1}{2}\epsilon^{abc}\left(\delta_{bI}\delta_{cJ} - \delta_{bJ}\delta_{cI}\right) - \left(\delta_{aI}\delta_{4J} - \delta_{aJ}\delta_{4I}\right)\right] \\
\left[T_5^i\right]_{IJ} &= -\frac{\imath}{\sqrt{2}}\left(\delta_{iI}\delta_{5J} - \delta_{iJ}\delta_{5I}\right) \\
\left[\hat{T}_6^r\right]_{IJ} &= -\frac{\imath}{\sqrt{2}}\left(\delta_{rI}\delta_{6J} - \delta_{rJ}\delta_{6I}\right) ,
\end{aligned} \tag{2.40}$$

where $a = 1, 2, 3$, $i = 1, \dots, 4$, $r = 1, \dots, 5$ and $I, J = 1, \dots, 6$.

The Goldstone matrix, encoding the dynamics of the pNGBs, is defined as

$$U\left[\vec{\Pi}\right] = \exp\left(\imath\frac{\sqrt{2}}{f}\Pi_r\hat{T}_6^r\right) \tag{2.41}$$

[13] For a concise discussion of the WZW term, see, e.g., [47].

with Π_r the five Goldstone modes and $f = \Lambda_c/(4\pi)$ the pNGB decay constant. The Π-fields transform in the fundamental representation of $SO(5)$, as can be seen when performing a $h \in SO(5)$ rotation on the general symmetry breaking field

$$\begin{aligned} h\,\Sigma = h\,U\left[\vec{\Pi}\right]\begin{pmatrix} 0_{5\times1} \\ f \end{pmatrix} &= \begin{pmatrix} h_4 & 0 \\ 0 & 1 \end{pmatrix} f \begin{pmatrix} \sin\left(\frac{|\Pi|}{f}\right)\cdot\frac{\vec{\Pi}}{|\Pi|} \\ \cos\left(\frac{|\Pi|}{f}\right) \end{pmatrix} \\ &= U\left[h\,\Pi\right]\begin{pmatrix} 0_{4\times1} \\ f \end{pmatrix}, \end{aligned} \tag{2.42}$$

where $\vec{\Pi} = \left(\Pi_1, \Pi_2, \Pi_3, \Pi_4, \Pi_5\right)^T$, also see [53]. Using the generators T^a_L, an $SU(2)_L$ gauge transformation can be performed such that

$$\vec{\Pi} \overset{SU(2)_L}{\to} \left(0, 0, 0, \Pi_4, \Pi_5\right)^T, \tag{2.43}$$

where three Higgs degrees of freedom are eaten by the EW gauge bosons, making them massive. However, using this parametrization would lead to a rather involved kinetic term involving trigonometric functions of Π_4 and Π_5 so it is further redefined as [47, 64]

$$\frac{h}{f} = \frac{\Pi_4}{\sqrt{\Pi_4^2+\Pi_5^2}}\sin\frac{\sqrt{\Pi_4^2+\Pi_5^2}}{f}, \quad \frac{S}{f} = \frac{\Pi_5}{\sqrt{\Pi_4^2+\Pi_5^2}}\sin\frac{\sqrt{\Pi_4^2+\Pi_5^2}}{f} \tag{2.44}$$

which is hereafter referred to as unitary gauge. This leads to the Goldstone matrix

$$U = \begin{pmatrix} \mathbb{I}_{3\times3} & & \\ & 1-\frac{h^2}{f^2+f\sqrt{f^2-h^2-S^2}} & -\frac{hS}{f^2+f\sqrt{f^2-h^2-S^2}} & \frac{h}{f} \\ & -\frac{hS}{f^2+f\sqrt{f^2-h^2-S^2}} & 1-\frac{S^2}{f^2+f\sqrt{f^2-h^2-S^2}} & \frac{S}{f} \\ & -\frac{h}{f} & -\frac{S}{f} & \frac{1}{f}\sqrt{f^2-h^2-S^2} \end{pmatrix} \tag{2.45}$$

and the composite sector kinetic term from (2.36) [66]

$$\begin{aligned} \mathcal{L}^{H,S}_{\text{kin}} =& \frac{f^2}{4}Tr(d_\mu d^\mu) \\ =& (D_\mu H)^\dagger D^\mu H + \frac{1}{2}(\partial_\mu S)^2 + \frac{1}{2f^2}\left[\partial_\mu(H^\dagger H) + \frac{1}{2}\partial_\mu S^2\right]^2 + \mathcal{O}\left(\frac{1}{f^4}\right), \end{aligned} \tag{2.46}$$

where the pNGB Higgs was rewritten as a complex $SU(2)_L$ doublet with $H = \frac{1}{\sqrt{2}}(0,h)^T$ in unitary gauge.

2.6.1 Fermion Embeddings

Before the Yukawa terms and the potential can be constructed, the representations of $SO(6)$ the composite resonances transform in and the SM fermions have to be

lifted into need to be specified. This discussion concentrates on the top quark, which, being the heaviest quark, couples to the composite sector the most – an extension to all other quarks is possible, but their contributions are very small in comparison.

The righthanded (RH) top quark t_R, which is a $\mathbf{1}_{2/3}$ of $SU(2)_L \times U(1)_Y$, can simply be encoded as a singlet of $SO(6)$ – it may even be *fully composite* instead. Regardless of its nature as fully or partially composite, this choice would not break $SO(6)$ and the potential would need to arise from the lefthanded (LH) fermions $q_L = (t_L, b_L)$. A short overview of the higher representations is given here. The spinorial **4** is not considered in general, as it does not obey custodial symmetry for the $Z\bar{b}b$ couplings [45]. On the other hand, **10**-representations are neglected because they do not break the $SO(2)_S \subset SO(6)$ subgroup [45], which corresponds to the shift symmetry of the singlet S. They therefore fail to produce a singlet potential and would not give different contributions than $\mathbf{1}_R$ and $\mathbf{6}_L$, as will be seen below. In contrast, the **20** and **20′** representations do not yield valid SM quark embeddings at all. Therefore, combinations of $Q_L \in (\mathbf{6}, \mathbf{15}, \mathbf{20'})$ and $t_R \in (\mathbf{1}, \mathbf{6}, \mathbf{15}, \mathbf{20'})$ are considered [45, 64, 65]. Note that to reproduce the correct hypercharge Y of the SM quarks, an additional $U(1)_X$ symmetry with charge $X = 2/3$ has to be introduced.

The **6** decomposes under $SO(6) \times U(1)_X \to SO(5) \times U(1)_X \to SO(4) \times U(1)_X \to SU(2) \times U(1)_Y$ as

$$\begin{aligned}\mathbf{6}_{2/3} &\to \mathbf{5}_{2/3} \oplus \mathbf{1}_{2/3} \\ &\to \left[\mathbf{4}_{2/3} \oplus \mathbf{1}_{2/3}\right] \oplus \mathbf{1}_{2/3} \\ &\to \left[\left(\mathbf{2}_{7/6} \oplus \mathbf{2}_{1/6}\right) \oplus \mathbf{1}_{2/3}\right] \oplus \mathbf{1}_{2/3}.\end{aligned}$$

As there is only one $\mathbf{2}_{1/6}$, the Q_L embedding in $SO(6)$ is unique, while t_R resides in a superposition of the two $\mathbf{1}_{2/3}$, parameterized by the angle θ_{6R}:

$$\begin{aligned}Q_L^6 &= \frac{1}{\sqrt{2}} \begin{pmatrix} (Q_L^4)^T & 0 & 0 \end{pmatrix}^T , \\ t_R^6 &= \begin{pmatrix} 0 & 0 & 0 & 0 & t_R e^{\imath\phi_{6R}} \cos\theta_{6R} & t_R \sin\theta_{6R} \end{pmatrix}^T ,\end{aligned} \tag{2.47}$$

where $Q_L^4 = \begin{pmatrix} \imath b_L & b_L & \imath t_L & -t_L \end{pmatrix}^T$. It is already apparent that Q_L^6 is conserved under $SO(2)_S$ rotations of the lower two components, such that this embedding will not break the singlet shift symmetry and S stays a pure Goldstone boson. By applying $\hat{T}_6^5$ to t_R^6 it becomes clear that its structure is conserved for $\phi_{6R} = \pm\pi/2, \theta_{6R} = \pm\pi/4$, such that these choices do not generate a singlet potential either.

The **15** decomposes as

$$\begin{aligned}\mathbf{15}_{2/3} &\to \mathbf{10}_{2/3} \oplus \mathbf{5}_{2/3} \\ &\to \left[\mathbf{3}_{2/3} \oplus \mathbf{3'}_{2/3} \oplus \mathbf{4}_{2/3}\right] \oplus \left[\mathbf{4}_{2/3} \oplus \mathbf{1}_{2/3}\right] \\ &\to \left[\mathbf{3}_{2/3} \oplus \left(\mathbf{1}_{5/3} \oplus \mathbf{1}_{2/3} \oplus \mathbf{1}_{-1/3}\right) \oplus \left(\mathbf{2}_{7/6} \oplus \mathbf{2}_{1/6}\right)\right] \oplus \left[\left(\mathbf{2}_{7/6} \oplus \mathbf{2}_{1/6}\right) \oplus \mathbf{1}_{2/3}\right] .\end{aligned}$$

Thus, q_L can be embedded in the **10** (A) or the **5** (B) of $SO(5)$,

$$Q_L^{15_\mathrm{A}} = (Q_L^4)_j T_5^j , \quad Q_L^{15_\mathrm{B}} = \imath (Q_L^4)_j \hat{T}_6^j . \tag{2.48}$$

A general embedding would be given by

$$Q_L^{15} = \cos\theta_{15L} e^{\imath\phi_{15L}} Q_L^{15_{\rm A}} + \sin\theta_{15L} Q_L^{15_{\rm B}}\,, \tag{2.49}$$

however, since $\mathbf{15}_{\rm B}$ is heavily constrained by $Zb\bar{b}$ couplings[14] [64] it is (mostly) dropped below, corresponding to $\theta_{15L} = 0$. Similarly, the t_R can be embedded as

$$t_R^{15} = \cos\theta_{15R} e^{\imath\phi_{15R}} T_R^3 t_R + \sin\theta_{15R} \hat{T}_6^5 t_R. \tag{2.50}$$

While t_R^{15} is generally invariant under $SO(2)_S$ transformations, Q_L^{15} is only for $\theta_{15L} = \pm\pi/4$.

Finally, the $\mathbf{20}'$ decomposes as

$$\begin{aligned}
\mathbf{20}'_{2/3} &\to \mathbf{14}_{2/3} \oplus \mathbf{5}_{2/3} \oplus \mathbf{1}_{2/3} \\
&\to \left[\mathbf{9}_{2/3} \oplus \mathbf{4}_{2/3} \oplus \mathbf{1}_{2/3}\right] \oplus \left[\mathbf{4}_{2/3} \oplus \mathbf{1}_{2/3}\right] \oplus \mathbf{1}_{2/3} \\
&\to \left[\left(\mathbf{3}_{5/3} \oplus \mathbf{3}_{2/3} \oplus \mathbf{3}_{-1/3}\right) \oplus \left(\mathbf{2}_{7/6} \oplus \mathbf{2}_{1/6}\right) \oplus \mathbf{1}_{2/3}\right] \oplus \left[\left(\mathbf{2}_{7/6} \oplus \mathbf{2}_{1/6}\right) \oplus \mathbf{1}_{2/3}\right] \oplus \mathbf{1}_{2/3}\,,
\end{aligned}$$

and we can write $Q_L^{20'}$ as a superposition of the embeddings in a $\mathbf{14}$ (A) and a $\mathbf{5}$ (B) of $SO(5)$,

$$Q_L^{20'_{\rm A}} = \frac{1}{2}\begin{pmatrix} 0_{4\times4} & Q_L^4 & 0_{4\times1} \\ \left(Q_L^4\right)^T & 0 & 0 \\ 0_{1\times4} & 0 & 0 \end{pmatrix}, \quad Q_L^{20'_{\rm B}} = \frac{1}{2}\begin{pmatrix} 0_{4\times4} & 0_{4\times1} & Q_L^4 \\ 0_{1\times4} & 0 & 0 \\ \left(Q_L^4\right)^T & 0 & 0 \end{pmatrix}, \tag{2.51}$$

with a general realization given by

$$Q_L^{20'} = \cos\theta_{20L} e^{\imath\phi_{20L}} Q_L^{20'_{\rm A}} + \sin\theta_{20L} Q_L^{20'_{\rm B}}, \tag{2.52}$$

which is $SO(2)_S$-invariant for $\theta_{20L} = \pm\pi/4$. Finally, t_R can be embedded in a superposition of the $\mathbf{14}$ (A), $\mathbf{5}$ (B) and $\mathbf{1}$ (C) representations,

$$\begin{aligned}
t_R^{20'_{\rm A}} &= \frac{1}{2\sqrt{5}}\begin{pmatrix} -\mathbb{I}_{4\times4} t_R & 0_{4\times2} \\ 0_{2\times4} & 2(\mathbb{I}_{2\times2} + \sigma^3) t_R \end{pmatrix}, \quad t_R^{20'_{\rm B}} = \frac{1}{\sqrt{2}}\begin{pmatrix} 0_{4\times4} & 0_{4\times2} \\ 0_{2\times4} & \sigma^1 t_R \end{pmatrix}, \\
t_R^{20'_{\rm C}} &= \frac{1}{\sqrt{30}}\begin{pmatrix} -\mathbb{I}_{5\times5} t_R & 0_{5\times1} \\ 0_{1\times5} & 5 t_R \end{pmatrix},
\end{aligned} \tag{2.53}$$

where σ^a are the Pauli matrices, leading to

$$t_R^{20'} = \cos\theta_{20R1} e^{\imath\phi_{20R1}} t_R^{20'_A} + \sin\theta_{20R1}\cos\theta_{20R2} e^{\imath\phi_{20R2}} t_R^{20'_B} + \sin\theta_{20R1}\sin\theta_{20R2} t_R^{20'_C}. \tag{2.54}$$

[14] This is due to mixings of the SM b_L with $\mathbf{3}_{2/3}$ and $\mathbf{1}_{-1/3}$ composite resonances modifying the physical b_Ls weak isospin charge.

2.6.2 Example: LO Spurion Analysis in the $(20', 1)$ model

To illustrate the construction of the Yukawa terms and pNGB potential to leading order (LO) in spurions, this section deals with a $(\mathbf{20'}_L, \mathbf{1}_R)$ model as considered in [66]. For a comparison of the most important combinations of $(\mathbf{1})$, $\mathbf{6}$, $\mathbf{15}$, $\mathbf{20}$ to next-to-leading order (NLO) in spurions, see [45].[15] The aforementioned paper, as well as [7, 64, 65] concentrate on realizing EWSB by dynamical $\mathbb{Z}_2$ breaking at EW scale, which can be obtained at renormalizable ($D = 4$) order. This thesis aims to expand the analysis to include $D > 4$ terms, which arise dynamically when assuming a UV completion and unlock a parameter space usually overlooked. In particular, a large S^6 term is desired, which is crucial for the envisioned $\mathbb{Z}_2$ non-restoration at high temperatures, see [15] or Ch. 3 and will be subject of Ch. 4.

Choosing the Q_L in a $\mathbf{20'}$ of $SO(6)$ and a fully composite t_R singlet allows for a viable EWSB from LO in the PC expansion [66]. While the parametrization used here is different from the source, the analysis is consistent with it, as will be commented on later. The general embedding of Eq. (2.52) can be rewritten as

$$\begin{aligned} Q_L^{20'} &= \cos\theta_{20L} e^{\imath\phi_{20L}} Q_L^{20'_A} + \sin\theta_{20L} Q_L^{20'_B} \\ &= \Lambda_L^1 b_L + \Lambda_L^2 t_L = \Lambda_L^\alpha q_{L\alpha}\,, \end{aligned} \tag{2.55}$$

where, abbreviating $\mathfrak{c}_\theta \equiv \cos\theta_{20L}$ and $\mathfrak{s}_\theta \equiv \sin\theta_{20L}$,

$$\Lambda_L^1 = \frac{1}{2}\begin{pmatrix} & & & & \imath e^{\imath\phi_{20L}}\mathfrak{c}_\theta & \imath\mathfrak{s}_\theta \\ & 0_{4\times4} & & & e^{\imath\phi_{20L}}\mathfrak{c}_\theta & \mathfrak{s}_\theta \\ & & & & 0 & 0 \\ & & & & 0 & 0 \\ \imath e^{\imath\phi_{20L}}\mathfrak{c}_\theta & e^{\imath\phi_{20L}}\mathfrak{c}_\theta & 0 & 0 & & \\ \imath\mathfrak{s}_\theta & \mathfrak{s}_\theta & 0 & 0 & 0_{2\times2} & \end{pmatrix},$$

$$\Lambda_L^2 = \frac{1}{2}\begin{pmatrix} & & & & 0 & 0 \\ & 0_{4\times4} & & & 0 & 0 \\ & & & & \imath e^{\imath\phi_{20L}}\mathfrak{c}_\theta & \imath\mathfrak{s}_\theta \\ & & & & -e^{\imath\phi_{20L}}\mathfrak{c}_\theta & -\mathfrak{s}_\theta \\ 0 & 0 & \imath e^{\imath\phi_{20L}}\mathfrak{c}_\theta & -e^{\imath\phi_{20L}}\mathfrak{c}_\theta & & \\ 0 & 0 & \imath\mathfrak{s}_\theta & -\mathfrak{s}_\theta & 0_{2\times2} & \end{pmatrix}, \tag{2.56}$$

provide the $SO(6)$ embeddings of the left-handed bottom and top sector, respectively.

As motivated in Subsec. 2.5.3, partial compositeness is assumed for the coupling of the SM to the composite sector, i.e., the multiplets above are coupled linearly to composite fermion resonances $\Psi^{T,t}$. For the following discussion, and in particular for the construction of the pNGB Higgs potential, it is therefore useful to lift the SM fermions to (spurious) $SO(6)$ multiplets by assigning the embedding matrices' Λ_L^i transformation properties under the full $SO(6)$ global symmetry in an intermediate

[15] One needs to be careful when comparing the resulting potentials however, as a different basis of generators is used.

step, making them the spurions of $SO(6)$. This allows to construct the Lagrangian with the help of the spurions from symmetry principles, i.e., an $SO(6)$ symmetry explicitly broken only by setting the spurions back to their actual background values of (2.56) in the end. Moreover, it is convenient to construct the $SO(6)$ Lagrangian in terms of $SO(5)$ objects as per the CCWZ construction of Subsec. 2.5.2. Using the transformation properties of U in (2.34), the dressed embedding matrices can be written down as

$$(\Lambda_L'^{\alpha})_{66} = (U^T)_{6I}(U^T)_{6J}(\Lambda_L^{\alpha})^{IJ}\,, \tag{2.57}$$
$$(\Lambda_L'^{\alpha})_{a6} = (U^T)_{aI}(U^T)_{6J}(\Lambda_L^{\alpha})^{IJ}\,, \tag{2.58}$$
$$(\Lambda_L'^{\alpha})_{ab} = (U^T)_{aI}(U^T)_{bJ}(\Lambda_L^{\alpha})^{IJ}\,, \tag{2.59}$$

where $a, b = 1, \dots, 5$, obtaining $SO(5)$-singlets, fiveplets and **14**-plets[16]. The resonances can be split similarly. One can then build a formally $SO(5)$ and thus, by virtue of U, $SO(6)$-invariant Langrangian, only broken by the spurions acquiring their background values. The PC Lagrangian then reads [65]

$$\mathcal{L}_{\text{PC}} = -y_L f \left(a(\bar{\Psi}_R^{T\prime})^{66}(\Lambda_L'^{\alpha})_{66} + b(\bar{\Psi}_R^{T\prime})^{6a}(\Lambda_L'^{\alpha})_{a6} + c(\bar{\Psi}_R^{T\prime})^{ab}(\Lambda_L'^{\alpha})_{ba}\right) q_{L\alpha} + \text{h.c.}\,, \tag{2.60}$$

where a, b, c are $\mathcal{O}(1)$ numbers.

To arrive at the low energy Yukawa Lagrangian $\mathcal{L}_{\text{Yuk}}$, one could integrate out the resonances, yielding form factors, as considered e.g., in [64, 65]. Alternatively, as explained, one can just construct $SO(5)$ invariants from only the SM fields, spurions and the Goldstone matrix to obtain $\mathcal{L}_{\text{Yuk}}$, where the heavy field contributions are absorbed. The Yukawa Lagrangian then reads (up to $\mathcal{O}(1)$ proportionality factors that will drop out in (2.62) below)

$$\begin{aligned}
\mathcal{L}_{\text{Yukawa}} =& y_L f\, \bar{t}_R (\Lambda_L'^{\alpha})_{66} q_{L\alpha} + \text{h.c.} \\
=& y_L\, \bar{t}_R \frac{1}{f}\left(-h\sqrt{f^2 - h^2 - S^2}\sin\theta_{20\text{L}} + \imath h S \cos\theta_{20\text{L}}\right) t_L + \text{h.c.} \\
=& -\sqrt{2} y_L\, \bar{q}_L H^c t_R \sin\theta_{20\text{L}}\left(1 - \frac{|H|^2}{f^2} - \frac{S^2}{2f^2} + \mathcal{O}\left(\frac{1}{f^4}\right)\right) \\
& - \imath\sqrt{2} y_L \cos\theta_{20\text{L}} \frac{S}{f} \bar{q}_L H^c t_R + \text{h.c.}\,.
\end{aligned} \tag{2.61}$$

To make S a real, CP-odd scalar, guaranteeing a $\mathbb{Z}_2$-symmetric form of the potential and allowing for spontaneous CPV,[17] $\phi_{20\text{L}} = -\pi/2$ was chosen in the second row and in the last row, $H^c = \imath\sigma_2 H^* = \frac{1}{\sqrt{2}}(h, 0)^T$ in unitary gauge. One can then identify

[16] The bottom spurion singlet vanishes in this configuration, related to the bottom quark being still massless. To account for a bottom mass, the embedding $Q_L^{20'}$ would have to be modified, c.f. [53] or the appendix, which would however not change the analysis notably.

[17] Note that in all CH models here, we impose overall CP-invariance on the Lagrangian.

$y_t \equiv \sqrt{2} y_L \sin\theta_{20\mathrm{L}}$ as the (LO) SM top-Higgs coupling and $\epsilon_Q \equiv \cot\theta_{20\mathrm{L}}$ as the mixing parameter of the embedding, such that, in agreement with [66],

$$\mathcal{L}_{\text{Yukawa}} = \frac{y_t}{\sqrt{2}} \bar{t}_R \frac{1}{f} \left(-h\sqrt{f^2 - h^2 - S^2} + \imath \epsilon_Q h S \right) t_L + \text{h.c.}\,. \tag{2.62}$$

Summarizing the results so far in the latter parametrization (including the other terms of Eq. (2.39)) and generalizing them to three quark families ($i, j = 1, ..3$), the effective Lagrangian for the model at hand, up to $D = 6$ is obtained (see also [66]):

$$\begin{aligned} \mathcal{L}^{D\leq 6}_{(\mathbf{20}',\mathbf{1})} \supset & (D_\mu H)^\dagger D^\mu H + \frac{1}{2}(\partial_\mu S)^2 + \frac{1}{2f^2}\left[\partial_\mu |H|^2 + \frac{1}{2}\partial_\mu S^2\right]^2 \\ & - \sum_{q_R = u_R, d_R} (y_q)_{ij} \bar{q}^i_L H q^j_R \left(1 + i\epsilon^i_Q \frac{S}{f} - \frac{1}{f^2}(|H|^2 + S^2/2)\right) + \text{ h.c.} \\ & + \frac{S}{16\pi^2 f}\left[n_B B_{\mu\nu}\tilde{B}^{\mu\nu} + n_W W^{I\mu\nu}\tilde{W}^I_{\mu\nu} + n_G G^{a\mu\nu}\tilde{G}^a_{\mu\nu}\right] - V(H,S)\,, \end{aligned} \tag{2.63}$$

where $H \to H^c$ for $q_R = u_R$ in the second line. The first term in the last line corresponds to the WZW Lagragian, with the anomaly coefficients fixed by the coset (with $n_W = n_B, n_G = 0$ for $SO(6)/SO(5)$ [47]). These couplings supplement the SM-fermion loops mediating the same transitions, if coupled to S. We will now turn to the evaluation of the scalar potential $V(H, S)$.

Finally, the potential can be constructed, based on the fact that it has to be proportional to explicit $SO(6)$ breaking effects, parameterized by the spurions Λ^α_L. Therefore, as mentioned before, formally $SO(6)$-invariant terms consisting of the dressed spurions are constructed. Setting them to their background values of (2.56) will then lead to the actual scalar potential. Moreover, to ensure that the terms also respect the SM gauge group, an even number of spurions (saturating the SM index) is needed. Assuming a one-scale-one-coupling framework as described, e.g., in [53, 66, 68], the scaling of any potential term can be determined by dimensional analysis,

$$V \propto N_C \frac{m_*^4}{g_*^2}\left(\frac{\hbar g_*^2}{16\pi^2}\right)^{\#Loops}\left(\frac{y_{L,R}\Lambda}{g_*}\right)^{\#spurions}\left(\frac{h}{f}\right)^{\#h}\left(\frac{S}{f}\right)^{\#S}, \tag{2.64}$$

where $m_* = g_* f$ is the resonance mass scale, with g_* the coupling of the composite sector, and N_C counts the QCD color multiplicity.

The (one-loop) invariants at LO in y_L read (setting $\hbar = 1$)

$$c_{\mathrm{s}2}\frac{N_C m_*^4}{16\pi^2}\frac{y_L^2}{g_*^2}(\Lambda'^\alpha_L)_{66}(\Lambda'^{\alpha\dagger}_L)^{66} = c_{\mathrm{s}2}\frac{N_C g_*^2 y_L^2}{16\pi^2}\left(h^2\left(f^2 - h^2 - S^2\right)\mathfrak{s}_\theta^2 + h^2 S^2 \mathfrak{c}_\theta^2\right), \tag{2.65}$$

$$\begin{aligned} c_{\mathrm{f}2}\frac{N_C m_*^4}{16\pi^2}\frac{y_L^2}{g_*^2}(\Lambda'^\alpha_L)_{a6}(\Lambda'^{\alpha\dagger}_L)^{a6} = c_{\mathrm{f}2}\frac{N_C g_*^2 y_L^2}{16\pi^2}\Big(& f^4\mathfrak{s}_\theta^2 + \frac{f^2}{4}h^2(\mathfrak{c}_\theta^2 - 7\mathfrak{s}_\theta^2) + h^4\mathfrak{s}_\theta^2 \\ & - h^2 S^2(\mathfrak{c}_\theta^2 - \mathfrak{s}_\theta^2) + f^2 S^2(\mathfrak{c}_\theta^2 - \mathfrak{s}_\theta^2)\Big), \end{aligned}$$

where the parameters $c_i \sim \mathcal{O}(1)$ encode the high energy dynamics and a formulation easily comparable with the ϵ_Q parametrization used in Ref. [66] is chosen.[18] This results in the LO potential

$$\begin{aligned} V\left(h,S\right) =& \frac{N_C g_*^2 y_L^2}{16\pi^2}\left(h^2 f^2\left[c_{\mathrm{s}2}\mathfrak{s}_\theta^2 + \frac{c_{\mathrm{f}2}}{4}\left(\mathfrak{c}_\theta^2 - 7\mathfrak{s}_\theta^2\right)\right] - h^4\mathfrak{s}_\theta^2\left(c_{\mathrm{s}2} - c_{\mathrm{f}2}\right)\right. \\ &\left. + h^2 S^2\left[\left(c_{\mathrm{s}2} - c_{\mathrm{f}2}\right)\left(\mathfrak{c}_\theta^2 - \mathfrak{s}_\theta^2\right)\right] + S^2 f^2 c_{\mathrm{f}2}\left(\mathfrak{c}_\theta^2 - \mathfrak{s}_\theta^2\right)\right). \end{aligned} \tag{2.66}$$

In turn the Higgs mass and quartic coupling, respectively μ_h^2 and λ_h, can be identified, allowing for a replacement of the UV parameters c_i below by connecting them to physical values at low energies. Note that no quartic S interaction is induced at LO in the spurion expansion. Minimizing with respect to h and S yields the $T = 0$ vevs

$$\langle h\rangle \equiv v = \frac{f}{2\sqrt{2}}\sqrt{\frac{4\mathfrak{s}_\theta^2 c_{\mathrm{s}2} + c_{\mathrm{f}2}\left(\mathfrak{c}_\theta^2 - 7\mathfrak{s}_\theta^2\right)}{\mathfrak{s}_\theta^2\left(c_{\mathrm{s}2} - c_{\mathrm{f}2}\right)}} = \sqrt{\frac{-\mu_h^2}{\lambda_h}}, \quad \langle S\rangle = 0 \tag{2.67}$$

where v is written in terms of μ_h^2 and λ_h. Employing $|H| = h/\sqrt{2}$ (in unitary gauge) finally leads to

$$\begin{aligned} V(H,S) =& \mu_h^2\left|H\right|^2 + \lambda_h\left|H\right|^4 + \lambda_h f^2\left(1 - 2\frac{v^2}{f^2}\right)\left(\frac{\epsilon_Q^2 - 1}{\epsilon_Q^2 - 3}\right)S^2 \\ &- \frac{1}{2}(\epsilon_Q^2 - 1)\lambda_h\, S^2\left|H\right|^2 . \end{aligned} \tag{2.68}$$

Note that, having reverted to the ϵ_Q parametrization, the result agrees with the one of Ref. [66]. For $\epsilon_Q^2 = 1$, the singlet becomes an exact Goldstone boson, making it massless and not entering the scalar potential.

[18] Note that the 14-plet is not included as, due to U being unitary, it does not induce linearly independent terms.

3 $\mathbb{Z}_2$ Symmetry Non-restoration

In this chapter, the Higgs potential is extended with a scalar singlet featuring a discrete $\mathbb{Z}_2$-symmetry to allow for electroweak baryogenesis. To avoid the common intermediate $\mathbb{Z}_2$-symmetry breaking at electroweak scale, which leads to cancellation between patches of baryon and antibaryon surplus or potentially dangerous domain walls (see Sec. 2.3), spontaneous $\mathbb{Z}_2$ breaking at high temperatures is proposed instead. While such a SNR scenario with a one-step electroweak phase transition $(0, w) \to (v, 0)$ cannot be realized when truncating the potential at renormalizable $D = 4$ level, it can be achieved by minimally extending the potential with a $D = 6$ singlet sextic term S^6. The parameter space allowing for a strong first order phase transition in the SNR scenario is then explored by analyzing the minima obtained from the 1-loop high temperature expansion of the scalar potential. This work was published as part of [15] and is recapitulated here.

3.1 One-loop high temperature corrections to the Scalar Potential up to $D = 6$

The tree level potential of the proposed Higgs plus scalar singlet EFT is given by

$$\begin{aligned} V_0(h, S) &= \mu_h^2 H^2 + \lambda_h H^4 + \frac{\mu_S^2}{2} + \frac{\lambda_S}{4} S^4 + \lambda_{hS} H^2 S^2 + \frac{1}{\Lambda_{\text{NP}}} S^6 \\ &= \frac{\mu_h^2}{2} h^2 + \frac{\lambda_h}{4} h^4 + \frac{\mu_S^2}{2} S^2 + \frac{\lambda_S}{4} S^4 + \frac{\lambda_{hS}}{2} h^2 S^2 + \frac{1}{\Lambda_{\text{NP}}} S^6 , \end{aligned} \tag{3.1}$$

where $H = \frac{1}{\sqrt{2}} (\Pi_1 + \imath \Pi_2, h - \imath \Pi_3)^T$. In the second row, the three EW Goldstone degrees of freedom are set to $\Pi_{1,2,3} = 0$ in unitary gauge and h and S denote the background values of the Higgs and singlet, respectively. Note the discrete $\mathbb{Z}_2 : S \leftrightarrow -S$ symmetry, which can be spontaneously broken by the singlet. In this section, the singlet can be either CP-even or CP-odd. Using the tools of Sec. 2.4, for our theory the 1-loop high-temperature approximation then reads

$$V_{\text{1-loop}}^T(h, S) = \frac{1}{24} \sum_{i=h,S,\Pi,W,Z,\gamma} n_i m_i^2(h, S)\, T^2 + \frac{1}{48} n_t m_t^2(h, S)\, T^2 , \tag{3.2}$$

where we used (2.30). Here, the "degrees of freedom" are given by[1]

$$n_h = 1, n_S = 1, n_\Pi = 3, n_W = 2 \cdot 3, n_Z = 3, n_\gamma = 1, n_t = 12\,. \tag{3.3}$$

For our EFT, given that the S is not charged under the EW gauge group, the shifted mass matrix $m^2_{ij}(h,S) = -\partial_i\partial_j \mathcal{L}_0(h,S)$ involves

$$\begin{aligned}
m^2_{hh}(h,S) &= \mu_h^2 + 3\lambda_h h^2 + \lambda_{hS} S^2 \\
m^2_{hS}(h,S) &= \lambda_{hS} h S \\
m^2_{SS}(h,S) &= \mu_S^2 + 3\lambda_S S^2 + \frac{30}{\Lambda_{\rm NP}} S^4 + \lambda_{hS} h^2 \\
m^2_{\Pi}(h,S) &= \mu_h^2 + \lambda_h h^2 + \lambda_{hS} S^2 \\
m^2_{\Pi h}(h,S) &= m^2_{\Pi S} = 0 \\
m^2_{W}(h,S) &= \frac{g^2}{4} h^2 \\
m^2_{Z}(h,S) &= \frac{g^2 + g'^2}{4} h^2 \\
m^2_{\gamma}(h,S) &= 0 \\
m^2_{q}(h,S) &= \frac{y_q^2}{2} h^2\,.
\end{aligned}$$

The physical scalar masses are then obtained by diagonalization,

$$M^2_\varphi = \begin{pmatrix} m^2_{hh} & m^2_{hS} \\ m^2_{hS} & m^2_{SS} \end{pmatrix}, \qquad \det M^2_\varphi - m^2_\varphi \mathbb{I} = 0 \tag{3.4}$$

$$\Leftrightarrow m^2_{\varphi_\pm} = \frac{1}{2}\left(m^2_{hh} + m^2_{SS} \pm \sqrt{m^4_{hh} + m^4_{SS} - 2m^2_{hh} m^2_{SS} + 4m^4_{hS}} \right)\,. \tag{3.5}$$

As in the sum of the thermal potential, the squareroots cancel out and we furthermore assume the electroweak vaccuum to be $\mathbb{Z}_2$-restoring, $m_{hS} = 0$, and we do not need to concern ourselves with this step. We obtain

$$V^T_{\text{1-loop}}(h,S) = \frac{T^2}{2}(c_h h^2 + c_S S^2) + \frac{5T^2}{4\Lambda^2_{\rm NP}} S^4\,, \tag{3.6}$$

with

$$c_h = \frac{1}{48}\left(9g^2 + 3g'^2 + 12y_t^2 + 24\lambda_h + 4\lambda_{hS}\right), \quad c_S = \frac{\lambda_{hS}}{3} + \frac{\lambda_S}{4}\,, \tag{3.7}$$

[1]The reader wondering, why despite $n_{W,Z} = 3$ suggests that transverse and longitudinal polarizations of the EW gauge bosons are considered, the three Goldstone bosons are still handled as degrees of freedom, is referred to Appendix C of [50]. Moreover, they note that this identification of $n_{W,Z}$ with 3 polarization degrees of freedom is only accidentally true in some gauges (Landau and unitary) in the first place.

as in [15], such that

$$V_{\text{eff}}(h,S) = \frac{1}{2}\left(\mu_h^2 + T^2 c_h\right) h^2 + \frac{\lambda_h}{4}h^4 + \frac{1}{2}\left(\mu_S + c_S T^2\right) S^2 + \frac{1}{4}\left(\lambda_S + \frac{5T^2}{\Lambda_{\text{NP}}^2}\right) S^4 + \frac{\lambda_{hS}}{2}h^2 S^2 + \frac{1}{\Lambda_{\text{NP}}} S^6 \,. \tag{3.8}$$

3.2 Thermal History of the EFT

The following constraints necessary for $\mathbb{Z}_2$ non-restoration can already be deduced:

1. The coexistence of two degenerate minima $(0, w)$ and $(v, 0)$ at a critical temperature T_c is required. For the singlet minimum to exist, it must be stable in h-direction,

$$\partial_h^2 V\left(0, w(T_c), T_c\right) = \mu_h^2 + c_h T_c^2 + \lambda_{hS} w(T_c)^2 > 0 \,. \tag{3.9}$$

   On the other hand, for the Higgs minimum to exist, the origin must be unstable along the h-direction,

$$\partial_h^2 V\left(0, 0, T_c\right) = \mu_h^2 + c_h T_c^2 < 0 \,. \tag{3.10}$$

   Therefore, $\lambda_{hS} > 0$ is a necessary condition.

2. Given the above, to have $\mathbb{Z}_2$ symmetry broken at high temperatures, we then need

$$\mu_S^2 + c_S T^2 < 0 \,. \tag{3.11}$$

   at high temperatures, making $c_S < 0$ the sufficient condition (this is not strictly necessary if $\mu_S < 0$).

3. For $c_S = \frac{\lambda_{hS}}{3} + \frac{\lambda_S}{4} < 0$, we then need to impose $\lambda_S < 0$, or more concretely $\lambda_S < -\frac{4}{3}\lambda_{hS}$.

Note that $\lambda_S < 0$ would lead to the potential not being bounded from below if the EFT is truncated at a renormalizable $D = 4$ order, such that SNR at high temperatures cannot be realized there. Instead, one would need to impose $\mu_S < 0$, making a singlet vev at low temperatures a possibility - this scenario was explored in [69] but will not be discussed further here. To sum the constraints up,

$$\mu_h^2 < 0, \quad \lambda_h > 0, \quad \lambda_{hS} > 0, \quad c_S < 0 \Leftrightarrow \lambda_S < -\frac{4}{3}\lambda_{hS} \,, \tag{3.12}$$

where the last condition is only strict if $\mu_S > 0$ is enforced. We turn to the analytical features, namely the critical points of the theory. The origin $(0, 0)$ starts as a saddle

point and may transform into a maximum for low temperatures. The EW minimum[2] $(0, v)$ with

$$v^2(T) = -\frac{\mu_h^2 + c_h T^2}{\lambda_h} \tag{3.13}$$

appears as a local minimum as soon as $v^2(T)$ becomes positive, then evolving into the global minimum for $T < T_c$. In vanishing h direction, the extrema $(0, \pm w_+)$ and $(0, \pm w_-)$ with

$$w_\pm^2 = \frac{\Lambda_{\mathrm{NP}}^2}{12}\left(-\lambda_S - \frac{5T^2}{\Lambda_{\mathrm{NP}}^2} \pm \sqrt{\lambda_S^2 - \frac{24\mu_S^2}{\Lambda_{\mathrm{NP}}^2} + \frac{4T^2}{\Lambda_{\mathrm{NP}}^2}(\lambda_S - 2\lambda_{hS}) + \frac{25T^4}{\Lambda_{\mathrm{NP}}^4}}\right) \tag{3.14}$$

arise due to the S^6 term. The $\pm w_+$ vacua are the symmetry breaking global minima at high temperatures and evolve into local minima below T_c. At lower temperatures they may remain local minima or become a saddle point. To make sure the EWPhT finishes and the universe cannot remain in a metastable state, it will be imposed that there should be no minima apart from v at low temperatures. Given that the $\pm w_-$ vacua exist, they are either maxima or saddle points.

The initial condition of only populating the $+w_+$ vacuum in our scenario could emerge from a symmetry breaking at much higher temperatures, with inflation blowing up the corresponding bubble. The full universe would then be baryon symmetric, as an opposing local antibaryon excess would be generated in $-w_+$ patches. In contrast to $\mathbb{Z}_2$ symmetry breaking after inflation, this would not be as problematic, as our whole visible universe would be contained in one of the bubbles.

In mixed direction, there are four additional extrema $\pm(v_{b_+}, w_{b_+})$ and $\pm(v_{b_-}, w_{b_-})$ with

$$v_{b_\pm}^2 = v^2(T) - \frac{\lambda_{hS}}{\lambda_h} w_{b_\pm}^2 \tag{3.15}$$

$$w_{b_\pm}^2 = \frac{\Lambda_{\mathrm{NP}}^2}{12}\left(-\lambda_S + \frac{\lambda_{hS}^2}{\lambda_h} \pm \sqrt{\left(\lambda_S - \frac{\lambda_{hS}^2}{\lambda_h}\right)^2 - \frac{24}{\Lambda_{\mathrm{NP}}^2}\left(\mu_S^2 + c_S T^2 + \lambda_{hS} v^2(T)\right)}\right).$$

At temperatures where (v_{b_-}, w_{b_-}) is real, it is a saddle point and acts as barrier between the EW and $\mathbb{Z}_2$ breaking minima, enforcing a first order phase transition. The (v_{b_+}, w_{b_+}) becomes real and a local minimum when $(0, w_+)$ becomes a saddle point.

In addition to the above, the following constraints are placed on our envisioned thermal history for the numerical analysis:

1. The EWPhT $(0, w_+) \to (0, v)$ should be the only phase transition in our model.

[2]As all minima presented here are derived from their quadratic quantities, there will always be a negative partner, in this case $-v$. We will omit this and concentrate only on the "positive" values.

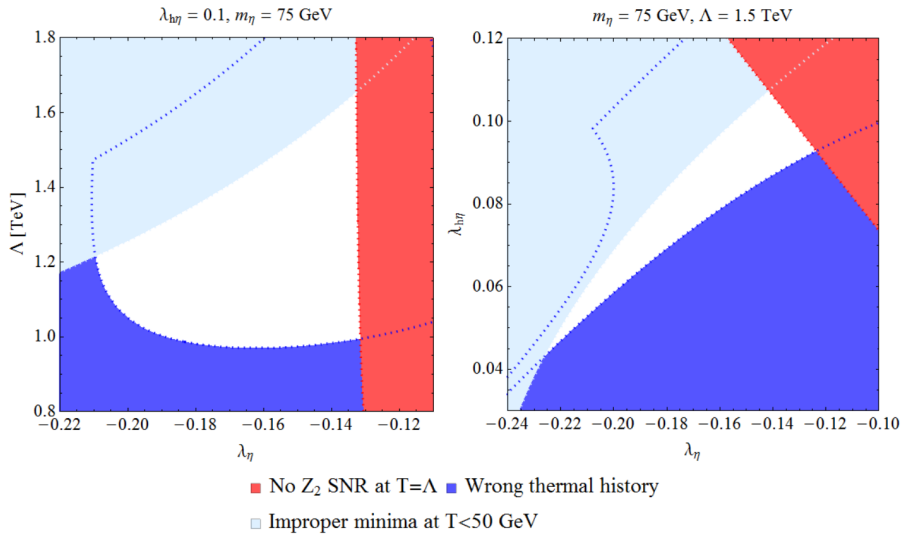

Figure 3.1: Visualization of the constraints we impose to safely achieve the sought thermal history, see the text. In both panels the singlet mass has been set to $m_S = 75\,\text{GeV}$, whereas in the left (right) panel $\lambda_{hS} = 0.1$ ($\Lambda_{\text{NP}} = 1.5\,\text{TeV}$) is fixed, and λ_S and Λ_{NP} (λ_S and λ_{hS}) are varied. This figure is taken from [15], with $\eta = S$ and $\Lambda = \Lambda_{\text{NP}}$.

2. To make sure the EWPhT completes[3], at low temperatures $T < 50\,\text{GeV}$ no minimum other than the EW vev should remain.

3. Invisible Higgs decay is tighly constrained by measurement [70, 71]. We therefore assume that the singlet is heavier than half the Higgs mass $m_S > m_h/2$, such that the dangerous $h \to SS$ channel is kinetically closed.[4]

Fig. 3.1 displays these constraints graphically for a benchmark point with $m_S = 75\,\text{GeV}$, where on the left (right), $\lambda_{hS} = 0.1$ ($\Lambda_{\text{NP}} = 1.5\,\text{TeV}$) is fixed, and λ_S and Λ_{NP} (λ_S and λ_{hS}) are varied. Most notably, the scale of new physics is bounded from above, promising impacts on experiments in the near future and reinforcing the crucial role of the $D = 6$ operator in our analysis. Next, $\Lambda_{\text{NP}} = 1.5\,\text{TeV}$ was fixed and a scan over the remaining three parameters was performed, enforcing the above constraints. Calculating T_c and evaluating the strength of the phase transition $\xi = v_c/T_c$ for each viable parameter point, the scatter plots in Fig. 3.2 were obtained. A strong first order phase transition with $\xi \gtrsim 1.3$ can be realized. It is apparent that relatively small (absolute) values of the quartic and portal couplings are preferred. Furthermore, the singlet is predicted to be rather light, $m_S < 85\,\text{GeV}$. Lastly, snapshots of the thermal evolution of the EFT potential for a benchmark point with $\lambda_S = -0.15, \lambda_{hS} = 0.1, \Lambda_{\text{NP}} = 1.5\,\text{TeV}$ and $m_S = 75\,\text{GeV}$ are given in

[3] In a numerical analysis, the bubble nucleation temperature could be calculated instead.

[4] As noted in [45], $m_S < m_h/2$ might be possible in principle but is not instrumental in a SFOEWPhT at tree level, as then $\lambda_{hS} \lesssim 0.01$.

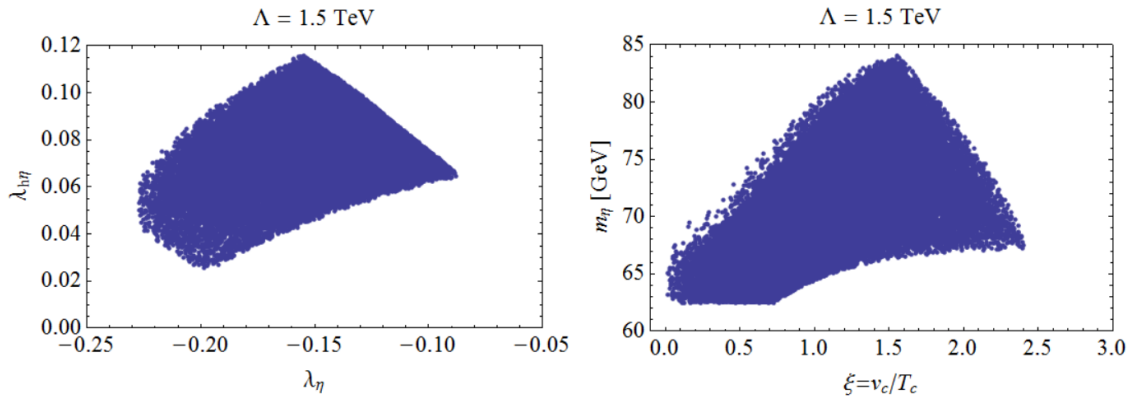

Figure 3.2: Scatter plots of the parameters for which the envisioned one-step (S)FOEWPhT occurs, assuming $\Lambda_{\rm NP} = 1.5\,\text{TeV}$. This figure is taken from [15], with $\eta = S$ and $\Lambda = \Lambda_{\rm NP}$.

Fig. 3.3. One can see how the universe starts in the $\mathbb{Z}_2$-breaking, EW symmetry conserving ω_+ vacuum at very high temperatures, the origin being a saddle point. As the plasma cools down, the EW minimum v starts to develop with the saddle point (v_{b_-}, w_{b_-}) acting as a potential barrier between the two minima. Once the critical temperature is reached, bubbles of v begin to nucleate. Below the critical temperature, the w_+ minimum turns into a saddle point and (v_{b_+}, w_{b_+}) emerges as a new minimum, before all minima except for the EW one disappear at low temperatures, as we imposed. There is a possibility that the (v_{b_+}, w_{b_+}) minimum arises before the EWPhT completes, leading to nucleation and collision of bubbles of this phase with the EW minimum, which will however not be discussed further.

Now that we have seen that we can obtain strong first order phase transitions in our $\mathbb{Z}_2$ nonrestoration scenario and explored the parameter space, we turn to constructing the potential from the composite Higgs model.

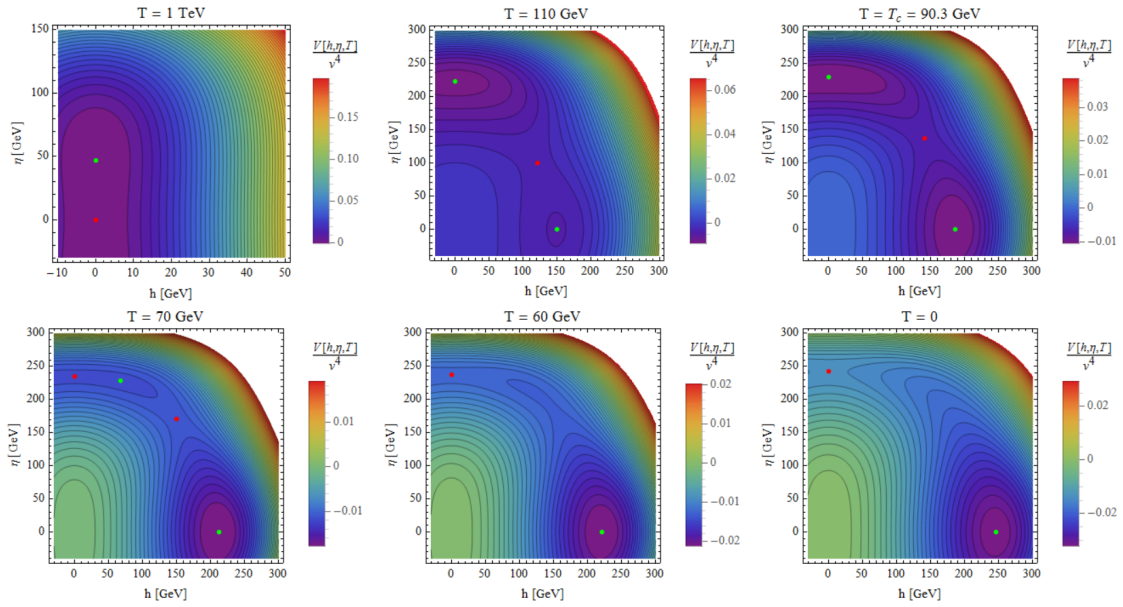

Figure 3.3: Thermal evolution of the EFT potential for a benchmark point with $\lambda_S = -0.15, \lambda_{hS} = 0.1, \Lambda_{\text{NP}} = 1.5\,\text{TeV}$ and $m_S = 75\,\text{GeV}$. The green dots denote local and global minima, whereas the red dots represent saddle points. This figure is taken from [15], with $\eta = S$ and $\Lambda = \Lambda_{\text{NP}}$.

4 $SO(6)/SO(5)$ Composite Higgs Potential for Different Fermion Embeddings

Given the fermion embeddings in Subsec. 2.6.1 and the framework presented in Subsec. 2.6.2, they can now be applied to calculate the Yukawa couplings and Higgs potential for all models combined from $Q_L \in (\mathbf{6}, \mathbf{15}, \mathbf{20'})$ and $t_R \in (\mathbf{1}, \mathbf{6}, \mathbf{15}, \mathbf{20'})$. Although other non-renormalizable terms may arise earlier, up to the first order in spurions which yields the S^6 term is considered, since the latter is crucial for realizing the SNR scenario. For a detailed explanation of how the specific embeddings are selected and the potential calculated, see the following sections. The reader only interested in the overview and discussion of the results may jump to Sec. 4.5. Finally, in Sec. 4.6, the most promising model will be matched to the EFT parameter space obtained in Sec. 3.2, finding that it readily fits the constraints to produce the correct baryon asymmetry.

4.1 Models with a singlet t_R

The scalar potential was already evaluated to LO in spurions for the $(\mathbf{20'}, \mathbf{1})$ model in Subsec. 2.6.2. Indeed, only this model provides a potential usable for EWBG for a singlet t_R. The singlet is a representation of $SO(6)$ anyway and cannot source a scalar potential. Meanwhile, the fermion embedding into the $\mathbf{6}_L$ in (2.47) only fills the upper four components of the $SO(6)$-fundamental, so a subgroup $SO(2)_S$ of rotations of the lower two components remains unbroken. This $SO(2)_S$-symmetry translates into the shift symmetry of the singlet S in the symmetry broken phase. An unbroken shift symmetry in turn preserves the Goldstone nature of the singlet such that no potential can be generated. We therefore cannot construct a potential from $\mathbf{6}_L$ alone and the EWPhT cannot be enhanced.

On the other hand, while the $\mathbf{15}_L$ does break the $SO(2)$ subgroup, its decomposition in (2.48) does not include an $SO(5)$ singlet. Accordingly, an $SO(5)$ invariant coupling between a lefthanded dressed spurion and the righthanded top is impossible and a SM top mass term of the form $\bar{t}_L h t_R$ cannot be generated.

Higher Order terms in the $(\mathbf{20'}_L, 1_R)$-Potential

To explore if a S^6 (and S^4) term can be obtained in the $(\mathbf{20'}_L, \mathbf{1}_R)$ model of Subsec. 2.6.2, in the following the invariants arising at higher order in spurion insertions

(i.e., higher order in y_L) will be inspected. At NLO and NNLO, in addition to naive powers of LO terms in (2.65), the new structures[1]

$$\begin{aligned}
&\tilde{c}_{\mathrm{f4}}\frac{N_C m_*^4}{16\pi^2}\,\frac{y_L^4}{g_*^4}(\Lambda_L'^{\alpha})_{a6}(\Lambda_L'^{\beta\dagger})^{a6}(\Lambda_L'^{\beta})_{b6}(\Lambda_L'^{\alpha\dagger})^{b6}\,,\\
&c_{\mathrm{sfsf}}\frac{N_C m_*^4}{16\pi^2}\,\frac{y_L^4}{g_*^4}(\Lambda_L'^{\alpha})_{66}(\Lambda_L'^{\beta\dagger})^{66}(\Lambda_L'^{\beta})_{b6}(\Lambda_L'^{\alpha\dagger})^{b6}\,,\\
&\tilde{c}_{\mathrm{f6}}\frac{N_C m_*^4}{16\pi^2}\,\frac{y_L^6}{g_*^6}(\Lambda_L'^{\alpha})_{a6}(\Lambda_L'^{\beta\dagger})^{a6}(\Lambda_L'^{\beta})_{b6}(\Lambda_L'^{\gamma\dagger})^{b6}(\Lambda_L'^{\gamma})_{c6}(\Lambda_L'^{\alpha\dagger})^{c6}\,,
\end{aligned}\tag{4.1}$$

as well as corresponding combinations need to be considered. For simplicity, only the leading contributions for each operator will be presented. The resulting potential reads

$$\begin{aligned}
\frac{16\pi^2}{N_C m_*^4}\,V[h,S] &= \tilde{\mu}_h h^2+\tilde{\mu}_S S^2+\tilde{\lambda}_{h4}h^4+\tilde{\lambda}_{h2S2}h^2S^2+\tilde{\lambda}_{S4}S^4\\
&\quad+\tilde{\lambda}_{h6}h^6+\tilde{\lambda}_{h4S2}h^4S^2+\tilde{\lambda}_{h2S4}h^2S^4+\tilde{\lambda}_{S6}S^6+\mathcal{O}((h,S)^8)
\end{aligned}\tag{4.2}$$

$$\begin{aligned}
\tilde{\mu}_h &= \frac{y_L^2}{g_*^2}\frac{1}{f^2}\left[\mathfrak{s}_\theta^2 c_{\mathrm{s2}}+\left(\mathfrak{c}_\theta^2-7\mathfrak{s}_\theta^2\right)\frac{c_{\mathrm{f2}}}{4}\right]\\
\tilde{\mu}_S &= \frac{y_L^2}{g_*^2}\frac{1}{f^2}\left(\mathfrak{c}_\theta^2-\mathfrak{s}_\theta^2\right)c_{\mathrm{f2}}\\
\tilde{\lambda}_{h4} &= -\frac{y_L^2}{g_*^2}\frac{1}{f^4}\mathfrak{s}_\theta^2\left(c_{\mathrm{s2}}-c_{\mathrm{f2}}\right)\\
\tilde{\lambda}_{h2S2} &= \frac{y_L^2}{g_*^2}\frac{1}{f^4}\left(\mathfrak{c}_\theta^2-\mathfrak{s}_\theta^2\right)\left(c_{\mathrm{s2}}-c_{\mathrm{f2}}\right)\\
\tilde{\lambda}_{S4} &= \frac{y_L^4}{g_*^4}\frac{1}{2f^4}\left(\mathfrak{c}_\theta^2-\mathfrak{s}_\theta^2\right)^2\left(2c_{\mathrm{f4}}+\tilde{c}_{\mathrm{f4}}\right)\\
\tilde{\lambda}_{h6} &= \frac{y_L^4}{g_*^4}\frac{1}{4f^6}\mathfrak{s}_\theta^2\Big[-8\mathfrak{s}_\theta^2 c_{\mathrm{s4}}-\left(\mathfrak{c}_\theta^2-11\mathfrak{s}_\theta^2\right)c_{\mathrm{s2f2}}\\
&\qquad+2\left(\mathfrak{c}_\theta^2-7\mathfrak{s}_\theta^2\right)c_{\mathrm{f4}}+2\left(\mathfrak{c}_\theta^2-5\mathfrak{s}_\theta\right)\tilde{c}_{\mathrm{f4}}-\left(\mathfrak{c}_\theta^2-9\mathfrak{s}_\theta\right)c_{\mathrm{sfsf}}\Big]\\
\tilde{\lambda}_{h4S2} &= \frac{y_L^4}{g_*^4}\frac{1}{4f^6}\left(\mathfrak{c}_\theta^2-\mathfrak{s}_\theta^2\right)\Big[8\mathfrak{s}_\theta^2 c_{\mathrm{s4}}+\left(\mathfrak{c}_\theta^2-15\mathfrak{s}_\theta^2\right)c_{\mathrm{s2f2}}\\
&\qquad-2\left(\mathfrak{c}_\theta^2-11\mathfrak{s}_\theta^2\right)c_{\mathrm{f4}}-2\left(\mathfrak{c}_\theta^2-7\mathfrak{s}_\theta^2\right)\tilde{c}_{\mathrm{f4}}+\left(\mathfrak{c}_\theta^2-11\mathfrak{s}_\theta^2\right)c_{\mathrm{sfsf}}\Big]\\
\tilde{\lambda}_{h2S4} &= \frac{y_L^4}{g_*^4}\frac{1}{2f^6}\left(\mathfrak{c}_\theta^2-\mathfrak{s}_\theta^2\right)^2\left(2c_{\mathrm{s2f2}}-4c_{\mathrm{f4}}-2\tilde{c}_{\mathrm{f4}}+c_{\mathrm{sfsf}}\right)\\
\tilde{\lambda}_{S6} &= \frac{y_L^6}{g_*^6}\frac{1}{4f^6}\left(\mathfrak{c}_\theta^2-\mathfrak{s}_\theta^2\right)^3\left(4c_{\mathrm{f6}}+2\tilde{c}_{\mathrm{f2f4}}+\tilde{c}_{\mathrm{f6}}\right)\,,
\end{aligned}$$

[1]The coefficients of terms with n powers of the singlet and m powers of the $SO(5)$-fundamental are denoted by a subscript snfm. For untilded coefficients, multiplets with adjacent indices are $SU(2)_L$-contracted, while tilded ones correspond to the other possible contraction.

extending the results of [66], where a form that allows for easy translation to the ϵ_Q parametrization of the reference is chosen. It is thus found that the S^4 and S^6 terms are indeed generated at orders $(y_L/g_*)^4$ and $(y_L/g_*)^6$, respectively. However, this significant suppression is in tension with a straightforward realization of the SNR scenario and in particular leads to a too large EFT suppression Λ_{NP}, see Sec. 4.6 below. Let us therefore turn to an exploration of the other embeddings to analyze if the suppression can get lifted. The results of this calculation are summarized again in Tab. 4.1, albeit formulated differently to be consistent with the following tables. Additionally, in the tables the coefficients are simply numbered, as the snfm notation would take up too much space.

4.2 Models with a t_R in a fundamental $\mathbf{6}_R$

The Yukawa terms for a fundamental embedding of the righthanded quark are given by

$$\begin{aligned}
\mathcal{L}_{\text{Yuk}}^{(6,6)} &= \frac{y_L y_R^*}{g_*} f \left(\bar{Q}_L'^6\right)_6 \left(t_R'^6\right)_6 M_1 + \text{h.c.} \qquad (4.3)\\
&= -\frac{y_L y_R^*}{\sqrt{2} g_* f} \bar{t}_L \left[h\sqrt{f^2 - h^2 - S^2}\mathfrak{s}_{\theta 6\text{R}} + e^{\imath\phi_{6R}} h S \mathfrak{c}_{\theta 6\text{R}}\right] M_1 t_R + \text{h.c.}\\
&\overset{\text{here}}{=} -\frac{y_L y_R^*}{\sqrt{2} g_* f} \bar{t}_L \left[h\sqrt{f^2 - h^2 - S^2}\mathfrak{s}_{\theta 6\text{R}} + \imath h S \mathfrak{c}_{\theta 6\text{R}}\right] M_1 t_R + \text{h.c.}\\
\mathcal{L}_{\text{Yuk}}^{(15,6)} &= \frac{y_L y_R^*}{g_*} f \left(\bar{Q}_L'^{15}\right)_{6a} \left(t_R'^6\right)_a M_5 + \text{h.c.} \qquad (4.4)\\
&= \frac{y_L y_R^*}{2 g_* f} \bar{t}_L h \left(\imath e^{\imath\phi_{6R} - \imath\phi_{15L}} \mathfrak{c}_{\theta 15\text{L}} \mathfrak{c}_{\theta 6\text{R}} + \mathfrak{s}_{\theta 15\text{L}} \mathfrak{s}_{\theta 6\text{R}}\right) M_5 t_R + \text{h.c.}\\
&\overset{\text{here}}{=} -\frac{y_L y_R^*}{2 g_* f} \bar{t}_L h \mathfrak{c}_{\theta 6\text{R}} M_5 t_R + \text{h.c.}\\
\mathcal{L}_{\text{Yuk}}^{(20',6)} &= \frac{y_L y_R^*}{g_*} f \left[\left(\bar{Q}_L'^{20'}\right)_{66} \left(t_R'^6\right)_6 M_1 + \left(\bar{Q}_L'^{20'}\right)_{6a} \left(t_R'^6\right)_a M_5\right] + \text{h.c.} \qquad (4.5)\\
&= \frac{y_L y_R^*}{2 g_* f^2} \bar{t}_L \Big[-f^2 h M_5 \left(e^{\imath\phi_{6R} - \imath\phi_{20L}} \mathfrak{c}_{\theta 20\text{L}} \mathfrak{c}_{\theta 6\text{R}} + \mathfrak{s}_{\theta 20\text{L}} \mathfrak{s}_{\theta 6\text{R}}\right)\\
&\qquad -2\left(M_1 - M_5\right)\Big(h S^2 e^{\imath\phi_{6R} - \imath\phi_{20L}} \mathfrak{c}_{\theta 20\text{L}} \mathfrak{c}_{\theta 6\text{R}}\\
&\qquad +h\left(f^2 - h^2 - S^2\right) \mathfrak{s}_{\theta 20\text{L}} \mathfrak{s}_{\theta 6\text{R}}\\
&\qquad +hS\sqrt{f^2 - h^2 - S^2} e^{-\imath\phi_{20L}} \mathfrak{c}_{\theta 20\text{L}} \mathfrak{s}_{\theta 6\text{R}}\\
&\qquad +hS\sqrt{f^2 - h^2 - S^2} e^{\imath\phi_{6R}} \mathfrak{s}_{\theta 20\text{L}} \mathfrak{c}_{\theta 6\text{R}}\Big)\Big] t_R + \text{h.c.}\\
&\overset{\text{here}}{=} \frac{y_L y_R^*}{2 g_* f^2} \bar{t}_L \Big[-f^2 h \mathfrak{c}_{\theta 6\text{R}} M_5 - 2 h S^2 \mathfrak{c}_{\theta 6\text{R}} \left(M_1 - M_5\right)\\
&\qquad +2\imath h S \sqrt{f^2 - h^2 - S^2} \mathfrak{s}_{\theta 6\text{R}} \left(M_1 - M_5\right)\Big] t_R + \text{h.c.}
\end{aligned}$$

where the dressed fermion multiplets are abbreviated as $(Q_L'^m)_{ij} = (\Lambda_L'^{m\alpha})_{ij}\, q_{L\alpha}$ with $i = 1, \ldots, 5\,\text{or}\,6$ and m denotes the $SO(6)$ representation (and similarly for the right-handed fermions). M_1, M_5 are the form factors associated to invariants from $SO(5)$ singlets and fiveplets. Fiveplets in the $(\mathbf{6}, \mathbf{6})$ do not play a role due to the unitarity of the U matrix. In each model, the respective third row enforces the specific embedding ϕ_i, θ_i we choose, as motivated below.

For the $(\mathbf{6}, \mathbf{6})$, as for almost all models below, a $D = 5$ term $\propto ihS$ arises naturally, giving us the chance to implement spontaneous CP-violation in an overall CP-invariant Lagrangian, c.f., Subsec. 2.3.1. We therefore assume a purely CP-odd singlet S by fixing $\phi_{6R} = \pm\pi/2$. If one would additionally fix $\theta_{6R} = \pm\pi/2$, the whole Lagrangian would feature a Z_2 symmetry, such that it can be a dark matter candidate [72]. However, CP-violation could then not be implemented in this model, as the h and hS^2 terms would have the same phase. A problem of the other naive limit of $\theta_{6R} = 0$ is that it would not yield a mass term for $\langle S \rangle = 0$, the EW vacuum at zero temperature is however assumed to be $(v, 0)$ in the SNR scenario (although a finite singlet vev at $T = 0$ is in principle not forbidden - this is e.g., explored in [69]). To sum it up, for both latter choices, a mass and a CP-violating term would not arise at the same time, whereas the needed singlet potential is not generated for $\theta_{6R} = \pi/4$. The embedding is therefore fixed to $\phi_{6R} = \pm\pi/2, \theta_{6R} \neq \{0, \pi/4, \pi/2\}$.[2]

The Yukawa Lagrangian of the general $(\mathbf{15}, \mathbf{6})$ depends only on h and constant quantities, so the complex phase of the term can be absorbed into the top quark – equivalently $\phi_{6R} - \phi_{15\mathrm{L}} = \pm\pi/2$ is chosen. As mentioned in Subsec. 2.6.1 already, a $\mathbf{15}$ contribution features corrections to the $Zb\bar{b}$ coupling, unless one chooses $\theta_{15L} = 0$ with $\langle S \rangle\,|_{T=0} = 0$ [64]. The angle is only displayed here to be sure that it does not generate the necessary CPV term. As it does not, this model is ruled out. Nonetheless, it is displayed in the table (in gray font) for $\theta_{15\mathrm{L}} = 0$, and $\phi_{6R} - \phi_{15L} = \pi/2$. When going to finite angles, one should steer clear of $\theta_{15L} = \pm\pi/4$, which does not break $SO(2)_S$ symmetry.

With the $\mathbf{20'}_L$, spontaneous CP-violation arises when fixing $\phi_{20L} = \pm\pi/2, \phi_{6R} = \pm\pi/2$. Again, we can already rule out the combination $\theta_{6R} = \pm\pi/4, \theta_{20L} \pm \pi/4$ which conserves $SO(2)_S$. This representation features similar $Zb\bar{b}$ modifications as the $\mathbf{15}_L$ above [65], such that $\theta_{20L} = 0$ is fixed, from which $\theta_{6R} \neq \{0, \pi/2\}$ follows directly to ensure a non-zero top mass and spontaneous CPV. The hierarchies in the potential may change when going to finite angles, as discussed in Sec. 4.5.

In none of the models above or below, explicit CP-violation for a otherwise purely CP-odd or -even scalar arises, as the phases of h and hS terms are always equal. Only spontaneous CPV will be considered hereafter.

In the following, the non-trivial invariants for the models will be written down, as in contrast to the $(\mathbf{20'}, \mathbf{1})$, mixed terms $\propto y_L^n y_R^m$ have to be considered, too. The SM Yukawa coupling y_t, as well as the Higgs mass and quartic coupling can be recovered in analogy to Subsec. 2.6.2.

[2]Note that all sign choices of ϕ_i are not relevant for the potential and can be absorbed into the scalar.

Invariants contributing to the 6_R-Potentials

The **6**-representations decompose into fiveplets and singlets of $SO(5)$. Only structures that cannot be inferred from powers of already displayed terms are listed. All leading contributions to the terms of (4.2) are summarized in Tab. 4.2.

6 invariants: The only relevant $\mathbf{6}_L$ and $\mathbf{6}_R$ invariants to n-th order in spurions are given by

$$(\Lambda_L^{\alpha\prime})_6(\Lambda_L^{\alpha\prime\dagger})^6, \quad (\Lambda_R^{\prime})_6(\Lambda_R^{\prime\dagger})^6 \tag{4.6}$$

and their powers, calculated in analogy to (2.65) and omitting the dimension factor, as well as the $\mathcal{O}(1)$ constant c. As a result of the unitarity of the Goldstone matrix U, any bilinear of the dressed spurion fiveplets can be rewritten, e.g.

$$\begin{aligned}(\Lambda_L^{\alpha\prime})_a(\Lambda_L^{\beta\prime\dagger})^b &= (U^T)_{aI}(\Lambda_L^{\alpha\prime})^I U^{bJ}(\Lambda_L^{\beta\prime\dagger})_J \\ &= (\Lambda_L^{\alpha\prime})^I(\Lambda_L^{\beta\prime\dagger})_J\left[\delta_I^J - (U^T)_{6I}U^{6J}\right] = |\Lambda|^2 - (\Lambda_L^{\alpha\prime})_6(\Lambda_L^{\alpha\prime\dagger})^6\,,\end{aligned} \tag{4.7}$$

where the fact that Λ^1 and Λ^2 are orthogonal to each other was used. As $|\Lambda|^2$ is not dependent on the Goldstone bosons, it can be handled as constant. The contribution of such a term will therefore always be subleading or expressed by a singlet bilinear already. Fiveplet invariants can therefore be omitted.

$\mathbf{15}_L$ invariants: This representation only decomposes into a **5** and **10**. With a calculation analogous to (4.7), **10**-plet terms can be omitted and only fiveplet terms, analogous to those of the $\mathbf{20'}_L$, displayed in (2.65) and (4.1), contribute. No LH-RH-mixed invariants except for products of LO (with NLO) invariants have to be considered. This is motivated as follows: possible additional invariants would be given by cross-contracting fiveplet $\mathbf{15}_L$ and fiveplet $\mathbf{6}_R$ spurions. Using (4.7), such an invariant could be always written as a sum of a term already present at LO (NLO), suppressed by an additional power of $(y_R/g_*)^2$, and a term already given at the same spurion order by LO $\times$ LO (LO $\times$ NLO) invariants. Therefore, all invariants of this type would be subleading, solely due to the fact that $\mathbf{6}_R$ fiveplet bilinears can always be written in terms of singlet ones.

$\mathbf{20'}_L$ invariants: There are dressed spurions in a $\mathbf{1}, \mathbf{5}$ and $\mathbf{14}$ of $SO(5)$, where in analogy to the discussion below (4.7), the latter are omitted due to the unitarity of the Goldstone matrix. The pure LH terms were already given in (2.65) and (4.1). As in the $(\mathbf{15}, \mathbf{6})$, no LH-RH cross-contracted invariants can be constructed.

4.3 Models with a t_R in an asymmetric $\mathbf{15}_R$

The $\mathbf{15}_R$ embedding by itself does not break the $SO(2)$ symmetry. Therefore the $(\mathbf{6},\mathbf{15})$ model will not be considered. The remaining Yukawa terms read

$$\begin{aligned}
\mathcal{L}_{\text{Yuk}}^{(15,15)} &= \frac{y_L y_R^*}{g_*} f \left(\bar{Q}_L'^{15}\right)_{6a} \left(t_R'^{15}\right)_{a6} M_5 + \text{h.c.} \qquad (4.8)\\
&= \frac{y_L y_R^*}{4 g_* f} \bar{t}_L \Big[h\sqrt{f^2-h^2-S^2}\left(\mathfrak{c}_{\theta 15\text{L}}\mathfrak{s}_{\theta 15\text{L}} + \sqrt{2}e^{\imath\phi_{15\text{R}}-\imath\phi_{15\text{L}}}\mathfrak{c}_{\theta 15\text{L}}\mathfrak{s}_{\theta 15\text{R}}\right)\\
&\qquad +\imath h S\left(e^{-\imath\phi_{15\text{L}}}\mathfrak{c}_{\theta 15\text{L}}\mathfrak{c}_{\theta 15\text{R}} + \sqrt{2}e^{\imath\phi_{15\text{R}}}\mathfrak{s}_{\theta 15\text{L}}\mathfrak{s}_{\theta 15\text{R}}\right)\Big] M_5 t_R + \text{h.c.}\\
&\overset{here}{=} \frac{y_L y_R^*}{4 g_* f} \bar{t}_L \left[\sqrt{2} h\sqrt{f^2-h^2-S^2}\mathfrak{s}_{\theta 15\text{R}} + \imath h S \mathfrak{c}_{\theta 15\text{R}}\right] M_5 t_R + \text{h.c.}\\
\mathcal{L}_{\text{Yuk}}^{(20',15)} &= \frac{y_L y_R^*}{g_*} f \left(\bar{Q}_L'^{20'}\right)_{6a} \left(t_R'^{15}\right)_{a6} M_5 + \text{h.c.} \qquad (4.9)\\
&= \frac{y_L y_R^*}{4 g_* f} \bar{t}_L \Big[h\sqrt{f^2-h^2-S^2}\left(\mathfrak{s}_{\theta 20\text{L}}\mathfrak{c}_{\theta 15\text{R}} + \imath e^{\imath\phi_{15\text{R}}-\imath\phi_{20\text{L}}}\sqrt{2}\mathfrak{c}_{\theta 20\text{L}}\mathfrak{s}_{\theta 15\text{R}}\right)\\
&\qquad +h S\left(e^{-\imath\phi_{20\text{L}}}\mathfrak{c}_{\theta 20\text{L}}\mathfrak{c}_{\theta 15\text{R}} - \imath e^{\imath\phi_{15\text{R}}}\sqrt{2}\mathfrak{s}_{\theta 20\text{L}}\mathfrak{s}_{\theta 15\text{R}}\right)\Big] M_5 t_R + \text{h.c.}\\
&\overset{here}{=} \frac{y_L y_R^*}{4 g_* f} \bar{t}_L \left[h\sqrt{f^2-h^2-S^2}\mathfrak{s}_{\theta 15\text{R}} - \imath h S \mathfrak{c}_{\theta 15\text{R}}\right] M_5 t_R + \text{h.c.}\,.
\end{aligned}$$

To ensure a CP-odd scalar, the phases are fixed to $\phi_{15\text{L}} = \phi_{15\text{R}} = 0\,(\phi_{15\text{R}} = 0, \phi_{20L} = \pm\pi/2)$. As before, $\theta_{15(20)\text{L}} = 0$ and $\langle S\rangle\,|_{T=0} = 0$ are fixed to prevent $Zb\bar{b}$ contributions. It follows that to generate nonvanishing mass terms at zero temperature and CPV terms, one must take care that $\theta_{15\text{R}} \neq \{0, \pi/2\}$. Apart from the $Zb\bar{b}$-constraint, going to finite angles is reasonable, as long as $\theta_{15(20)L} \neq \pi/4$, for which the singlet potential vanishes.

A $D = 6$ explicitly CP violating term is not viable for both models. The invariants can be constructed in analogy to Sec. 4.2 and are summarized to leading contributions in Tab. 4.3.

Mixed invariants: The non-trivial mixed invariants for the $(\mathbf{15}(\mathbf{20}),\mathbf{15})$ are given by

$$\text{NLO: } (\Lambda_L'^{\alpha})_{6a}(\Lambda_R'^{\dagger})^{a6}(\Lambda_R')_{6b}(\Lambda_L'^{\alpha\dagger})^{b6} + \text{h.c.}\,, \qquad (4.10)$$

$$\text{NNLO: } (\Lambda_L'^{\alpha})_{6a}(\Lambda_L'^{\beta\dagger})^{a6}(\Lambda_L'^{\beta})_{6b}(\Lambda_R'^{\dagger})^{b6}(\Lambda_R')_{6c}(\Lambda_L'^{\alpha\dagger})^{c6} + \text{h.c.}\,. \qquad (4.11)$$

Note that no cross-contracted terms can arise for righthanded spurions.

4.4 Models with a t_R in a symmetric $\mathbf{20'}_R$

The Yukawa Lagrangians for a t_R in a symmetric $\mathbf{20'}_R$ are displayed below.

$$
\begin{aligned}
\mathcal{L}_{\text{Yuk}}^{(6,20')} &= \frac{y_L y_R^*}{g_*} f \left[(\bar{Q}_L'^6)_6 (t_R'^{20'})_{66} M_1 + (\bar{Q}_L'^6)_a (t_R'^{20'})_{a6} M_5 \right] + \text{h.c.} \qquad (4.12)\\
&= \frac{y_L y_R^*}{g_* f^2} \bar{t}_L \Bigg[- f^2 h \Big\{ \left(\frac{1}{2\sqrt{10}} e^{\imath \phi_{20R1}} \mathfrak{c}_{\theta 20\text{R}1} + \sqrt{\frac{3}{5}} \mathfrak{s}_{\theta 20\text{R}1} \mathfrak{s}_{\theta 20\text{R}2} \right) M_5 \\
&\qquad\qquad - \frac{\sqrt{15}}{6} \mathfrak{s}_{\theta 20\text{R}1} \mathfrak{s}_{\theta 20\text{R}2} M_1 \Big\} \\
&\qquad + hS\sqrt{f^2 - h^2 - S^2} e^{\imath \phi_{20R2}} \mathfrak{c}_{\theta 20\text{R}2} \mathfrak{s}_{\theta 20\text{R}1} (M_5 - M_1) \\
&\qquad + \frac{hS^2 \left(\sqrt{2} e^{\imath \phi_{20R1}} \mathfrak{c}_{\theta 20\text{R}1} - \sqrt{3} \mathfrak{s}_{\theta 20\text{R}1} \mathfrak{s}_{\theta 20\text{R}2} \right)}{\sqrt{5}} (M_5 - M_1) \\
&\qquad - \frac{h^3 \left(\sqrt{2} e^{\imath \phi_{20R1}} \mathfrak{c}_{\theta 20\text{R}1} + 4\sqrt{3} \mathfrak{s}_{\theta 20\text{R}1} \mathfrak{s}_{\theta 20\text{R}2} \right)}{4\sqrt{5}} (M_5 - M_1) \Bigg] t_R \\
&\qquad + \text{h.c.} \\
&\overset{here}{=} - \frac{y_L y_R^*}{g_* f^2} \bar{t}_L \Bigg[f^2 h \frac{\cos(\theta_{20R1})}{2\sqrt{10}} M_5 \\
&\qquad\qquad + \imath \cdot hS\sqrt{f^2 - h^2 - S^2} \mathfrak{s}_{\theta 20\text{R}1} (M_5 - M_1) \\
&\qquad\qquad + \left(\sqrt{\frac{2}{5}} hS^3 - \frac{1}{2\sqrt{10}} h^3 \right) \mathfrak{c}_{\theta 20\text{R}1} (M_5 - M_1) \Bigg] + \text{h.c.} \\
\mathcal{L}_{\text{Yuk}}^{(15,20')} &= \frac{y_L y_R^*}{g_*} f (\bar{Q}_L'^{15'})_{6a} (t_R'^{20'})_{a6} M_5 + \text{h.c.} \qquad (4.13)\\
&= \frac{y_L y_R^*}{4 g_* f} \bar{t}_L \imath e^{-\imath \phi_{15\text{L}}} \Bigg[\sqrt{2} h e^{\imath \phi_{20R2}} \mathfrak{s}_{\theta 20\text{R}1} \mathfrak{c}_{\theta 20\text{R}2} \sqrt{f^2 - h^2 - S^2} \\
&\qquad\qquad + \sqrt{5} hS e^{\imath \phi_{20R1}} \mathfrak{c}_{\theta 20\text{R}1} \Bigg] M_5 t_R + \text{h.c.} \\
&\overset{here}{=} - \frac{y_L y_R^*}{4 g_* f} \bar{t}_L \left[h\sqrt{f^2 - h^2 - S^2} \sqrt{2} \mathfrak{s}_{\theta 20\text{R}1} + \imath hS\sqrt{5} \mathfrak{c}_{\theta 20\text{R}1} \right] t_R M_5 + \text{h.c.}
\end{aligned}
$$

$$\mathcal{L}_{\rm Yuk}^{(20',20')} = \frac{y_L y_R^*}{g_*} f\left[(\bar{Q}_L'^{20'})_{66}(t_R'^{20'})_{66}M_1 + (\bar{Q}_L'^{20'})_{6a}(t_R'^{20'})_{a6}M_5\right] + \text{h.c.} \tag{4.14}$$

$$\begin{aligned}
&= \frac{y_L y_R^*}{g_* f^3}\bar{t}_L e^{\imath\phi_{20\rm L}}\Bigg[- f^2 h\sqrt{f^2-h^2-S^2}e^{\imath\phi_{20\rm R2}}\frac{\mathfrak{s}_{\theta 20\rm R1}\mathfrak{c}_{\theta 20\rm R2}M_5}{2\sqrt{2}} \\
&\qquad - f^2 hS\frac{2\sqrt{6}\mathfrak{s}_{\theta 20\rm R1}\mathfrak{s}_{\theta 20\rm R2}(5M_1-6M_5) + 9e^{\imath\phi_{20\rm R1}}\mathfrak{c}_{\theta 20\rm R1}M_5}{12\sqrt{5}} \\
&\qquad - hS^2\sqrt{f^2-h^2-S^2}e^{\imath\phi_{20\rm R2}}\sqrt{2}\mathfrak{c}_{\theta 20\rm R2}\mathfrak{s}_{\theta 20\rm R1}(M_1-M_5) \\
&\qquad - hS^3\frac{-\sqrt{6}\mathfrak{s}_{\theta 20\rm R1}\mathfrak{s}_{\theta 20\rm R2} + 2e^{\imath\phi_{20\rm R1}}\mathfrak{c}_{\theta 20\rm R1}}{\sqrt{5}}(M_1-M_5) \\
&\qquad + h^3 S\frac{2\sqrt{6}\mathfrak{s}_{\theta 20\rm R1}\mathfrak{s}_{\theta 20\rm R2} + e^{\imath\phi_{20\rm R1}}\mathfrak{c}_{\theta 20\rm R1}}{2\sqrt{5}}(M_1-M_5)\Bigg]t_R + \text{h.c.} \\
&\overset{here}{=} \frac{y_L y_R^*}{g_* f^3}\bar{t}_L\Bigg[- f^2 h\sqrt{f^2-h^2-S^2}\frac{\mathfrak{s}_{\theta 20\rm R1}M_5}{2\sqrt{2}} - \imath f^2 hS\frac{3\mathfrak{c}_{\theta 20\rm R1}M_5}{4\sqrt{5}} \\
&\qquad - hS^2\sqrt{f^2-h^2-S^2}\sqrt{2}\mathfrak{s}_{\theta 20\rm R1}(M_1-M_5) \\
&\qquad + \frac{\imath}{2\sqrt{5}}\left(h^3 S - 4hS^3\right)\mathfrak{c}_{\theta 20\rm R1}(M_1-M_5)\Bigg]t_R + \text{h.c.}\,.
\end{aligned}$$

In the $(\mathbf{20'},\mathbf{20'})$, to avoid the contribution to $Zb\bar{b}$ coupling, $\theta_{20\rm L}=0$ and $\langle S\rangle|_{T=0}=0$ is assumed. To generate the top mass, $\theta_{20R1}\neq 0$ and $\theta_{20R2}\neq\pi/2$, i.e. a $\mathbf{20'}_{{\rm B}R}$ contribution is then needed. For spontaneous CPV, $\theta_{20R2}=0$ ($\mathbf{20'}_{{\rm AB}R}$ model) with $\phi_{20\rm R1}=\pm\pi/2, \phi_{20\rm R2}=0$, or $\theta_{20R1}=\pi/2$ ($\mathbf{20'}_{{\rm BC}R}$ model) with $\phi_{20\rm R1}=\pm\pi/2, \phi_{20\rm R2}=\pm\pi/2$ needs to be fixed. On the other hand, for a general ($\mathbf{20'}_{{\rm ABC}R}$) model, only a CP-even scalar could retain overall CP conservation and a $\mathbb{Z}_2$ symmetry of the potential would need to be imposed. Otherwise, the scalar explicitly breaks CP invariance.

Similarly, in the $(\mathbf{15},\mathbf{20'})$, where $\theta_{20\rm L}=0$ is already fixed, $\theta_{20\rm R1}\neq\{0,\pi/2\}, \theta_{20\rm R2}\neq\pi/2$ (AB-contribution) is needed to obtain both a top mass and spontaneous CPV term. Meanwhile, a $\mathbf{20'}_{{\rm C}R}$-contribution does not add any structure to the Lagrangian. Therefore, the embeddings are fixed to $\phi_{20\rm R1}-\phi_{15\rm L}=\pm\pi/2, \phi_{20\rm R2}-\phi_{15\rm L}=0$ and $\theta_{20\rm R2}=0$ but going back to a general model is entirely reasonable.

For the $(\mathbf{6},\mathbf{20'})$, with $\phi_{20\rm R1}=0$ and $\phi_{20\rm R2}=\pm\pi/2$ a general model is viable. In addition, both a $\mathbf{20'}_{{\rm AB}R}$ and a $\mathbf{20'}_{{\rm BC}R}$ would work equally fine.

All models above will therefore be restricted to $\theta_{20R2}=0$ in Tab. 4.4. Going to nonzero angles does not change the hierarchy of terms for any of the $\mathbf{20'}_R$ models, but it changes their correlations in a significant way, as we will see in the next section.

Mixed invariants: In addition to those of last section, the $(\mathbf{20},\mathbf{20})$ features the invariant

$$\text{NLO: } (\Lambda_L'^{\alpha})_{66}(\Lambda_R'^{\dagger})^{66}(\Lambda_R')_{6a}(\Lambda_L'^{\alpha\dagger})^{a6} + \text{h.c.}\,. \tag{4.15}$$

4.5 Scalar Potential for Various Fermion Embeddings

In this section we will compare the potentials for various fermion embeddings, aiming to carve out differences in the hierarchies of couplings and analyzing their usefulness with regard to the $\mathbb{Z}_2$ non-restoration scenario of Ch. 3.

In Tab. 4.1–4.4 we provide an overview of the spurion-order ($y_{L,R}^n$) at which the different terms in the potential appear for various viable combinations of q_L and t_R embeddings. We already analyzed the Yukawa terms and the embeddings in detail in Sec. 4.1–4.4. To recapitulate the constraints we imposed :

1. A non-zero top mass term $h\bar{t}_L t_R$ should arise in $\mathcal{L}_{\text{Yuk}}$.

2. Only embeddings featuring no explicit CP-breaking, i.e., that only generate even powers of the pseudoscalar S in the potential are taken into account. To fulfill the second Sakharov criterion, a term of the form $\imath S h\bar{t}\gamma^5 t$ should arise in $\mathcal{L}_{\text{Yuk}}$ to induce spontaneous CP-violation instead, as described in Subsec. 2.3.1.[3] In combination with the last point, this fixes the phases ϕ_i and rules out some combination of angles θ_i. In particular, whenever an angle is displayed in the tables, it needs to be $\theta_i \neq \{0, \pi/2\}$.

3. A singlet potential $V(S) \neq 0$ should arise, ruling out combinations of $Q_L \in \{\mathbf{6}, \mathbf{15}\,\text{with}\,\theta_{15L} = \pi/4, \mathbf{20}\,\text{with}\,\theta_{20L} = \pi/4\}$ with $t_R \in \{\mathbf{1}, \mathbf{6}\,\text{with}\,\theta_{6R} = \pi/4, \mathbf{15}\}$ that do not break the singlet shift symmetry, see Subsec. 2.6.1.

Furthermore, to minimize corrections to $Zb\bar{b}$, we restrict ourselves to $\mathbf{15}(\mathbf{20})_{\text{A}L}$ ($\theta_{15(20)L} = 0$) and assume $\langle S\rangle|_{T=0} = 0$ (c.f. [64, 65]).

Note that wherever we display only a limit $\theta_{L,R} = 0$, going to finite values of the angle does not change the hierarchy of the terms, except for the $(\mathbf{20'}_L, \mathbf{6}_R)$ and $(\mathbf{20'}_L, \mathbf{15}_R)$, see below, and the above cases of vanishing S-potential. Finally, we will assess whether the respective models fit the SNR scenario of Section 3.

Let us start in Tab. 4.1 with the models where the t_R is realized as a composite singlet. Here, only Q_L in a $\mathbf{20'}_L$ yields a viable setup. For the $\mathbf{6}_L$, no singlet potential is generated as the embedding does not break the singlet shift symmetry, whereas for the $\mathbf{15}_L$ the top quark remains massless. For the $(\mathbf{20'}_L, \mathbf{1}_R)$ model, as discussed before, the singlet sextic (quartic) interaction is generated at order $(y_L/g_*)^6$ ($(y_L/g_*)^4$), making it challenging to realize the $\mathbb{Z}_2$ SNR scenario with natural $\mathcal{O}(1)$ dimensionless coefficients, as shown in the next section. Finally, note that both

[3] As also noted there, in the EFT of Ch. 3, the necessary CP-violation could be injected via a $\mathbb{Z}_2$ conserving ($D=6$) $\imath S^2 h\bar{t}\gamma^5 t$ operator. The term does not arise in any of the CH models considered - the $D=5$ term is however obtainable in all of them. The latter is therefore chosen, such that the CH model features only a (spontaneously broken) CP symmetry and no additional $\mathbb{Z}_2$ (in the Yukawa Lagrangian). Nonetheless, regarding the discussed thermal evolution both setups are equivalent.

the renormalizable scalar portal and the pure ($D \leq 4$) Higgs terms arise at LO in spurions, whereas the scalar quartic only arises at NLO.

Next, consider the models with a $\mathbf{6}_R$ embedding in Tab. 4.2. Despite the fact that no CPV inducing term arises for $(\mathbf{15}_L, \mathbf{6}_R)$, we still display the model (in gray font). When going to finite angles $\theta_{20L} \neq 0$ in the $(\mathbf{20'}_L, \mathbf{6}_R)$ model despite the $Zb\bar{b}$ constraint, the hierarchies change to fit the $(\mathbf{20'}_L, \mathbf{1}_R)$ model: the Higgs sextic (quartic) interaction is generated at $(y_L/g_*)^4$ ($(y_L/g_*)^2$) – the purely left-handed invariants dictate the leading contributions to these terms. As mentioned above, for $\theta_{6R} = \pi/4$ and $\theta_{20L} = \pi/4$, the singlet becomes a true Goldstone boson in both the $(\mathbf{20'}_L, \mathbf{6}_R)$ model and the $(\mathbf{6}_L, \mathbf{6}_R)$. For all other cases, as before, the S^n terms arise at the nth order in spurions. On the other hand, besides for the $(\mathbf{20'}_L, \mathbf{6}_R)$, the renormalizable portal emerges only at NLO in spurions. More importantly – with the exception of $(\mathbf{20'}_L, \mathbf{6}_R)$ with $\theta_{20L} \neq 0$ –, the Higgs quartic coupling always emerges only at NLO in spurions. Both the Higgs portal and quartic couplings are thus generically suppressed, whereas the Higgs mass term arises at LO. Especially the latter hierarchy leads to a higher fine-tuning of the model, see, e.g., [73–75].[4]

The models with a $\mathbf{15}_R$ are displayed in Tab. 4.3. While the $(\mathbf{6}_L, \mathbf{15}_R)$ in general does not generate a singlet potential, for the other two models, this is only the case when going to $\theta_{15(20)\mathrm{L}} = \pi/4$, which is not advised anyway (see above). Once more, the S^4 (S^6) terms arise only at NLO (NNLO) in spurions, while for the $(\mathbf{20'}_L, \mathbf{15}_R)$ the Higgs mass and quartic coupling can arise at the same order when going to finite angle $\theta_{20\mathrm{L}} \neq 0$.

Finally, let us move on to the $\mathbf{20'}_R$ models displayed in Tab. 4.4, which will turn out to be the most interesting for the SNR scenario. Out of all the models, the one that fits the sought-for hierarchies and coupling constraints of Sec. 3.2 best is the $(\mathbf{20'}_{\mathrm{A}L}, \mathbf{20'}_R)$. Here, while we need a $\mathbf{20'}_{\mathrm{B}R}$ contribution to generate the top mass, determined by $y_t \propto y_L y_R^* \sin\theta_{20R1}$, and $\mathbf{20'}_{\mathrm{A}R}$ *or* $\mathbf{20'}_{\mathrm{C}R}$ to generate the CPV-inducing operator, a general (ABC) model would only admit a CP-even scalar without CPV terms, or a CP-mixed scalar.

In the $(\mathbf{15}_{\mathrm{A}L}, \mathbf{20'}_{\mathrm{AB}R})$ setup, only a $\mathbf{20'}_{\mathrm{AB}}$ fulfills the conditions and a $\mathbf{20'}_{\mathrm{C}}$ admixture would not change anything, whereas for the $(\mathbf{6}_L, \mathbf{20'}_R)$, both $\mathbf{20'}_{\mathrm{AB}R}$ and $\mathbf{20'}_{\mathrm{BC}R}$ would work equally fine again. Therefore, we display only $\theta_{20R2} = 0$ models in the table. Note that here, the $\mathbf{6}_L$ and $\mathbf{15}_{\mathrm{A}L}$ models predict opposite signs for the h^4 and h^2S^2 terms and thus do not fulfill the conditions for the $\mathbb{Z}_2$ SNR scenario, c.f., (3.12).

This can be remedied by allowing nonzero θ_{R2}, where we can fulfill the constraints on signs and magnitude of the couplings for points within $\theta_{20R2} \in (0.70, 1.50) \cup (1.64, 2.45)$ for $\theta_{20R1} \in (1.11, 1.50) \cup (1.11, 1.50) + \pi$ and $\theta_{20R2} \in (0.70, 1.50) + \pi \cup$

[4] Consider the constraints on the tuning parameter $\xi_{\mathrm{CH}} = v^2/f^2 \lesssim 0.1$ when matching to the EFT parameters, where $v = -\mu_h^2/(2\lambda_h)$. If both Higgs mass and quartic terms emerge at LO, the ratio is given by $v^2/f^2 = c_\mu/(4c_\lambda)$, where c_μ and c_λ are the cumulative of the contributions to h^2 and h^4 as they would be displayed in the table. A tuning of $\xi_{\mathrm{CH}} \lesssim 0.1$ can then be obtained with $\mathcal{O}(1)$ coefficients. In contrast, if the quartic term emerges at NLO instead, λ_h would be additionally suppressed and $v^2/f^2 = c_\mu/(4c_\lambda) \cdot (g_*/y_{L,R})^2$. Assuming $g_* = 4$ or higher, this can only be achieved with $O(10)$ or larger coefficients, reintroducing fine-tuning.

$(1.64, 2.45)+\pi$ for $\theta_{20R1} \in (0.70, 1.11) \cup (0.70, 1.11)+\pi$. These intervals were obtained by respectively solving the set of inequalities in (3.12) for one of the angles θ_{Ri} while scanning over the other angle $\theta_{Rj\neq i}$.

Coming back to our model of choice, the $(\mathbf{20'}_{AL}, \mathbf{20'}_{\mathrm{AB}R})$, we can easily create the sought-out pattern of couplings to realize the $\mathbb{Z}_2$ SNR scenario, where the S^6 (S^4) terms arise already at NLO (LO) in spurions, which allows for non-negligible contributions. Also, the fact that the quartic Higgs coupling arises at LO in spurions is interesting regarding the naturalness of the setup. (Only for $\theta_{20\mathrm{R}1} = \pi/2$, which does not concern us, arises the quartic at NLO.) We will provide a more quantitative evaluation of this model in the next section.

Finally, Tab. 4.5 shows a compact overview of the order at which each term is generated.

Table 4.1: $V(h,S)$ terms obtained via spurion analysis for t_R a $SO(6)$ singlet. Only leading terms are shown and each entry should be multiplied by $N_c m_*^4/16\pi^2$, while every h or S comes with a factor $1/f$ and every $y_{L,R}$ with a $1/g_*$. The coefficients c_i of the various invariants are just numbered consecutively. Parameters that contribute in the same way in the given approximation were collected into single c_i and we abbreviate $\mathfrak{c}_{2\theta} = \cos 2\theta_{20\mathrm{L}}$, $\mathfrak{s}_\theta^2 = \sin^2\theta_{20\mathrm{L}}$.

		$\mathbf{1}_R$
$\mathbf{6}_L$	h^2 h^4 h^6 S^2 S^4 S^6 h^2S^2 h^2S^4 h^4S^2	No S-potential
$\mathbf{15}_{\mathrm{A}\,L}$	h^2 h^4 h^6 S^2 S^4 S^6 h^2S^2 h^2S^4 h^4S^2	No top mass
$\mathbf{20}'_L$	h^2	$y_L^2\left(\mathfrak{s}_\theta^2 c_1 + \frac{1}{4}\left(4\mathfrak{c}_{2\theta} - 3\right)c_2\right)$
	h^4	$-y_L^2\mathfrak{s}_\theta^2\left(c_1 - c_2\right)$
	h^6	$\frac{1}{4}y_L^4\mathfrak{s}_\theta^2\left(-c_4 + 2c_5 + 2c_6 - c_7 - 2\mathfrak{s}_\theta^2\left(4c_3 - 6c_4 + 8c_5 + 6c_6 - 5c_7\right)\right)$
	S^2	$y_L^2\mathfrak{c}_{2\theta}\,c_2$
	S^4	$\frac{1}{2}y_L^4\mathfrak{c}_{2\theta}{}^2\left(2c_5 + c_6\right)$
	S^6	$\frac{1}{4}y_L^6\mathfrak{c}_{2\theta}{}^3 4c_8$
	h^2S^2	$y_L^2\mathfrak{c}_{2\theta}\,\left(c_1 - c_2\right)$
	h^2S^4	$-\frac{1}{2}y_L^4\mathfrak{c}_{2\theta}{}^2\left(-2c_4 + 4c_5 + 2c_6 - c_7\right)$
	h^4S^2	$\frac{1}{4}y_L^4\mathfrak{c}_{2\theta}\,\left(4\mathfrak{s}_\theta^2\left(2c_3 - 4c_4 + 6c_5 + 4c_6 - 3c_7\right) - \left(-c_4 + 2c_5 + 2c_6 - c_7\right)\right)$

Table 4.2: $V(h,S)$ terms obtained via our spurion analysis for t_R in a $SO(6)$ sextuplet. Only leading terms are shown and each entry should be multiplied by $N_c m_*^4/16\pi^2$, while every h or S comes with a factor $1/f$ and every $y_{L,R}$ with a $1/g_*$. The $\mathbf{15}_L$ model does not generate a CPV-inducing term and is thus displayed in gray. Parameters that contribute in the same way in the given approximation were collected into single c_i and we abbreviate $\mathfrak{c}_{2\theta} = \cos 2\theta_{6\mathrm{R}}$ and $\mathfrak{s}_\theta^2 = \sin^2\theta_{6\mathrm{R}}$, while the other angle is set to zero, respectively. As discussed in the text, going to finite values of the displayed angle changes the hierarchy of terms for the $\mathbf{20'}_L$ model.

		$\mathbf{6}_R$
$\mathbf{6}_L$	h^2	$\frac{1}{2}y_L^2 c_1 - y_R^2\mathfrak{s}_\theta^2 c_2$
	h^4	$\frac{1}{4}y_L^4 c_4 - \frac{1}{2}y_L^2 y_R^2\mathfrak{s}_\theta^2(-2c_3) + y_R^4\mathfrak{s}_\theta^4 c_5$
	h^6	$\frac{1}{8}\left(y_L^6 c_8 - 2y_L^4 y_R^2\mathfrak{s}_\theta^2 c_6 + 4y_L^2 y_R^4\mathfrak{s}_\theta^4 c_7 - 8y_R^6\mathfrak{s}_\theta^6 c_9\right)$
	S^2	$y_R^2\mathfrak{c}_{2\theta}\, c_2$
	S^4	$y_R^4\mathfrak{c}_{2\theta}{}^2 c_5$
	S^6	$y_R^6\mathfrak{c}_{2\theta}{}^3 c_9$
	h^2S^2	$\frac{1}{2}y_R^2\mathfrak{c}_{2\theta}\left(-2y_L^2 c_3 - 4y_R^2\mathfrak{s}_\theta^2 c_5\right)$
	h^2S^4	$\frac{1}{2}y_R^4\mathfrak{c}_{2\theta}{}^2\left(y_L^2 c_7 - 6y_R^2\mathfrak{s}_\theta^2 c_9\right)$
	h^4S^2	$\frac{1}{4}y_R^2\mathfrak{c}_{2\theta}\left(y_L^4 c_6 - 4y_L^2 y_R^2\mathfrak{s}_\theta^2 c_7 + 12y_R^4\mathfrak{s}_\theta^4 c_9\right)$
$\mathbf{15}_{\mathrm{A}L}$	h^2	$\frac{1}{4}y_L^2 c_1 - y_R^2\mathfrak{s}_\theta^2 c_2$
	h^4	$\frac{1}{16}y_L^4\left(c_4 + c_5\right) - \frac{1}{4}y_L^2 y_R^2\mathfrak{s}_\theta^2 c_3 + y_R^4\mathfrak{s}_\theta^4 c_6$
	h^6	$\frac{1}{64}h^6\left(16c_9 y_L^2 y_R^4\mathfrak{s}_\theta^4 - 4\left(c_7+c_8\right)y_L^4 y_R^2\mathfrak{s}_\theta^2 + \left(c_{10}+c_{11}-8c_{12}\right)y_L^6 - 64c_{13}y_R^6\mathfrak{s}_\theta^6\right)$
	S^2	$y_L^2 c_1 + y_R^2\mathfrak{c}_{2\theta}\, c_2$
	S^4	$y_L^2 y_R^2\mathfrak{c}_{2\theta}\, c_3 + \frac{1}{2}y_L^4\left(2c_4+c_5\right) + y_R^4\mathfrak{c}_{2\theta}{}^2 c_6$
	S^6	$\frac{1}{2}\left(y_L^4 y_R^2\mathfrak{c}_{2\theta}\left(2c_7+c_8\right) + y_L^2 y_R^4(\mathfrak{c}_{4\theta}+1)c_9 + y_L^6\left(2c_{10}+c_{11}\right) + 2y_R^6\mathfrak{c}_{2\theta}{}^3 c_{13}\right)$
	h^2S^2	$\frac{1}{4}y_L^4\left(2c_4+c_5\right) + \frac{1}{4}y_L^2 y_R^2(3\mathfrak{c}_{2\theta}-2)c_3 - 2y_R^4\mathfrak{s}_\theta^2\mathfrak{c}_{2\theta}\, c_6$
	h^2S^4	$\frac{1}{8}\left(2y_L^4 y_R^2(2\mathfrak{c}_{2\theta}-1)\left(2c_7+c_8\right) + 2y_L^2 y_R^4\mathfrak{c}_{2\theta}\left(5\mathfrak{c}_{2\theta}-4\right)c_9 + 3y_L^6\left(2c_{10}+c_{11}\right) - 24y_R^6\mathfrak{s}_\theta^2\mathfrak{c}_{2\theta}{}^2 c_{13}\right)$
	h^4S^2	$\frac{1}{16}\left(y_L^4 y_R^2\left(c_7(5\mathfrak{c}_{2\theta}-4)c_7 + (3\mathfrak{c}_{2\theta}-2)c_8\right) + 8y_L^2 y_R^4\mathfrak{s}_\theta^2(1-2\mathfrak{c}_{2\theta})c_9 + y_L^6\left(3c_{10}+2c_{11}\right) + 48y_R^6\mathfrak{s}_\theta^4\mathfrak{c}_{2\theta}\, c_{13}\right)$
$\mathbf{20'}_{\mathrm{A}L}$	h^2	$y_L^2\frac{1}{4}c_2 - y_R^2\mathfrak{s}_\theta^2 c_3$
	h^4	$\frac{1}{64}\left(4y_L^4\left(c_9+c_{10}\right) + 2y_L^2 y_R^2\left(\left(3\mathfrak{c}_{2\theta}-1\right)c_5 - 4\mathfrak{s}_\theta^2 c_6\right) + y_R^4\left(3\mathfrak{c}_{2\theta}-1\right)^2 c_{12}\right)$
	h^6	$\frac{1}{64}\left(y_L^6 c_{16} - 4y_L^4 y_R^2\mathfrak{s}_\theta^2 c_{13} + 16y_L^2 y_R^4\mathfrak{s}_\theta^4 c_{14} - 64y_R^6\mathfrak{s}_\theta^6 c_{15}\right)$
	S^2	$y_L^2 c_2 + y_R^2\mathfrak{c}_{2\theta}\, c_3$
	S^4	$\frac{1}{2}y_L^4\mathfrak{c}_{2\theta}{}^2\left(2c_9+c_{10}\right)$
	S^6	$\frac{1}{4}y_L^6 4c_{17}$
	h^2S^2	$y_L^2\left(c_1-c_2\right)$
	h^2S^4	$\frac{1}{2}y_L^4\left(2c_8 - 4c_9 - 2c_{10} + c_{11}\right)$
	h^4S^2	$\frac{1}{4}y_L^4\left(c_8 - 2c_9 - 2c_{10} + c_{11}\right) + \frac{1}{8}y_L^2 y_R^2\left(3\mathfrak{c}_{2\theta}-1\right)\left(c_4-c_5\right)$

Table 4.3: $V(h,S)$ terms obtained via our spurion analysis for t_R in a **15** of $SO(6)$. Only leading terms are shown and each entry should be multiplied by $N_c m_*^4/16\pi^2$, while every h or S comes with a factor $1/f$ and every $y_{L,R}$ with a $1/g_*$. Parameters that contribute in the same way in the given approximation were collected into single c_i and we abbreviate $\mathfrak{c}_{2\theta} = \cos 2\theta_{15\mathrm{R}}$ and $\mathfrak{s}_\theta^2 = \sin^2\theta_{15\mathrm{R}}$, while the other angle is set to zero, respectively. As discussed in the text, going to finite values of the displayed angle changes the hierarchy of terms for the $\mathbf{20'}_L$ model.

		$\mathbf{15}_R$
$\mathbf{6}_L$	h^2 h^4 h^6 S^2 S^4 S^6 h^2S^2 h^2S^4 h^4S^2	No S-potential
$\mathbf{15}_{\mathrm{A}L}$	h^2	$\frac{1}{4}y_L^2 c_1 + \frac{1}{8}y_R^2\left(3\mathfrak{c}_{2\theta}-1\right)c_2$
	h^4	$\frac{1}{64}\left(2y_L^2y_R^2\left((3\mathfrak{c}_{2\theta}-1)c_3 - 4\mathfrak{s}_\theta^2 c_4\right) + 4y_L^4\left(c_5+c_6\right) + y_R^4(1-3\mathfrak{c}_{2\theta})^2 c_7\right)$
	h^6	$\frac{1}{512}\Big(4y_L^4y_R^2\left((3c_8+3c_9+2c_{12}+2c_{13})\,\mathfrak{c}_{2\theta} - c_8 - c_9 - 2c_{12} - 2c_{13}\right)$ $+2y_L^2y_R^4(3\mathfrak{c}_{2\theta}-1)\left((3c_{10}+2c_{11})\,\mathfrak{c}_{2\theta} - c_{10} - 2c_{11}\right) + 8\left(c_{14}+c_{15}+c_{16}\right)y_L^6 + c_{17}y_R^6(3\mathfrak{c}_{2\theta}-1)^3\Big)$
	S^2	$y_L^2 c_1$
	S^4	$y_L^4\frac{1}{2}\left(2c_5+c_6\right)$
	S^6	$\frac{1}{4}y_L^6\left(4c_{14}+2c_{15}+c_{16}\right)$
	h^2S^2	$\frac{1}{32}y_L^2\left(8\left(2c_5+c_6\right)y_L^2 + \left(4c_3+c_4\right)y_R^2(3\mathfrak{c}_{2\theta}-1)\right)$
	h^2S^4	$\frac{1}{64}y_L^4\left(12\left(4c_{14}+2c_{15}+c_{16}\right)y_L^2 + \left(8c_8+4c_9+2c_{12}+c_{13}\right)y_R^2(3\mathfrak{c}_{2\theta}-1)\right)$
	h^4S^2	$\frac{1}{256}y_L^2\Big(y_L^2y_R^2\left((48c_8+24c_9+22c_{12}+14c_{13})\,\mathfrak{c}_{2\theta} - 16c_8 - 8c_9 - 18c_{12} - 10c_{13}\right)$ $+8\left(6c_{14}+4c_{15}+3c_{16}\right)y_L^4 + \left(4c_{10}+c_{11}\right)y_R^4(1-3\mathfrak{c}_{2\theta})^2\Big)$
$\mathbf{20'}_{\mathrm{A}L}$	h^2	$\frac{1}{4}y_L^2 c_2 + \frac{1}{8}y_R^2\left(3\mathfrak{c}_{2\theta}-1\right)c_3$
	h^4	$\frac{1}{64}\left(4y_L^4\left(c_9+c_{10}\right) + 2y_L^2y_R^2\left(\left(3\mathfrak{c}_{2\theta}-1\right)c_5 - 4\mathfrak{s}_\theta^2 c_6\right) + y_R^4\left(3\mathfrak{c}_{2\theta}-1\right)^2 c_{12}\right)$
	h^6	$\frac{1}{256}\left(y_L^6 4c_{17} + y_L^4y_R^2\left(2\left(3\mathfrak{c}_{2\theta}-1\right)c_{13} + 8\mathfrak{s}_\theta^2 c_{14}\right)\right.$ $\left.+y_L^4y_R^2\left(\left(3\mathfrak{c}_{2\theta}-1\right)^2 c_{15} + 4\mathfrak{s}_\theta^2\left(3\mathfrak{c}_{2\theta}-1\right)c_{16}\right) + \frac{1}{2}y_R^6\left(3\mathfrak{c}_{2\theta}-1\right)^2 c_{18}\right)$
	S^2	$y_L^2 c_2$
	S^4	$y_L^4\frac{1}{2}\left(2c_9+c_{10}\right)$
	S^6	$\frac{1}{4}y_L^6 4c_{19}$
	h^2S^2	$y_L^2\left(c_1-c_2\right)$
	h^2S^4	$\frac{1}{2}y_L^4\left(2c_8-4c_9-2c_{10}+c_{11}\right)$
	h^4S^2	$\frac{1}{4}y_L^4\left(c_8-2c_9-2c_{10}+c_{11}\right) + \frac{1}{4}y_L^2y_R^2\left(3\mathfrak{c}_{2\theta}-1\right)\left(c_4-c_5\right)$

Table 4.4: $V(h,S)$ terms obtained via our spurion analysis for t_R in a $\mathbf{20'}_{\mathrm{AB}}$ of $SO(6)$ ($\theta_{20R2}=0$). This configuration is chosen in order to reproduce a heavy top quark and simultaneously a CPV-inducing term, combining viably with the $\mathbf{20'}_{\mathrm{A}\,L}$ such as to generate a S^6 term at NLO and fitting our SNR criteria. Only leading terms are shown and each entry should be multiplied by $N_c m_*^4/16\pi^2$, while every h or S comes with a factor $1/f$ and every $y_{L,R}$ with a $1/g_*$. Parameters that contribute in the same way in the given approximation were collected into single c_i and we abbreviate $\mathfrak{c}_{2\theta} = \cos 2\theta_{20\mathrm{R}1}$ and $\mathfrak{s}_\theta^2 = \sin^2\theta_{20\mathrm{R}1}$, while $\theta_{15L},\theta_{20L}=0$. The smaller left-handed embeddings do not fit the SNR coupling pattern in this choice of angles – for a discussion of nonzero θ_{20R2}, which does allow SNR also in those cases, see main text.

		$\mathbf{20'}_R$
$\mathbf{6}_L$	h^2	$\frac{1}{2}y_L^2 c_1 + \frac{1}{40}y_R^2\left(11\mathfrak{c}_{2\theta}-9\right)c_3$
	h^4	$\frac{1}{20}y_R^2\mathfrak{c}_\theta^2\left(c_2-c_3\right)$
	h^6	$\frac{1}{800}\mathfrak{c}_\theta^2\left(20y_L^2y_R^2\left(-2c_4\right)+y_R^4\left(11\mathfrak{c}_{2\theta}-9\right)\left(c_6-2c_7\right)\right)$
	S^2	$y_R^2\left(2\mathfrak{s}_\theta^2 c_2+\frac{1}{5}\left(7\mathfrak{c}_{2\theta}-3\right)c_3\right)$
	S^4	$y_R^2\frac{1}{5}\left(7\mathfrak{c}_{2\theta}-3\right)\left(c_2-c_3\right)$
	S^6	$\frac{4}{25}y_R^4\left(7\mathfrak{c}_{2\theta}-3\right)\left(c_6-2c_7+\mathfrak{s}_\theta^2\left(5c_5-6c_6+7c_7\right)\right)$
	h^2S^2	$y_R^2\frac{2}{5}\left(2\mathfrak{c}_{2\theta}-3\right)\left(c_2-c_3\right)$
	h^2S^4	$\frac{1}{10}y_L^2y_R^2\left(7\mathfrak{c}_{2\theta}-3\right)\left(-2c_4\right)$ $+\frac{1}{200}y_R^4\Big(-64\mathfrak{s}_\theta^2\left(25c_5-29c_6+33c_7\right)+\mathfrak{s}_{2\theta}^2\left(320c_5-461c_6+602c_7\right)-56\left(c_6-2c_7\right)\Big)$
	h^4S^2	$\frac{1}{5}y_L^2y_R^2\left(2\mathfrak{c}_{2\theta}-3\right)\left(-2c_4\right)+\frac{1}{200}y_R^4\left(2\mathfrak{s}_\theta^2\left(5c_5-28c_6+51c_7\right)-2\left(49\mathfrak{c}_{2\theta}-51\right)\left(c_6-2c_7\right)\right)$
$\mathbf{15}_{\mathrm{A}\,L}$	h^2	$\frac{1}{4}y_L^2 c_1 + \frac{1}{40}y_R^2\left(11\mathfrak{c}_{2\theta}-9\right)c_3$
	h^4	$\frac{1}{20}y_R^2\mathfrak{c}_\theta^2\left(c_2-c_3\right)$
	h^6	$\frac{1}{800}y_R^2\mathfrak{c}_\theta^2\left(10y_L^2c_4+y_R^2\left(11\mathfrak{c}_{2\theta}-9\right)\left(c_6-2c_7\right)\right)$
	S^2	$y_L^2c_1+y_R^2\left(2\mathfrak{s}_\theta^2c_2+\frac{1}{5}\left(7\mathfrak{c}_{2\theta}-3\right)c_3\right)$
	S^4	$\frac{1}{5}y_R^2\left(7\mathfrak{c}_{2\theta}-3\right)\left(c_2-c_3\right)$
	S^6	$\frac{1}{25}y_R^2\left(7\mathfrak{c}_{2\theta}-3\right)\left(5c_4y_L^2+y_R^2\left(2\left(\mathfrak{c}_{2\theta}-1\right)\left(-5c_5+6c_6-7c_7\right)+4\left(c_6-2c_7\right)\right)\right)$
	h^2S^2	$\frac{2}{5}y_R^2\left(2\mathfrak{c}_{2\theta}-3\right)\left(c_2-c_3\right)$
	h^2S^4	$\frac{1}{200}y_R^2\Big(10y_L^2\left(23\mathfrak{c}_{2\theta}-27\right)c_4$ $+y_R^2\mathfrak{s}_\theta^2\left(-64\left(25c_5-29c_6+33c_7\right)+\mathfrak{s}_{2\theta}^2\left(320c_5-461c_6+602c_7\right)-56\left(c_6-2c_7\right)\right)\Big)$
	h^4S^2	$\frac{1}{200}y_R^2\left(5y_L^2\left(9\mathfrak{c}_{2\theta}-11\right)c_4-y_R^2\left(2\left(49\mathfrak{c}_{2\theta}-51\right)\left(c_6-2c_7\right)-2\mathfrak{s}_{2\theta}^2\left(5c_5-28c_6+51c_7\right)\right)\right)$
$\mathbf{20'}_{\mathrm{A}\,L}$	h^2	$y_L^2\frac{1}{4}c_2 + \frac{1}{40}y_R^2\left(11\mathfrak{c}_{2\theta}-9\right)c_4$
	h^4	$\frac{1}{20}y_R^2\mathfrak{c}_\theta^2\left(c_3-c_4\right)$
	h^6	$\mathfrak{c}_\theta^2\left(\frac{1}{80}y_L^2y_R^2\left(c_7-c_8\right)+\frac{1}{800}y_R^4\left(11\mathfrak{c}_{2\theta}-9\right)\left(c_{17}-2c_{18}\right)\right)$
	S^2	$y_L^2c_2+\frac{1}{5}y_R^2\left(5c_3-3c_4+\mathfrak{c}_{2\theta}\left(-5c_3+7c_4\right)\right)$
	S^4	$\frac{1}{5}y_R^2\left(7\mathfrak{c}_{2\theta}-3\right)\left(c_3-c_4\right)$
	S^6	$\frac{1}{5}y_L^2y_R^2\left(7\mathfrak{c}_{2\theta}-3\right)\left(c_7-c_8\right)$ $-\frac{2}{25}y_R^4\left(7\mathfrak{c}_{2\theta}-3\right)\left(-5c_{16}+4c_{17}-3c_{18}+\mathfrak{c}_{2\theta}\left(5c_{16}-6c_{17}+7c_{18}\right)\right)$
	h^2S^2	$y_L^2\left(c_1-c_2\right)+\frac{2}{5}y_R^2\left(2\mathfrak{c}_{2\theta}-3\right)\left(c_3-c_4\right)$
	h^2S^4	$y_L^4\frac{1}{2}\left(2c_{12}-4c_{13}-2c_{14}+c_{15}\right)$ $-\frac{1}{20}y_L^2y_R^2\left(-20c_5+12c_6+47c_7-39c_8+44c_9-24c_{10}+\mathfrak{c}_{2\theta}\left(20c_5-28c_6-43c_7+51c_8-56c_9+36c_{10}\right)\right)$ $+\frac{1}{400}y_R^4\left(64\mathfrak{c}_{2\theta}\left(25c_{16}-29c_{17}+33c_{18}\right)+\mathfrak{c}_{4\theta}\left(-320c_{16}+461c_{17}-602c_{18}\right)-1280c_{16}+1283c_{17}-1286c_{18}\right)$
	h^4S^2	$\frac{1}{4}y_L^4\left(c_{12}-2c_{13}-2c_{14}+c_{15}\right)$ $+\frac{1}{40}y_L^2y_R^2\left(\mathfrak{c}_{2\theta}\left(11c_6+9c_7-20c_8+17c_9-17c_{10}\right)-9c_6-11c_7+20c_8-23c_9+23c_{10}\right)$ $+\frac{1}{200}y_R^4\left(-98\mathfrak{c}_{2\theta}\left(c_{17}-2c_{18}\right)+\mathfrak{c}_{4\theta}\left(-5c_{16}+28c_{17}-51c_{18}\right)+5c_{16}+74c_{17}-153c_{18}\right)$

Table 4.5: Overview of $V(h,S)$ terms arising at nth order in spurions, with brackets denoting special cases of embeddings described in the text (not noting the cases for which S remains a Goldstone boson), i.e., in the $\mathbf{20'}_L$ block, $\theta_{20\mathrm{L}} = 0$ in the first column, $\theta_{20\mathrm{L}} \neq 0$ for the second and third and $\theta_{20\mathrm{R1}} = 0$ for the $(\mathbf{20'}_{\mathrm{A}L}, \mathbf{20'}_R)$.

		$\mathbf{1}_R$	$\mathbf{6}_R$	$\mathbf{15}_R$	$\mathbf{20'}_R$
$\mathbf{6}_L$	h^2	No S-pot.	2^{nd}	No S-pot.	2^{nd}
	h^4		4^{th}		2^{nd}
	h^6		6^{th}		4^{th}
	S^2		2^{nd}		2^{nd}
	S^4		4^{th}		2^{nd}
	S^6		6^{th}		4^{th}
	h^2S^2		2^{nd}		2^{nd}
	h^2S^4		4^{th}		4^{th}
	h^4S^2		6^{th}		4^{th}
$\mathbf{15}_{\mathrm{A}L}$	h^2	No top mass	No CPV	2^{nd}	2^{nd}
	h^4			4^{th}	2^{nd}
	h^6			6^{th}	4^{th}
	S^2			2^{nd}	2^{nd}
	S^4			4^{th}	2^{nd}
	S^6			6^{th}	4^{th}
	h^2S^2			4^{th}	2^{nd}
	h^2S^4			6^{th}	4^{th}
	h^4S^2			6^{th}	4^{th}
$\mathbf{20'}_L$	h^2	2^{nd}	2^{nd}	2^{nd}	2^{nd}
	h^4	2^{nd} (4^{th})	4^{th} (2^{nd})	4^{th} (2^{nd})	2^{nd} (4^{th})
	h^6	4^{th} (6^{th})	6^{th} (4^{th})	6^{th} (4^{th})	4^{th} (6^{th})
	S^2	2^{nd}	2^{nd}	2^{nd}	2^{nd}
	S^4	4^{th}	4^{th}	4^{th}	2^{nd}
	S^6	6^{th}	6^{th}	6^{th}	4^{th}
	h^2S^2	2^{nd}	2^{nd}	2^{nd}	2^{nd}
	h^2S^4	4^{th}	4^{th}	4^{th}	4^{th}
	h^4S^2	4^{th}	4^{th}	4^{th}	4^{th}

4.6 Matching the $SO(6)/SO(5)$ Composite Higgs Model to the SNR scenario

We now turn to matching the parameters of the EFT in Equation 3.1 to the parameters from last section. For simplicity, we set $y_L = y_R = 1$, but the couplings can be reinserted by counting coupling dimensions. It was already mentioned that an S^6 term arising at NNLO, thus being suppressed by $(y_{L,R}/g_*)^6$, is in tension with the SNR scenario. This can be motivated as follows: the coupling of the composite sector is assumed to be strong, $g_* \in (1, 4\pi)$ - we conservatively pick $g_* = 4$. The Goldstone boson scale needs to be $f \gtrsim 800\,\text{GeV}$, as smaller values are constrained by experiment [52]. If we pick the NP scale near the upper limit that works for the SNR scenario, $\Lambda_{\text{NP}} \approx 1.5\,\text{TeV}$, an NNLO term S^6 term, scaling like

$$\frac{S^6}{\Lambda_{\text{NP}}^2} = \frac{N_c m_*^4}{16\pi^2}\left(\frac{y_{L,R}}{g_*}\right)^6 \frac{S^6}{f^6}\bar{c}_6 = \frac{N_c}{16\pi^2}\left(\frac{y_{L,R}^6}{g_*^2 f^2}\right)\bar{c}_6 S^6 \tag{4.16}$$

would ask for $\bar{c}_6 \sim 240$, where $\bar{c}_6$ denotes the sum of all contributions to this term at NNLO (sixth order in spurions). In contrast, for an NLO term

$$\frac{N_c m_*^4}{16\pi^2}\left(\frac{y_{L,R}}{g_*}\right)^4 \frac{S^6}{f^6}\bar{c}_4 = \frac{N_c}{16\pi^2}\left(\frac{y_{L,R}^4}{f^2}\right)\bar{c}_4 S^6\,, \tag{4.17}$$

a cumulative $\bar{c}_4 \sim 15$ suffices, which can indeed arise from the number of $\mathcal{O}(1)$ coefficients encountered in the $\mathbf{20'}_R$ models.

Moreover, as actually all the coefficients of dimension six operators h^6, h^4S^2, h^2S^4, S^6 depend on $\mathcal{O}(10)$ different parameters c_i in the $\mathbf{20'}_R$ models, the cutoff Λ_{NP} can be treated as a free parameter, as long as it fits within the range given by $y_{L,R}/g_*$ such that the coefficients are still of $\mathcal{O}(1 \sim 10)$. In this case, we could, e.g., choose values between $\Lambda_{\text{NP}} \sim 1\,\text{TeV} - 6\,\text{TeV}$, which goes quite beyond the realm of the SNR scenario. We assume the coefficients of h^4S^2 and h^2S^4 are small enough to not impact our analysis, which is readily accounted for, given the large number of degrees of freedom in their coefficients.

As in the $(\mathbf{6}, \mathbf{20'})$ and the $(\mathbf{15}, \mathbf{20'})$ models only very specific embeddings allow for the SNR scenario at all, we concentrate on the analysis of the $(\mathbf{20'}, \mathbf{20'})$ model, although it can be extended to the other two models.

The remaining five IR parameters, namely $\mu_h^2, \mu_S^2, \lambda_h, \lambda_S, \lambda_{hS}$, depend on $\cos\theta_{20R1}$ and four c's. We can express the latter in terms of the EFT couplings. In particular, λ_h and λ_S depend on the same combination of c's (c.f., Tab. 4.4), such that the mixing parameter can be determined by their ratio:

$$\cos\theta_{20R1}^2 = \frac{5}{7}\left(1 - \frac{\lambda_S}{56\lambda_h}\right)^{-1}. \tag{4.18}$$

Given the range of λ_S in Fig. 3.2 and the SM quartic coupling λ_h, this is found to lie between $\cos\theta_{20R1} \approx 0.83 - 0.84$. This is safely within the range of values that can

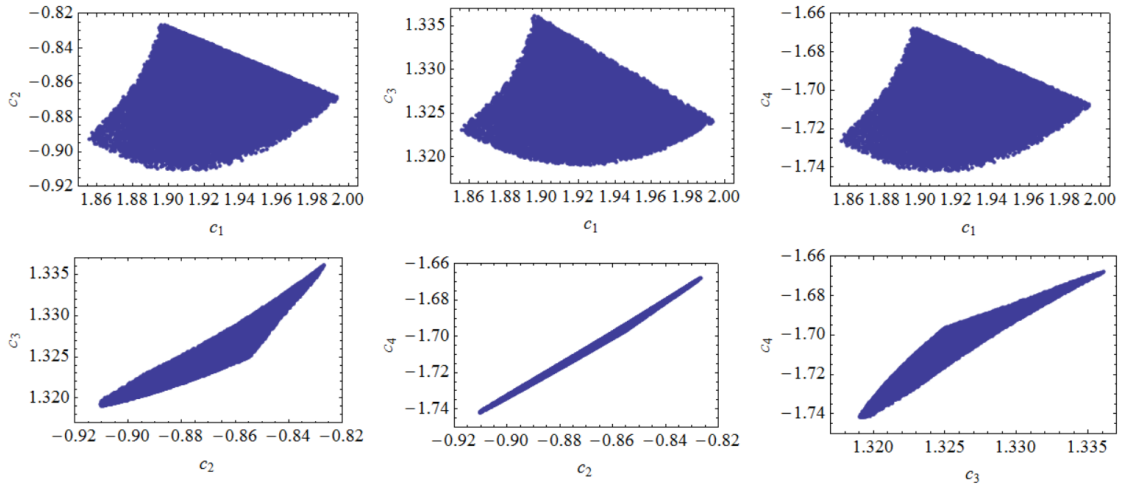

Figure 4.1: Values of UV-parameters of the $(\mathbf{20}', \mathbf{20}')$ model that reproduce the IR values plotted in Fig. 3.2, under the assumption that $f = 800\,\text{GeV}$ and $g_* = 4$. The figure was taken from [15].

successfully generate the BAU during the EWPhT, as motivated in the following. In particular, for the benchmark point used in Sec. 3.2, where $\lambda_S = -0.15, \lambda_{hS} = 0.1, \Lambda_{\text{NP}} = 1.5\,\text{TeV}, m_S = 75\,\text{GeV}$ and the other parameters are fixed by SM values,

$$V(v(T), 0, T_c) = V(0, w_+, T_c) \quad \Rightarrow \quad \begin{aligned} T_c &\approx 90\,\text{GeV}\,, \\ v_c &\approx 186\,\text{GeV}\,, w_c \approx 230\,\text{GeV}\,, \end{aligned} \tag{4.19}$$

yielding $\xi = \dfrac{v_c}{T_c} \approx 2$. With (2.19) and (4.14), we can now estimate the value of the CP violating phase for $\cos\theta_{20R1} = 0.835,\ f = 800\,\text{GeV}$

$$\Delta\Theta_t \approx \frac{b\Delta w_c}{y_t f} \approx \frac{3\cos\theta_{20R1}}{4\sqrt{5}} \frac{2\sqrt{2}}{\sin\theta_{20R1}} \frac{230\,\text{GeV}}{f} \approx 0.41\,, \tag{4.20}$$

which is safely above the strength $\Delta\Theta_t \gtrsim 0.1$ needed to generate the BAU - if not a bit too strong, when compared with the plots in [7]. These are only valid for $m_S = 80\,\text{GeV}$ (and above) though, where we would find $T_c \approx 90\,\text{GeV}, \xi \approx 1.33$ and $\Delta\Theta_t \approx 0.37$, which fits very well with their values.

Lastly, the values of UV parameters fitting the IR parameters from Fig. 3.2 are plotted in Fig. 4.1. One can see that they are nicely constrained to order unity parameters. The correlation between each two $c_{2,3,4}$ is much stronger than between each of them with c_1 because c_2, c_3 (c_3, c_4) determine the Higgs mass (quartic), which are fixed by the SM. They incidentally also fully determine the singlet mass and quartic. The parameter c_1 is then left to be fixed by the viable parameter space of the portal coupling.

5 Conclusion

In this thesis, I investigated a novel method to explain the baryon-asymmetry of the universe, realized in a way that can also solve the hierarchy problem and account for the hierarchy in quark masses. The BAU can be generated using the well-established model of electroweak baryogenesis by extending the standard model with a scalar singlet S, often taken $\mathbb{Z}_2$-symmetric, potentially allowing it to be a dark matter candidate and realizing EWBG with a two-step phase transition. Such a scenario featuring spontaneous $\mathbb{Z}_2$ breaking at the electroweak scale however leads to phenomenological problems, which can be avoided by not restoring $\mathbb{Z}_2$ at high temperatures instead. As was shown here, this scenario can be obtained by minimally extending the scalar potential with a non-renormalizable sextic singlet term and allows for a strong first order phase transition while not being ruled out by current collider limits. Calculating the critical points of the finite temperature scalar potential, the parameter space for which the envisioned one-step phase transition $(h, S) = (0, w) \to (v, 0)$ can be made strongly first order was explored. Therein, it was taken care that the electroweak phase transition definitely completes. In particular, the scale of new physics is constrained to $\Lambda_{\text{NP}} \approx 1 - 1.6\,\text{TeV}$, which is quite accessible to experiments. Further investigations may elaborate on the impact of other critical points present in the course of the phase transition, or a numerical analysis can be used to explore for which parameter sets the phase transition completes instead of imposing that only the electroweak minimum survives at low temperatures. It would also be interesting to investigate potential mechanisms that could lead to dynamical $\mathbb{Z}_2$ breaking before inflation. Moreover, investigating what gravitational wave signals follow from the proposed thermal history may be promising to discriminate models.

Assuming a UV-completion in form of a $SO(6)/SO(5)$ composite Higgs model, the proposed EFT arises dynamically. The Higgs and scalar singlet arise as pseudo-Nambu-Goldstone-bosons of a strongly coupled new sector, eliminating the hierarchy problem. Other, heavier resonances of this composite sector are coupled linearly to the SM elementary fermions in the partial compositeness framework, which generates the quark masses while offering an explanation to their curiously different values. Lifting the SM fermions to spurion multiplets of $SO(6)$, the low-energy potential was then constructed using the CCWZ formalism. A comprehensive overview of the Yukawa terms and the potential, generated for various models to non-renormalizable order, was given. Namely, all combinations of SM fermions in $((\mathbf{1}), \mathbf{6}, \mathbf{15}, \mathbf{20'})$ representations of $SO(6)$ were considered. The specific models were fixed to obtain non-zero top mass, a spontaneous CP violating term involving the Higgs and the singlet, and a non-vanishing singlet potential. The latter helps to enhance the EWPhT at tree level, as preferred in singlet extensions to realize EWBG. Models

with a top quark in a $\mathbf{20'}_R$ can generate the sextic singlet term at NLO in the spurion expansion and thus may be suited to realize the SNR scenario, unlike all other models where this term is highly suppressed. While combinations with the $\mathbf{6}_L$ and the $\mathbf{15}_L$ are tightly constrained to very specific embeddings, the $(\mathbf{20'}_{\mathrm{A}}, \mathbf{20'}_{\mathrm{AB}})$ features no such limitations and was therefore identified as the most promising option. It was subsequently matched to the general EFT parameters, showing that it fits the given parameter space very well. Additionally, the CPV-term of this incarnation should be able to generate the correct BAU, as motivated by comparing it with previous analyses. The model therefore fulfills all Sakharov criteria, most likely generates the correct BAU and additionally features solutions to the hierarchy problem and the flavor hierarchy puzzle. One could explore if the envisioned thermal history can also be obtained in other motivated models beyond the SM, such as, e.g., a $SU(6)$ gauge-Higgs-grand-unification with an extra scalar singlet [76] or models with extended scalar sectors.

Acknowledgements

First and foremost, I would like to thank my supervisor, Florian Goertz, very much for his guidance and patience, for answering my questions, keeping in touch online and of course for taking me under his wing in the first place. Many thanks also goes to Mr. Pawlowski, who agreed to be my second referee on rather short notice. Special thanks goes to Andrei Angelescu, who patiently answered my questions about the EFT part and who kindly showed me his code. The MPIK also has my gratitude for letting me write my thesis there.

Love and thanks to Paul, for loving me and fighting to keep me confident every day. Alena and Imke, who kept me company in our "digital office", also have my gratitude. A huge thank you goes to Sebastian, who proofread this thesis, performed some LaTeX-wizardry, and managed to make me laugh even on the day of submission. Thanks also goes to Joerg for the spontaneous discussions about physics during lockdown.

Last, but not least, a big thank you goes to my parents and my grandparents, who supported me throughout my studies and my brother, who often helps with sorting out my feelings – I love you.

Appendix

A Embedding SM fermions into multiplets of $SO(6)$

In the main text, the viable SM fermion embeddings into $SO(6)$ multiplets are given. Here, it is elaborated why some embeddings cannot be used and how the spurions are constructed explicitly. For an introduction on group theory for physicists, see, for example, [77]. To begin with, the spinorial **4** decomposes under $SO(6) \times U(1)_X \to SO(4) \times U(1)_X \cong SU(2) \times SU(2) \times U(1)_X \to SU(2) \times U(1)_Y$ as

$$\begin{aligned}\mathbf{4}_{2/3} &\to (\mathbf{2},\mathbf{1})_{2/3} \oplus (\mathbf{1},\mathbf{2})_{2/3} \\ &\to \mathbf{2}_{2/3} \oplus \left(\mathbf{1}_{7/6} \oplus \mathbf{1}_{1/6}\right),\end{aligned}$$

which one can check by, e.g., using the `LieArt` Mathematica package or filing through Slansky [78]. Obviously, a q_L can be embedded. However, in beyond the standard model (BSM) physics one always needs to take care to not destroy any relations that are well described by the SM and hold experimentally, such as the EW boson mass ratio. Corrections to the latter can be protected by a global $SU(2)_L \times SU(2)_R$ symmetry in the Higgs potential, which is called the *custodial symmetry* and was first formulated to construct realistic technicolor models [79]. As can be seen above, the spinorial representation does not contain a $(\mathbf{2},\mathbf{2})_{2/3}$ decomposition and the fermions would therefore not obey this symmetry.

The decompositon of **6** is already given in Subsec. 2.6.1 To obtain the concrete embedding of the fermions from there, one may apply a small transformation with the generators of $SU(2)_L$ and the third $SU(2)_R$ operator to a full $SO(6)$ fundamental and consider its component's charges. The right-handed top quark is a singlet of $SU(2)_L$ and has to be embedded in components five and six in our choice of generators. It fixes the X-charge of the representation by requiring that $Y = I_R^3 + X = 2/3$, where $I_R^3 = 0$ is the charge under the T_R^3 generator. The left-handed quarks are doublets of $SU(2)_L$ and therefore need to be realized in the first four components. Applying the hypercharge generator,

$$\begin{aligned}T_Y Q^6 &= \left(T_R^3 + X T_X\right)\begin{pmatrix}a & b & c & d & 0 & 0\end{pmatrix}^T \\ &= \begin{pmatrix}Xa - \frac{i}{2}b & \frac{i}{2}a + Xb & Xc + \frac{i}{2}d & -\frac{i}{2}c + Xd & 0 & 0\end{pmatrix},\end{aligned} \tag{A.1}$$

it is apparent that to ensure proper $U(1)_Y$ symmetry, a, b and c, d need to contain the same particles with the same charges, which yields $b = \pm ia, d = \pm ic$. Choosing $c, d \sim t_L$ then yields a nonzero top mass term in the CCWZ construction, as

opposed to $c, d \sim b_L$, which yields a massive bottom quark instead.[1] Requiring $Y(t_L, b_L) = 1/6$ then fixes

$$Q_L^6 = (b_L, -ib_L, t_L, it_L, 0, 0)^T . \tag{A.2}$$

Next, one can take a look at the tensor product of two fundamentals,

$$\mathbf{6} \otimes \mathbf{6} = \mathbf{1} \oplus \mathbf{15} \oplus \mathbf{20'}, \tag{A.3}$$

by which the asymmetric **15** and the symmetric **20** representation can be obtained. Writing down every possible combination of the two 6-elements, $Q_{i,j}$ with $i, j = 1, \ldots, 6$, and analyzing them with respect to their symmetry and quantum numbers leads to the embeddings in Subsec. 2.6.1. To which $SO(5)$ representation they belong can be seen by testing how they transform under the subgroup.

[1] Note that b_R would also require a different X-charge.

B Lists

B.1 List of Figures

B.2 List of Tables

C Bibliography

[1] The CMS Collaboration. Observation of a new boson at a mass of 125 GeV with the CMS experiment at the LHC. *Physics Letters B*, 716(1):30–61, September 2012. arXiv:1207.7235, doi:10.1016/j.physletb.2012.08.021.

[2] Particle Data Group. Review of Particle Physics. *Progress of Theoretical and Experimental Physics*, 2020(8):083C01, August 2020. doi:10.1093/ptep/ptaa104.

[3] Elena Graverini. Flavour anomalies: a review. *Journal of Physics: Conference Series*, 1137:012025, January 2019. arXiv:1807.11373, doi:10.1088/1742-6596/1137/1/012025.

[4] J. R. Espinosa and M. Quirós. The electroweak phase transition with a singlet. *Physics Letters B*, 305(1-2):98–105, May 1993. arXiv:hep-ph/9301285, doi:10.1016/0370-2693(93)91111-Y.

[5] Jose Ramon Espinosa and Mariano Quiros. Novel Effects in Electroweak Breaking from a Hidden Sector. *Physical Review D*, 76(7):076004, October 2007. arXiv:hep-ph/0701145, doi:10.1103/PhysRevD.76.076004.

[6] Stefano Profumo, Michael J. Ramsey-Musolf, and Gabe Shaughnessy. Singlet Higgs Phenomenology and the Electroweak Phase Transition. *Journal of High Energy Physics*, 2007(08):010–010, August 2007. arXiv:0705.2425, doi:10.1088/1126-6708/2007/08/010.

[7] Jose R. Espinosa, Ben Gripaios, Thomas Konstandin, and Francesco Riva. Electroweak Baryogenesis in Non-minimal Composite Higgs Models. *Journal of Cosmology and Astroparticle Physics*, 01:012, January 2012. arXiv:1110.2876, doi:10.1088/1475-7516/2012/01/012.

[8] Jose R. Espinosa, Thomas Konstandin, and Francesco Riva. Strong Electroweak Phase Transitions in the Standard Model with a Singlet. *Nuclear Physics B*, 854(3):592–630, January 2012. arXiv:1107.5441, doi:10.1016/j.nuclphysb.2011.09.010.

[9] Vernon Barger, Daniel J. H. Chung, Andrew J. Long, and Lian-Tao Wang. Strongly First Order Phase Transitions Near an Enhanced Discrete Symmetry Point. *Physics Letters B*, 710(1):1–7, March 2012. arXiv:1112.5460, doi:10.1016/j.physletb.2012.02.040.

[10] James M. Cline and Kimmo Kainulainen. Electroweak baryogenesis and dark matter from a singlet Higgs. *Journal of Cosmology and Astroparticle Physics*, 2013(01):012–012, January 2013. arXiv:1210.4196, doi:10.1088/1475-7516/2013/01/012.

[11] David Curtin, Patrick Meade, and Chiu-Tien Yu. Testing Electroweak Baryogenesis with Future Colliders. *Journal of High Energy Physics*, 2014(11):127, November 2014. arXiv:1409.0005, doi:10.1007/JHEP11(2014)127.

[12] Gowri Kurup and Maxim Perelstein. Dynamics of Electroweak Phase Transition In Singlet-Scalar Extension of the Standard Model. *Physical Review D*, 96(1):015036, July 2017. arXiv:1704.03381, doi:10.1103/PhysRevD.96.015036.

[13] Marcela Carena, Zhen Liu, and Marc Riembau. Probing Electroweak Phase Transition via Enhanced Di-Higgs Production. *Physical Review D*, 97(9):095032, May 2018. arXiv:1801.00794, doi:10.1103/PhysRevD.97.095032.

[14] Ya. B. Zeldovich, I. Yu. Kobzarev, and L. B. Okun. Cosmological Consequences of the Spontaneous Breakdown of Discrete Symmetry. *Zhurnal Eksperimental'noi i Teoreticheskoi Fiziki*, 67:3–11, 1974. URL: https://www.jetp.ras.ru/cgi-bin/dn/e_040_01_0001.pdf.

[15] Andrei Angelescu, Florian Goertz, and Aika Tada. Z_2 Non-Restoration and Composite Higgs: Singlet-Assisted Baryogenesis w/o Topological Defects. March 2022. arXiv:2112.12087.

[16] Michael Edward Peskin and Daniel V. Schroeder. *An introduction to quantum field theory*. Addison-Wesley, Reading, Mass, 1995.

[17] B. R. Martin and G. Shaw. *Particle physics*. Wiley, Chichester, UK ; New York, 3rd ed edition, 2008.

[18] Matthew Dean Schwartz. *Quantum field theory and the standard model*. Cambridge University Press, New York, 2014.

[19] Christian Grefe. *Detector Optimization Studies and Light Higgs Decay into Muons at CLIC*. PhD thesis, Rheinische Friedrich-Wilhelms-Universität Bonn, February 2014. arXiv:1402.2780.

[20] C. S. Wu, E. Ambler, R. W. Hayward, D. D. Hoppes, and R. P. Hudson. Experimental Test of Parity Conservation in Beta Decay. *Physical Review*, 105(4):1413–1415, February 1957. doi:10.1103/PhysRev.105.1413.

[21] Julian Schwinger. A theory of the fundamental interactions. *Annals of Physics*, 2(5):407–434, November 1957. doi:10.1016/0003-4916(57)90015-5.

[22] Sheldon L. Glashow. Partial-symmetries of weak interactions. *Nuclear Physics*, 22(4):579–588, February 1961. doi:10.1016/0029-5582(61)90469-2.

[23] Peter W. Higgs. Broken Symmetries and the Masses of Gauge Bosons. *Physical Review Letters*, 13(16):508–509, October 1964. doi:10.1103/PhysRevLett.13.508.

[24] F. Englert and R. Brout. Broken Symmetry and the Mass of Gauge Vector Mesons. *Physical Review Letters*, 13(9):321–323, August 1964. doi:10.1103/PhysRevLett.13.321.

[25] G. S. Guralnik, C. R. Hagen, and T. W. B. Kibble. Global Conservation Laws and Massless Particles. *Physical Review Letters*, 13(20):585–587, November 1964. doi:10.1103/PhysRevLett.13.585.

[26] Jeffrey Goldstone, Abdus Salam, and Steven Weinberg. Broken Symmetries. *Physical Review*, 127(3):965–970, August 1962. doi:10.1103/PhysRev.127.965.

[27] Leonard Susskind. Dynamics of spontaneous symmetry breaking in the Weinberg-Salam theory. *Physical Review D*, 20(10):2619–2625, November 1979. doi:10.1103/PhysRevD.20.2619.

[28] H. Georgi, H. R. Quinn, and S. Weinberg. Hierarchy of Interactions in Unified Gauge Theories. *Physical Review Letters*, 33(7):451–454, August 1974. doi:10.1103/PhysRevLett.33.451.

[29] Steven Weinberg. Implications of dynamical symmetry breaking. *Physical Review D*, 13(4):974–996, February 1976. doi:10.1103/PhysRevD.13.974.

[30] Stephen P. Martin. *A Supersymmetry Primer*, volume 18, pages 1–98. World Scientific, arXiv:hep-ph/9709356v7 edition, July 1998. arXiv:hep-ph/9709356, doi:10.1142/9789812839657_0001.

[31] Kenneth Lane. Two Lectures on Technicolor. February 2002. arXiv:hep-ph/0202255.

[32] Roberto Contino. Tasi 2009 lectures: The Higgs as a Composite Nambu-Goldstone Boson. May 2010. arXiv:1005.4269.

[33] Peter von Ballmoos. Antimatter in the Universe : Constraints from Gamma-Ray Astronomy. *Hyperfine Interactions*, 228(1-3):91–100, October 2014. arXiv:1401.7258, doi:10.1007/s10751-014-1024-9.

[34] James M. Cline. Baryogenesis. November 2006. arXiv:hep-ph/0609145.

[35] Ryley Hill, Kiyoshi W. Masui, and Douglas Scott. The Spectrum of the Universe. *Applied Spectroscopy*, 72(5):663–688, May 2018. arXiv:1802.03694, doi:10.1177/0003702818767133.

[36] Gordan Krnjaic. Can the Baryon Asymmetry Arise From Initial Conditions? *Physical Review D*, 96(3):035041, August 2017. arXiv:1606.05344, doi:10.1103/PhysRevD.96.035041.

[37] J. L. Barrow, Leah Broussard, James M. Cline, P. S. Bhupal Dev, Marco Drewes, Gilly Elor, Susan Gardner, Jacopo Ghiglieri, Julia Harz, Yuri Kamyshkov, Juraj Klaric, Lisa W. Koerner, Benoit Laurent, Robert McGehee, Marieke Postma, Bibhushan Shakya, Robert Shrock, Jorinde van de Vis, and Graham White. Theories and Experiments for Testable Baryogenesis Mechanisms: A Snowmass White Paper. March 2022. arXiv:2203.07059.

[38] Gilly Elor, Julia Harz, Seyda Ipek, Bibhushan Shakya, Nikita Blinov, Raymond T. Co, Yanou Cui, Arnab Dasgupta, Hooman Davoudiasl, Fatemeh Elahi, Kåre Fridell, Akshay Ghalsasi, Keisuke Harigaya, Chandan Hati, Peisi Huang, Azadeh Maleknejad, Robert McGehee, David E. Morrissey, Kai Schmitz, Michael Shamma, Brian Shuve, David Tucker-Smith, Jorinde van de Vis, and Graham White. New Ideas in Baryogenesis: A Snowmass White Paper. March 2022. arXiv:2203.05010.

[39] Andrei D Sakharov. Violation of CP Invariance, C asymmetry, and baryon asymmetry of the universe. *Soviet Physics Uspekhi*, 34(5):392–393, May 1991. doi:10.1070/PU1991v034n05ABEH002497.

[40] G. 't Hooft. Symmetry Breaking through Bell-Jackiw Anomalies. *Physical Review Letters*, 37(1):8–11, July 1976. doi:10.1103/PhysRevLett.37.8.

[41] M. B. Gavela, P. Hernández, J. Orloff, and O. Pène. Standard Model CP-violation and Baryon asymmetry. *Modern Physics Letters A*, 09(09):795–809, March 1994. arXiv:hep-ph/9312215, doi:10.1142/S0217732394000629.

[42] Mariano Quiros. Finite temperature field theory and phase transitions. January 1999. arXiv: hep-ph/9901312. arXiv:hep-ph/9901312.

[43] K. Rummukainen, M. Tsypin, K. Kajantie, M. Laine, and M. Shaposhnikov. The universality class of the electroweak theory. *Nuclear Physics B*, 532(1-2):283–314, October 1998. arXiv:hep-lat/9805013, doi:10.1016/S0550-3213(98)00494-5.

[44] Sidney Coleman. Fate of the false vacuum: Semiclassical theory. *Physical Review D*, 15(10):2929–2936, May 1977. doi:10.1103/PhysRevD.15.2929.

[45] Stefania De Curtis, Luigi Delle Rose, and Giuliano Panico. Composite Dynamics in the Early Universe. *Journal of High Energy Physics*, 12:149, 2019. arXiv:1909.07894, doi:10.1007/JHEP12(2019)149.

[46] James M. Cline, Avi Friedlander, Dong-Ming He, Kimmo Kainulainen, Benoit Laurent, and David Tucker-Smith. Baryogenesis and gravity waves from a

UV-completed electroweak phase transition. *Physical Review D*, 103(12):123529, June 2021. arXiv:2102.12490, doi:10.1103/PhysRevD.103.123529.

[47] Ben Gripaios, Alex Pomarol, Francesco Riva, and Javi Serra. Beyond the Minimal Composite Higgs Model. *Journal of High Energy Physics*, 04:070, 2009. arXiv:0902.1483, doi:10.1088/1126-6708/2009/04/070.

[48] Ville Vaskonen. Electroweak baryogenesis and gravitational waves from a real scalar singlet. *Physical Review D*, 95(12):123515, June 2017. arXiv:1611.02073, doi:10.1103/PhysRevD.95.123515.

[49] Sidney Coleman and Erick Weinberg. Radiative Corrections as the Origin of Spontaneous Symmetry Breaking. *Physical Review D*, 7(6):1888–1910, March 1973. doi:10.1103/PhysRevD.7.1888.

[50] C. Delaunay, C. Grojean, and J. D. Wells. Dynamics of Non-renormalizable Electroweak Symmetry Breaking. *Journal of High Energy Physics*, 2008(04):029–029, April 2008. arXiv:0711.2511, doi:10.1088/1126-6708/2008/04/029.

[51] Peter Arnold and Larry McLerran. Sphalerons, small fluctuations, and baryon-number violation in electroweak theory. *Physical Review D*, 36(2):581–595, July 1987. doi:10.1103/PhysRevD.36.581.

[52] Veronica Sanz and Jack Setford. Composite Higgs models after Run2. February 2018. arXiv:1703.10190.

[53] Giuliano Panico and Andrea Wulzer. *The Composite Nambu-Goldstone Higgs*, volume 913 of *Lecture Notes in Physics*. Springer, 2016. arXiv:1506.01961, doi:10.1007/978-3-319-22617-0.

[54] Savas Dimopoulos and John Preskill. Massless composites with massive constituents. *Nuclear Physics B*, 199(2):206–222, May 1982. doi:10.1016/0550-3213(82)90345-5.

[55] David B. Kaplan and Howard Georgi. SU(2) $\times$ U(1) breaking by vacuum misalignment. *Physics Letters B*, 136(3):183–186, March 1984. doi:10.1016/0370-2693(84)91177-8.

[56] David B. Kaplan, Howard Georgi, and Savas Dimopoulos. Composite Higgs scalars. *Physics Letters B*, 136(3):187–190, March 1984. doi:10.1016/0370-2693(84)91178-X.

[57] Howard Georgi, David B. Kaplan, and Peter Galison. Calculation of the composite Higgs mass. *Physics Letters B*, 143(1):152–154, August 1984. doi:10.1016/0370-2693(84)90823-2.

[58] Thomas Banks. Constraints on SU2×U1 breaking by vacuum misalignment. *Nuclear Physics B*, 243(1):125–130, August 1984. doi:10.1016/0550-3213(84)90389-4.

[59] Howard Georgi and David B. Kaplan. Composite Higgs and custodial SU(2). *Physics Letters B*, 145(3):216–220, September 1984. doi:10.1016/0370-2693(84)90341-1.

[60] David B. Kaplan. Flavor at ssc energies: A new mechanism for dynamically generated fermion masses. *Nuclear Physics B*, 365(2):259–278, November 1991. doi:10.1016/S0550-3213(05)80021-5.

[61] S. Coleman, J. Wess, and Bruno Zumino. Structure of Phenomenological Lagrangians. I. *Physical Review*, 177(5):2239–2247, January 1969. doi:10.1103/PhysRev.177.2239.

[62] Curtis G. Callan, Sidney Coleman, J. Wess, and Bruno Zumino. Structure of Phenomenological Lagrangians. II. *Physical Review*, 177(5):2247–2250, January 1969. doi:10.1103/PhysRev.177.2247.

[63] Kaustubh Agashe, Roberto Contino, and Alex Pomarol. The minimal composite Higgs model. *Nuclear Physics B*, 719:165–187, 2005. arXiv:hep-ph/0412089, doi:10.1016/j.nuclphysb.2005.04.035.

[64] Ligong Bian, Yongcheng Wu, and Ke-Pan Xie. Electroweak phase transition with composite Higgs models: calculability, gravitational waves and collider searches. *Journal of High Energy Physics*, 2019(12):28, December 2019. arXiv:1909.02014, doi:10.1007/JHEP12(2019)028.

[65] Ke-Pan Xie, Ligong Bian, and Yongcheng Wu. Electroweak baryogenesis and gravitational waves in a composite Higgs model with high dimensional fermion representations. *Journal of High Energy Physics*, 12:047, December 2020. arXiv:2005.13552, doi:10.1007/JHEP12(2020)047.

[66] Mikael Chala, Gauthier Durieux, Christophe Grojean, Leonardo de Lima, and Oleksii Matsedonskyi. Minimally extended SILH. *Journal of High Energy Physics*, 06:088, June 2017. arXiv:1703.10624, doi:10.1007/JHEP06(2017)088.

[67] Christoph Niehoff, Peter Stangl, and David M. Straub. Electroweak symmetry breaking and collider signatures in the next-to-minimal composite Higgs model. *Journal of High Energy Physics*, 04:117, April 2017. arXiv:1611.09356, doi:10.1007/JHEP04(2017)117.

[68] G. F. Giudice, C. Grojean, A. Pomarol, and R. Rattazzi. The Strongly-Interacting Light Higgs. *Journal of High Energy Physics*, 06:045, 2007. arXiv:hep-ph/0703164, doi:10.1088/1126-6708/2007/06/045.

[69] Marcela Carena, Zhen Liu, and Yikun Wang. Electroweak phase transition with spontaneous Z_2-breaking. *Journal of High Energy Physics*, 2020(8):107, August 2020. arXiv:1911.10206, doi:10.1007/JHEP08(2020)107.

[70] Albert M Sirunyan and others. Search for invisible decays of a Higgs boson produced through vector boson fusion in proton-proton collisions at $\sqrt{s} = 13$ TeV. *Physics Letters B*, 793:520–551, 2019. arXiv:1809.05937, doi:10.1016/j.physletb.2019.04.025.

[71] Morad Aaboud et al. Combination of searches for invisible Higgs boson decays with the ATLAS experiment. *Physical Review Letters*, 122(23):231801, 2019. arXiv:1904.05105, doi:10.1103/PhysRevLett.122.231801.

[72] Michele Redi and Andrea Tesi. Implications of a Light Higgs in Composite Models. *Journal of High Energy Physics*, 10:166, 2012. arXiv:1205.0232, doi:10.1007/JHEP10(2012)166.

[73] Giuliano Panico, Michele Redi, Andrea Tesi, and Andrea Wulzer. On the Tuning and the Mass of the Composite Higgs. *Journal of High Energy Physics*, 03:051, 2013. arXiv:1210.7114, doi:10.1007/JHEP03(2013)051.

[74] Oleksii Matsedonskyi, Giuliano Panico, and Andrea Wulzer. Light Top Partners for a Light Composite Higgs. *Journal of High Energy Physics*, 2013(1):164, January 2013. arXiv:1204.6333, doi:10.1007/JHEP01(2013)164.

[75] Adrian Carmona and Florian Goertz. A naturally light Higgs without light Top Partners. *Journal of High Energy Physics*, 2015(5):2, May 2015. arXiv:1410.8555, doi:10.1007/JHEP05(2015)002.

[76] Andrei Angelescu, Andreas Bally, Simone Blasi, and Florian Goertz. Minimal SU(6) Gauge-Higgs Grand Unification. *Physical Review D*, April 2021. arXiv:2104.07366, doi:10.1103/PhysRevD.105.035026.

[77] A. Zee. *Group theory in a nutshell for physicists*. In a nutshell. Princeton University Press, Princeton, 2016.

[78] R. Slansky. Group theory for unified model building. *Physics Reports*, 79(1):1–128, December 1981. doi:10.1016/0370-1573(81)90092-2.

[79] P. Sikivie, L. Susskind, M. Voloshin, and V. Zakharov. Isospin breaking in technicolor models. *Nuclear Physics B*, 173(2):189–207, October 1980. doi:10.1016/0550-3213(80)90214-X.

Erklärung:

Ich versichere, dass ich diese Arbeit selbstständig verfasst habe und keine anderen als die angegebenen Quellen und Hilfsmittel benutzt habe.

Dossenheim, den 01. Mai 2022 .....